SPELEOGENESIS ON CAYMAN BRAC, CAYMAN ISLANDS, BRITISH WEST INDIES.

SPELEOGENESIS ON CAYMAN BRAC, CAYMAN ISLANDS,

BRITISH WEST INDIES

by

ROZEMARIJN FREDERIKE ANTOINETTE LIPS

A Thesis

Submitted to the School of Graduate Studies

in Partial Fulfilment of the Requirements

for the Degree

Master of Science

McMaster University

December 1993

MASTER OF SCIENCE (1993) McMASTER UNIVERSITY

(GEOGRAPHY) Hamilton, Ontario

TITLE: Speleogenesis on Cayman Brac, Cayman Islands, British West Indies

AUTHOR: ROZEMARIJN FREDERIKE ANTOINETTE LIPS,

Licence en Science Géographiques (Université de Liège, Belgium)

SUPERVISOR: Professor D.C. FORD

NUMBER OF PAGES: xviii, 223

ABSTRACT

Due to differential tectonic uplift the core of Cayman Brac (Tertiary dolostone of the Bluff Group) reaches ~45 m in the east and is overlain by the Pleistocene limestone, the Ironshore Formation, in the west. The Bluff Group creates a cliff along most of the island in which an erosional notch of the last interglacial period is present at about 6 m amsl. The entrances of the caves are in the cliff, rarely on the plateau.

The notch caves lie a few meters above the notch and show a similar morphology: smooth rounded walls, bellholes and not much speleothem. The higher caves differ in morphology and speleothem abundance. Tibbetts Turn Cave shows morphological similarities with the notch caves but contains much more speleothems, which could indicate that it is older. Little Cayman Brac Cave follows a pre-existing vertical joint pattern sub-parallel to the cliff. The passages in Peter's Cave are also sub-parallel but appear to be determined by an arching joint.

Dating of the speleothems revealed that speleothem growth was not continuous over time and that the periods of growth cessation or dissolution were not necessarily linked to the glacial-interglacial sequence of the Quaternary. Periods of growth cessation were dated at >350 ka, ~200 ka and 75-20 ka. The present is for the majority of the speleothems a period of growth cessation.

In the caves three different speleothem dissolution types were identified. Type 1 consist of speleothem that has lost its initial morphology and is dissolved in the same manner as the walls in which they are present. Type 2 speleothems have lost an extensive part of their volume but their original morphology is still recognisable. Finally, Type 3 speleothems, often still actively growing, only show point dissolution or none at all.

ACKNOWLEDGEMENTS

My greatest gratitude is to Dr. Derek Ford, for giving me the wonderful opportunity to study under his guidance and for his excellent academic and financial support which enabled me to see some of the wonders of "the other side of the Atlantic Ocean".

Special thanks go to Dr. Brian Jones and Ian Hunter who made our stay on Cayman Brac very comfortable and for their succinct introduction to the geology of the island. Many thanks to Karen Lazzari and Mr. Bernstein of the Water Authority on Cayman Brac for using their facilities, for their great help and their friendship. Thanks also to the Mosquito Control Unit of Cayman Brac for their rainfall data and all the people on the island who received us with warm hospitality.

I am also thankful to Mike Bagosy, my hard working field assistent, Nicki Robinson for the alpha spectrometry, Bob Bignell for photography and for showing me some of Ontario's beautiful places, Mr. Zwicker for cutting my rock and speleothem samples and Jim McAndrew for mineral analysis. Further I would like to thank Dr. John Mylroie and Dr. Jim Carew for introducing me to the karst of the small island of San Salvador, Bahamas, and the USGS, especially Dr. Joe Troester and Dr. Carol Wicks, for the opportunity to study the caves on Isla de Mona, Puerto Rico. Dr. Yavor Shopov, Dr. Amos Frumkin, Dr. Steve Worthington and Markus Buck are especially thanked for the many fruitful discussions I had with them. Space precludes me from listing by name all the other people who helped me in various ways to bring this work to fruition. Their contribution is most appreciated.

Last but not least I would like to express my gratitude to Susan Vajoczki and Craig Malis for their friendship and support during my stay far from home. Of course, without the support and love of my family and Aondover Tarhule nothing would have gone as well as it did.

DEDICATION

TO MY PARENTS

BEDANKT VOOR JULLIE ENORME STEUN IN ALLES WAT IK ONDERNEEM

TABLE OF CONTENT

LIST OF FIGURES

LIST OF TABLES

LIST OF PHOTOS

ABBREVIATIONS

BC	Bats Cave
CC	Cross Island Road Cave
GC	Great Cave
HC	Hospital Cave
HRC	Hurricane Cave (= Peter's Cave)
LC	Little Cayman Brac Cave
PB	Pollard Bay Caves
PC	Peter's Cave
RC	Rebecca's Cave
TC	Tibbetts Turn Cave

CHAPTER ONE

INTRODUCTION

1.1 Objectives.

Caves and karst in continental settings have been studied in detail since the last century but the caves and karst found on small oceanic, carbonate islands have been largely ignored. Of course, the existence of caves was known but few researchers tried to determine why they were there, how they formed etc. Recent studies make it clear that many caves formed on small tropical oceanic islands where the rocks are comparatively young have formed under different conditions than those of caves in older rocks in a continental setting. The only water responsible for the dissolution of the bedrock is the rain water falling on the island and the saline water underlying the freshwater; there are no allogenic streams, such as are common on continental karst. Taking into account the relative young age of the rocks (Tertiary and Pleistocene) and the size of the caves, the dissolution mechanism must be very powerful. No past model for cave development explains these caves fully and further study of more islands and their caves is necessary.

Therefore, the purpose of this study is first to describe the karst and especially the caves on Cayman Brac, an example of a small oceanic island; second to determine the genetic type(s) of the caves and so to further advance the study of speleogenesis; third, to conduct a preliminary survey of the cave deposits, especially the chemical deposits.

Chemical deposits (speleothems) form when the cave is air filled and by dating them a minimum age of the cave can be determined. Furthermore, their characteristics may contain more useful information about the history of the cave. For instance the presence of growth hiatuses in a stalactite indicates that during some periods in the past the growth must have stopped for one reason or another. Dating these growth hiatuses and growth periods can lead to a better understanding of the events responsible for the growth cessation. This then may yield some more information on the environmental conditions of the Quaternary in the Caribbean Region.

The balance of Chapter One discusses the study area, including new data on the surface karst, and a review of pertinent literature. Chapter Two introduces the caves, cave geometry, direction of cave development, bellholes (typical tropical cave structures) and the clastic sediments. The water chemistry analysis is discussed in Chapter Three while Chapter Four contains the speleothem analysis. This includes the description of the speleothem dissolution types and the causes of dissolution, and the distribution of the different types of speleothem inside the caves. Uranium-series disequilibrium dating of some speleothems by alpha spectrometry is treated in Chapter Five. The last chapter contains the conclusions and proposals of further study.

1.2 Geographic and topographic description of Cayman Brac.

The Cayman Islands, a group of three islands, lie on isolated volcanic blocks of the Cayman Ridge, the northern margin of the Cayman Trench. They are situated approximately 740 km east of the Yucatan Peninsula, Mexico, and 240 km west of Cabo Cruz, Cuba, in the trend of the Sierra Maestra (Fig. 1.1). The islands consist of a core of Tertiary strata - the Bluff Group (Jones *et al.*, in press (b)) that is fringed by a Pleistocene limestone - the Ironshore Formation.

The topography of the three islands is quite different. Grand Cayman, with 197 km^2 is the biggest of the three, it consists mainly of low land with swamps and has a maximum elevation of 15 m. Of the island, 79% lies under 6 m of elevation which is believed to be the maximum elevation of the sea level high stand of the last interglacial (oxygen isotope stage 5e). Little Cayman (16.3 km^2) has a maximum altitude of only 13 m and 87% of its surface is below 6 m. Cayman Brac is the most eastern and the highest island with cliffs of up to 45 m and only 14% of the land below 6 m (mainly as a relatively narrow strip along the coast) (Woodroffe *et al.*, 1983).

Throughout the Caribbean, both glacio-eustatic sea-level changes and tectonic movements have taken place, causing elevated shoreline erosional features (notches and erosional benches) on Grand Cayman Island and Cayman Brac. Due to tectonic movements, the eastern ends of the islands are higher than the western ends. The preserved shoreline erosional features, however, do not show any evidence of tilting,

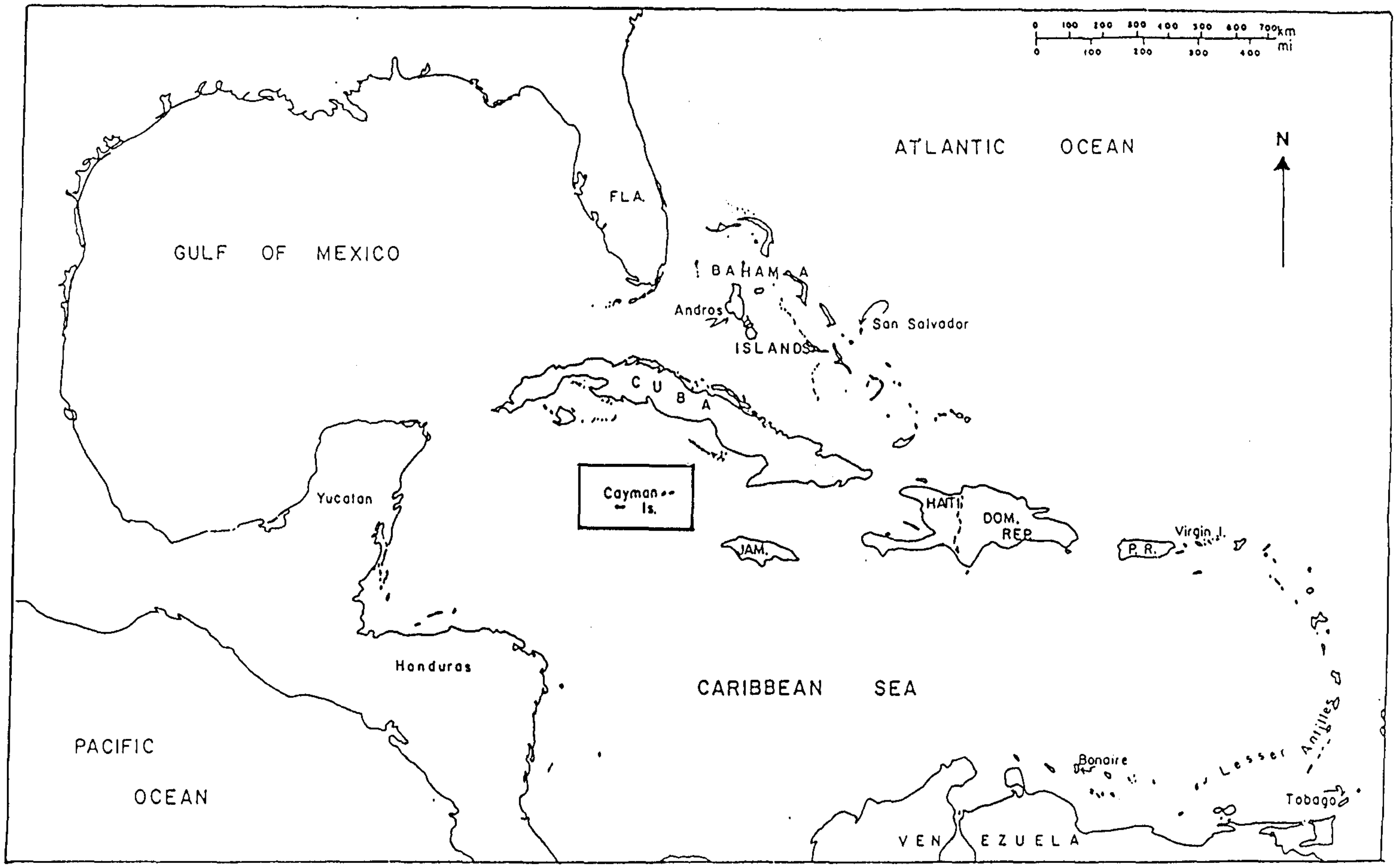

Fig. 1.1. Location of the Cayman Islands.

indicating a tectonic stability since the last sea level high stand (*op. cit.*).

Cayman Brac is a 19 km long island with a width that decreases from 3 km in the east to 1.5 km in the west (Fig. 1.2). The elevation varies from sea level in the west to an altitude of 45 m in the east. Beaches of white sand occur on the west end and at a few places along the north side of the island where the wave energy is reduced. However, along the north shore people have removed sand for different purposes which seems to have increased erosion of the remaining sand.

1.3 Geology.

On Cayman Brac the Bluff Group reaches about 45 m in the east and is overlain by the Ironshore Formation in the west. The Bluff strata create a cliff around most of the island with the Ironshore limestone forming a coastal platform at the cliff foot.

1.3.1 The Tertiary Bluff Group

Until recently the Bluff Group was termed the "Bluff Limestone", so called by Matley in 1926 and copied by many workers since then (e.g. Brunt *et al.*, 1973; Woodroffe *et al.*, 1983; Spencer, 1985). Jones and Hunter (1989) renamed the Bluff

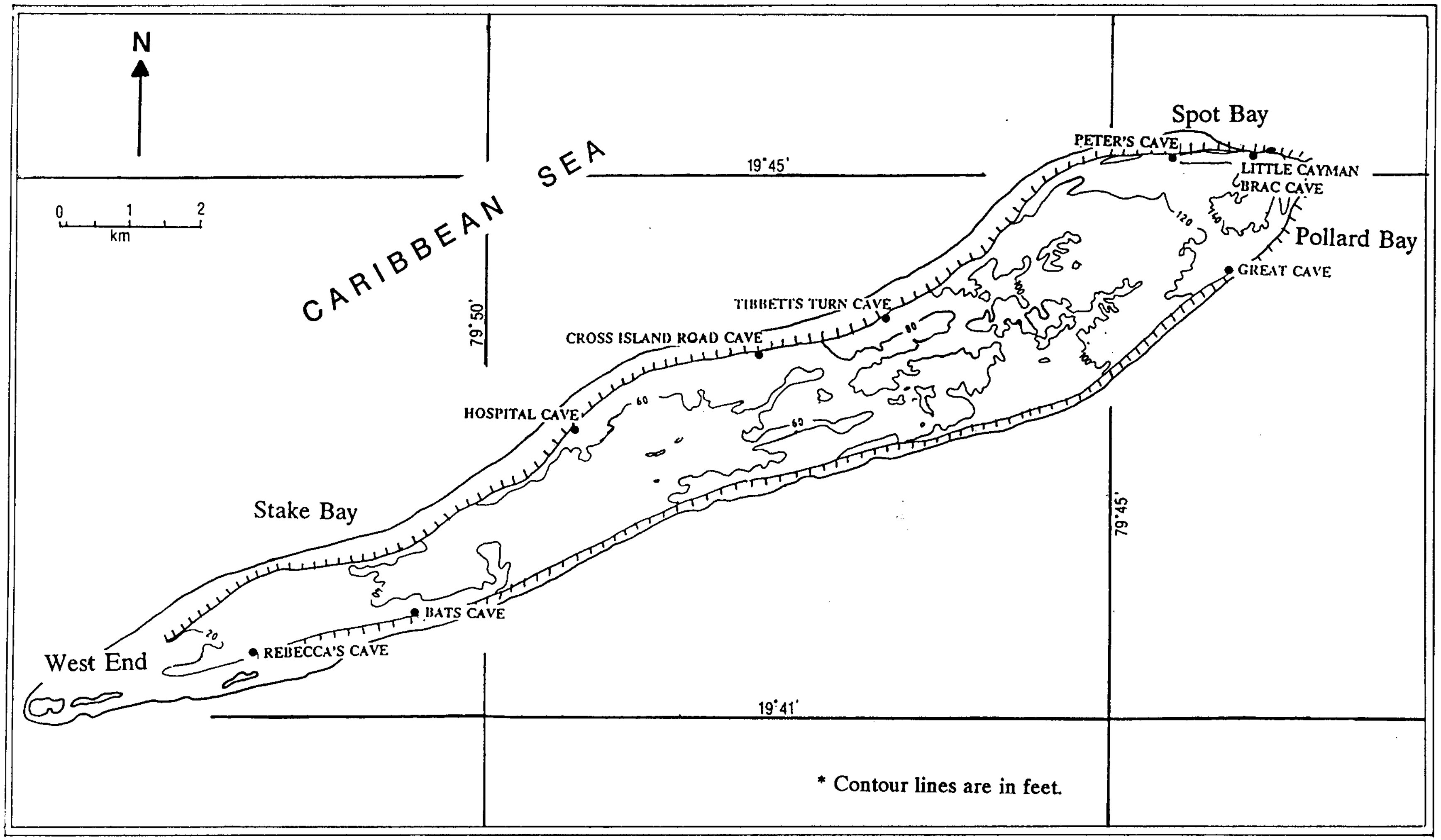

Fig. 1.2. Cayman Brac.

Limestone the "Bluff Formation" because it is composed of dolostone for the most part, and subdivided it into the "Cayman" and the "Pedro Castle" members. Further study by Jones *et al* (in press (a)) led them to designate a "Brac Formation" that underlies the Bluff Formation and to revise the stratigraphic nomenclature of the Tertiary strata by giving the Cayman and Pedro Castle members formational status and elevating the Bluff Formation to group status (in press (b)). The Bluff Group thus includes the Brac, Cayman and Pedro Castle formations, each separated by unconformities that represent periods of emergence and erosion, and each dipping at about 0.5° to the southwest along the long axis of the island (Fig. 1.3) (*op. cit.*).

1.3.1.1 The Brac Formation

The Brac Formation is exposed in the lower part of the cliffs around the high eastern end of Cayman Brac, roughly from Booby Point in the north to Pollard Bay in the south (Fig. 1.3) and has a maximum exposed thickness of approximately 33 m at North East Point. It consists of *Lepidocyclina*-rich limestones on the north side and dolostones on the south side. The limestones are wackestones to grainstones and near the top of the formation there is one bed of large articulated, smooth-shells bivalves and gastropods. Pods of skeletal wackestones occur at various levels in the dolostones on the south side. Fossil-moulded vugs, often containing internal sediment or dolomite cement, can now be seen instead of the bivalves and gastropods. Cavities filled with caymanite (see below), in association with *Lepidocyclina*, suggest that there was some karst

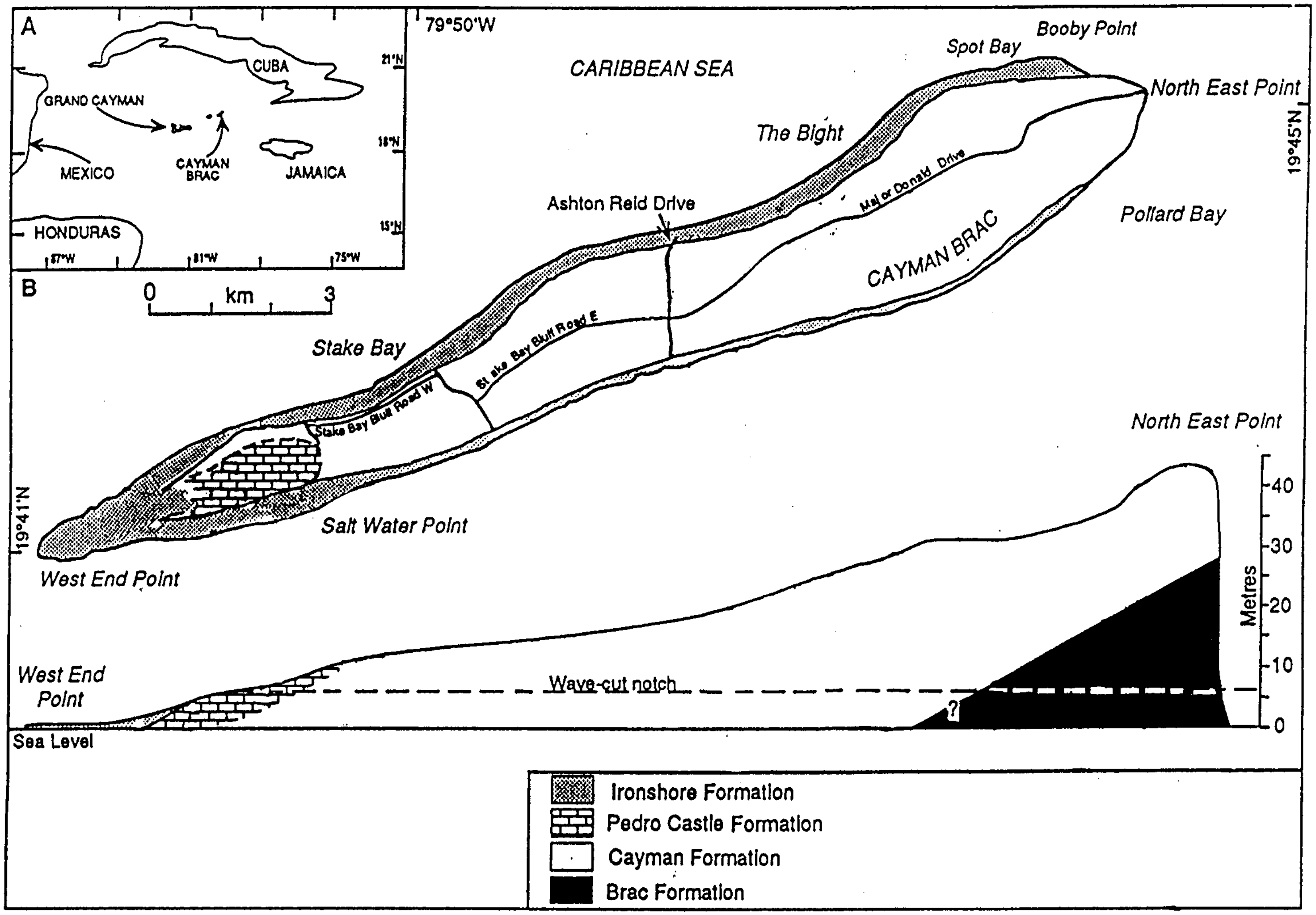

Fig. 1.3. The geology of Cayman Brac (modified from Jones *et al.*, in press (a), Fig. 1).

development before deposition of the ensuing Cayman Formation (Jones *et al.*, in press (a)). On the basis of the foraminiferal fauna and the $^{87}Sr/^{86}Sr$ ratio (0.70808 indicating an age of about 28 Ma) from the limestones, Jones *et al.* (*op. cit.*) determined the age of the Brac Formation to be late Early Oligocene (Rupelian).

1.3.1.2 The Cayman Formation.

Most of Cayman Brac is composed of fabric-retentive dolostones of the Cayman Formation (Fig. 1.3), which has a thickness of approximately 100 m if a regional dip of 0.5° to the west is assumed. Mudstones and wackestones dominate in this formation where beds and lenses of rhodolites, rudstone, packstone and grainstone are also present. Bedding planes are difficult to trace from one end of the island to the other and marker beds are absent. Leaching of fossils has occurred and fossil-moulded vugs are now visible. Due to the absence of age-determining fossils and the disruption of the initial $^{87}Sr/^{86}Sr$ ratio as a result of dolomitisation it is not possible to assign a definite age to the formation. However, a Lower to Middle Miocene age is suspected (Jones *et al.*, in press (a)).

1.3.1.3 The Pedro Castle Formation.

On Cayman Brac this formation is only found over a small area in the western part of the island where the Bluff Group meets the Ironshore Formation (Fig. 1.3). It consists of limestones, fabric-retentive dolomitic limestones and dolostones having an estimated total thickness of 15 to 17 m. According to lithology and biota the formation in its reference core on Grand Cayman can be subdivided into five units. The lower unit consists of poorly cemented white to off-white skeletal wackestone containing in general less than 10% dolomite. The second unit is formed of white to off-white, poorly-sorted skeletal grainstone; cavities, filled or lined with thick coatings of flowstone, are found in the lower part. The next unit is a white to off-white packstone that differs from the second unit because of its higher mud content; dolomitisation is extensive. The fourth unit consists of a light grey skeletal wackestone in which there are cavities, one of which is floored by flowstone. Dolomitisation has only occurred in the lower part. The upper most unit is a grey, recrystallised limestone that contains numerous cavities filled with terrestrial oncoids and/or terra rossa. The presence of *Stylophora*, a branching coral that became extinct in the Caribbean region towards the end of the Pliocene, and an average $^{87}Sr/^{86}Sr$ ratio of 0.70912 from the limestones, suggesting a minimal age of approximately 2 million years, are good indicators of the Pliocene age of this formation (Jones *et al.*, in press (a,b)).

1.3.1.4 Caymanite.

"Caymanite is a multicoloured microcrystalline dolostone with laminae that dip at angles up to 60°" (Jones, 1992, p. 720). It occurs only in cavities in the Tertiary strata and was deposited before the dolomitisation of the bedrock 2-5 Ma ago. The dolomitisation has not destroyed the original sedimentary fabric or structures and pigmentation was inherited from the original limestone. The colours, white, red and black, are due to pigmenting agents from the source area of the material forming the caymanite: white from the marine calcareous muds, red from iron and black from manganese, both originating from terra rossa, swamps, ponds and/or cave deposits such as guano. These materials were washed into cavities developed in the Tertiary strata, by storms and hurricanes in early stages of marine transgressions (Fig. 1.4). The sedimentary structures and the angle of deposition of the caymanite are both highly variable and depend on the point of sediment introduction into the cavities and the viscosity of the sediment-laden water. Angles steeper than the angle of repose were formed in cavities that were air-filled rather than water-filled at the moment of deposition so that the sediment-laden water could not flow easily. The angle of dip can thus not be used as an indicator for postdepositional tilting (Jones, 1992).

The abundance of caymanite-filled cavities indicate that the Tertiary strata were well karstified before the deposition of the Pleistocene Ironshore Formation. The cavities many with flowstones, in the Pedro Castle Formation may also have been formed before the deposition of the Ironshore Formation. Although the flowstone might have formed much later than the cavities, dating them could indicate a minimum age that is probably older than the last interglaciation.

1.3.2 The Pleistocene Ironshore Formation.

The formation owes its name to the sound the case-hardened surface makes

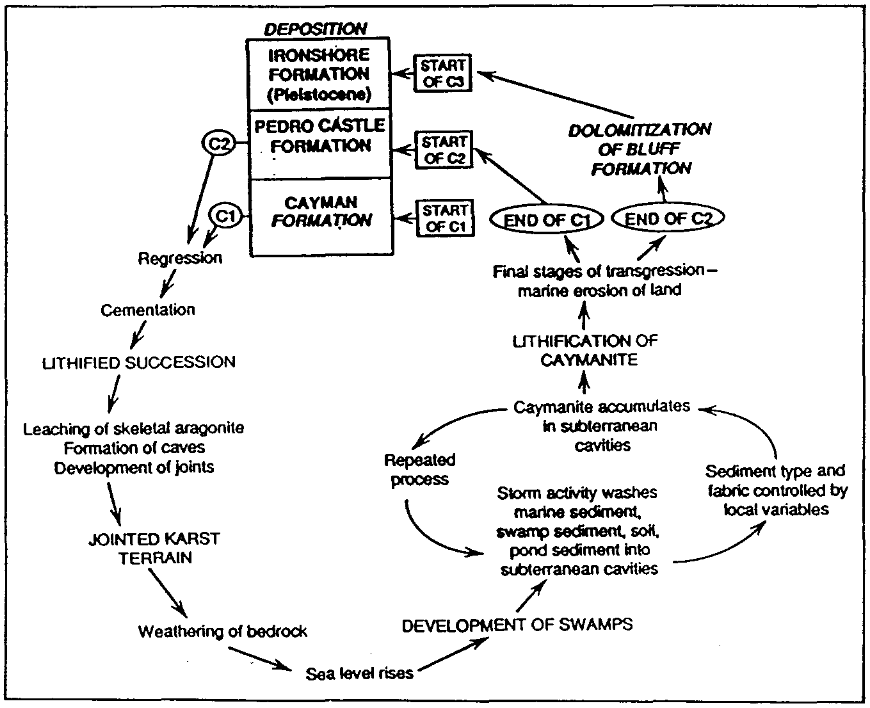

Fig. 1.4. Time of caymanite formation relative to the transgressive-regressive cycles (C1, C2 and C3) that led to the carbonate cycle present on the Cayman Islands (modified from Jones, 1992, Fig. 15).

when it is struck. It consists of poorly consolidated reef limestones, calcarenites of varying origins and lagoonal mud and sands. An unconformity separates this Pleistocene formation from the underlying Tertiary strata. Within this formation six depositional environments are recognised: reef, patch reef, back reef, lagoonal, shoal and beach ridge facies (Brunt *et al.*, 1973; Woodroffe, 1988). On all three Cayman Islands the reef facies dominates along the coast and is situated almost everywhere below 2 m above sea level. This uniform elevation together with the presence of corals in the growth position suggests that the reef was a constructional feature restricted in its growth by a past sea level. Dating of some of the corals revealed an average age of 124,000 $\pm$ 8000 years, which indicates formation during the Last Interglacial (oxygen isotope stage 5e) (Woodroffe *et al.*, 1983).

1.3.3 Tectonic movements of the islands.

The three Cayman Islands are each situated on a separate fault block on the Cayman Ridge. The latter is parallel to the Cayman Trench, a complex feature reaching more than 7000 m in depth and containing the mid-Cayman spreading centre (Fig. 1.5). The Cayman Ridge and the Nicaraguan Plateau have been moving apart at an average rate of 0.4 cm/a since the Eocene (Woodroffe, 1988). An average subsidence rate of 0.006 cm/a (*op.cit.*) is believed to occur along the Cayman Ridge but can not be applied to the Cayman Islands, which have experienced uplift since the formation of their Tertiary strata. The general dip to the west on all three islands but especially Cayman

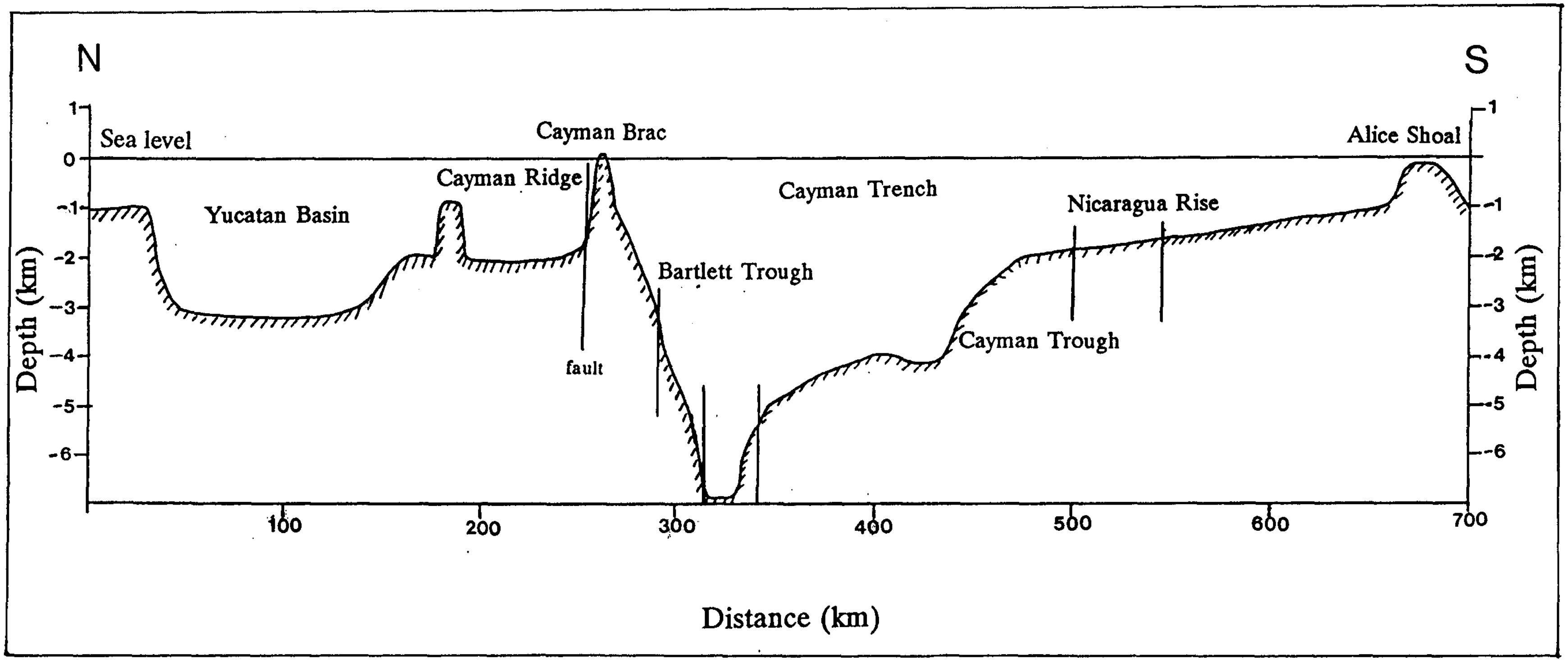

Fig. 1.5. Cross section of the Cayman Trench.

Brac seems to be in accord with Horsfield's (1975) theory of a domed regional uplift centred on eastern Cuba and northwestern Haiti in the Caribbean region during the Quaternary. The different elevation of the Tertiary strata on the different islands is most likely due to differential tectonic movement of the three fault blocks and is not a result of past geoidal configuration. This contention agrees with the existence of faulting and differential movement along the north coast of Jamaica, which is on the other side of the Cayman Trench (Woodroffe, 1988).

The different elevations of shoreline erosional features on Grand Cayman and Cayman Brac and their absence on Little Cayman suggest that the differential tectonic movements persisted into the Quaternary Period. However, the consistency of the elevation of the Ironshore Formation within each of the three islands indicates that there has not been any substantial differential movement since its formation during the Last Interglacial. The elevations are consistent with elevations of Sangamon sea level determined elsewhere in the Caribbean Region (Woodroffe *et al.*, 1983).

1.3.4 Past Sea level fluctuations

Although the Cayman Islands are situated in a tectonically unstable region, the periods of unconformity in their geological records as determined by Jones *et al.* (in press(a)) roughly agree with the periods of global low eustatic sea level during the Tertiary as described by Hallam (1984) (Figs. 1.6 and 1.7). The late Eocene to early Oligocene sea level fall of about 150 m was probably due to a substantial glacial build-up

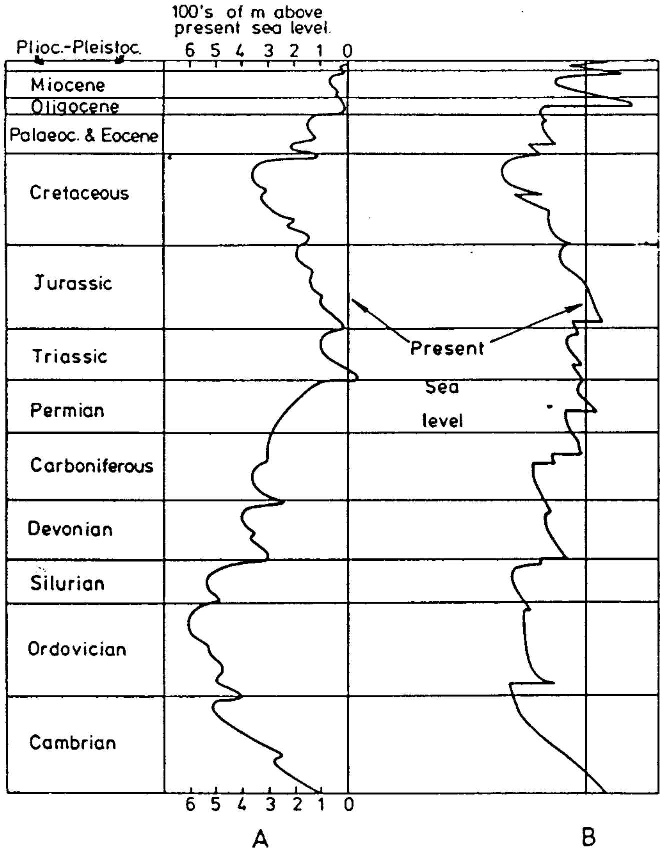

Fig. 1.6.
Eustatic curves for the Phanerozoic. A. After Hallam (1984). B. After Vail *et al.* (1977) (Hallam, 1984, Fig. 5).

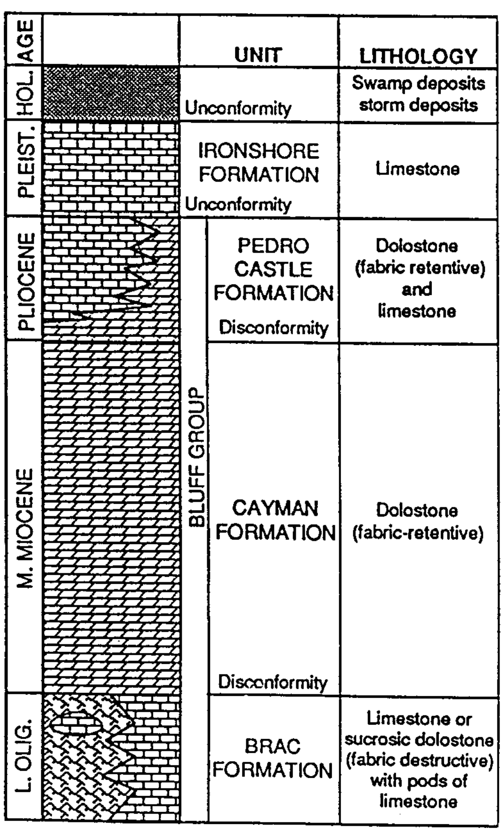

Fig. 1.7.
Stratigraphic sequence of the Tertiary strata of the Cayman Islands (Jones *et al.*, in press (b), Fig. 2)

on the Antarctic continent, although oxygen isotope data suggest that this did not occur until the mid-Miocene time (Hallam, 1984). The latter glacial build-up is thought to be responsible for the approximately 100 m eustatic fall at the end of the Miocene which was then followed by a rise due to deglaciation during the early Pliocene (*op. cit.*).

During the Pleistocene sea level fluctuated with continental ice volume variations as a result of global climatic changes. Temperature fluctuations were recorded as oxygen isotopic variations in the calcium carbonate of foraminifera preserved in deep sea cores. The time resolution of the oxygen isotopic records from the deep sea cores is not very good because of slow and varying sedimentation rates. However, high resolution oxygen isotopic records for the last 800,000 years (Imbrie *et al.*, 1984) and even higher resolution for the last 300,000 years (Martinson *et al.*, 1987) have been constructed based on orbitally tuned timescales (Fig. 1.8b).

On the basis of elevation and dates obtained from drowned speleothems and raised coral reefs in tectonically stable areas (e.g. Bermuda; Bahamas) curves of sea level fluctuation over time have also been constructed (e.g. Land *et al.*, 1967; Harmon *et al.*, 1983; Lundberg, 1990; Richards *et al.*, in litt.) (Figs. 1.8). Unfortunately they are not continuous and they can only give a maximum height for sea level because speleothem growth can occur at all elevations as long as it is above sea level (Richards *et al.*, in litt.).

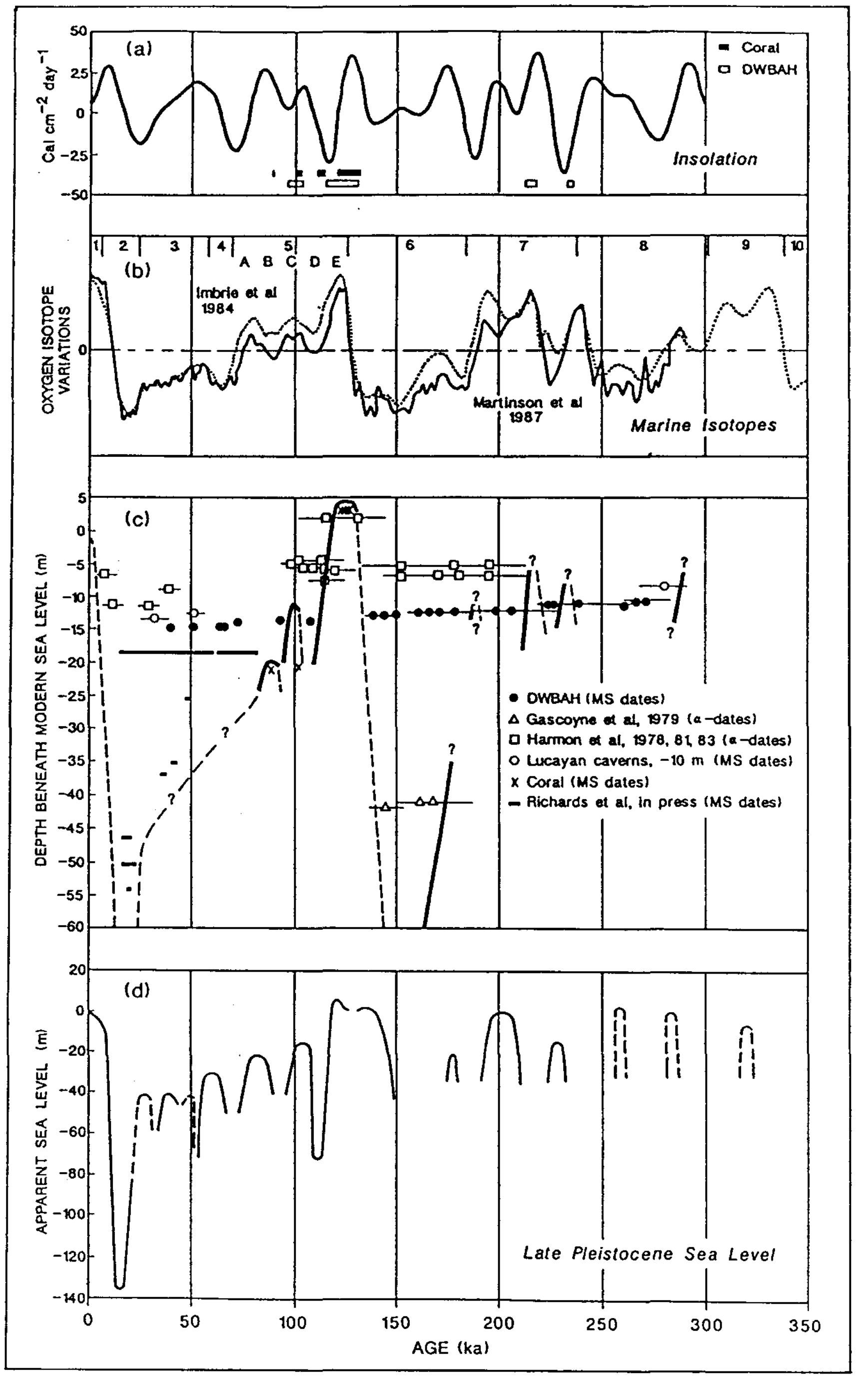

Fig. 1.8. Pleistocene sea level curve for Bahamas. (a) Average solar insolation received at the top of the atmosphere at 65°N for the summer half year expressed as deviations from the 1950 value (Berger, 1978). (b) Marine foraminiferal oxygen isotopic record. (c) Sea level curve reconstructed from speleothem dates. (d) Late Pleistocene sea level curve (Lundberg and Ford, in litt., Fig. 4.).

1.4 Marine notches.

In the cliff around most of the island a notch can be seen at about +6.4 m (Woodroffe *et al.*, 1983). The notch extends up to 7 m into the cliff and is symmetrical. The obvious horizontality and the sharpness of this feature over the whole island indicates that it postdates the tilting of the Tertiary strata in which it is formed (*op. cit.*). Along the east end where the cliff is not protected by a coastal platform or a fringing reef, a modern notch is also being formed. In the "Man of War", an isolated rock along the north eastern coast of the island, close to Little Cayman Brac Cave, which shows both the Sangamon and the modern notch, the modern notch is about 2 m deep. It is possible that its depth exceeds 2 m at the extreme east point, but this has not been determined conclusively.

Notches are very common in the tropics where vertical cliffs of carbonate rock are present. Several processes such as dissolution by sea water, bioerosion, wave and spray action, abrasion, wetting-drying and salt weathering, are held to be responsible for the formation of these notches. Various workers (e.g. Trudgill, 1976; Focke, 1978) have tried to determine the contribution of the different processes but it has to be kept in mind that their relationship is not always evident and that they can be highly dependent on one another (Trudgill, 1985). The studies by Trudgill (1976) on the Aldabra Atoll and Focke (1978) on Curaçao reveal that biological erosion is very important if not dominant (Fig. 1.9; Table 1.1) in the formation of a notch and that the morphology of the coast,

Table 1.1 Erosion processes responsible for surface removal (mm/a) (Trudgill, 1985, Table 10.2).

Results: *sand present*			*Inferences*		
1. All intertidal processes	(MEM)	1.25			
2. Minus grazing	(Tablet)	0.80	Effect of grazing:		0.45
3. Minus grazing and abrasion	(Tablet)	0.39	Effect of grazing and abrasion:		0.81
			Effect of abrasion:	0.41	
Conclusions:		mm a^{-}			% Erosion
Effect of abrasion		0.41			32.8
Effect of grazing		0.45			36.0
Effect of other processes		0.39			31.2
	Total	1.25			100.0
Results: *sand absent*			*Inference*		
1. All processes	(MEM)	1.01			
2. Minus grazing	(Tablet)	0.40	Effect of grazing:		0.61
Conclusions:			mm a^{-1}	% Erosion	
Effect of grazing			0.61	64	
Effect of other processes			0.40	36	
			Total 1.01	100	

(Modified from Trudgill, 1976a)

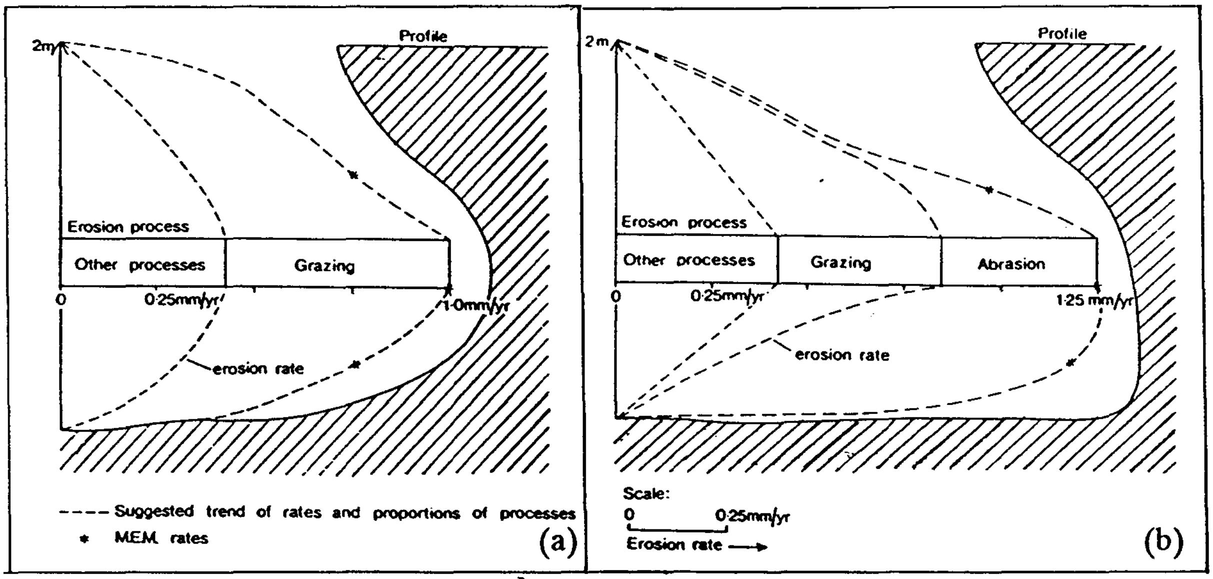

Fig. 1.9. Erosion rates and processes in an intertidal notch on Aldabra Atoll (MEM = Micro Erosion Meter). (a) sand absent. (b) sand present (Trudgill, 1976, Fig. 14 and 15).

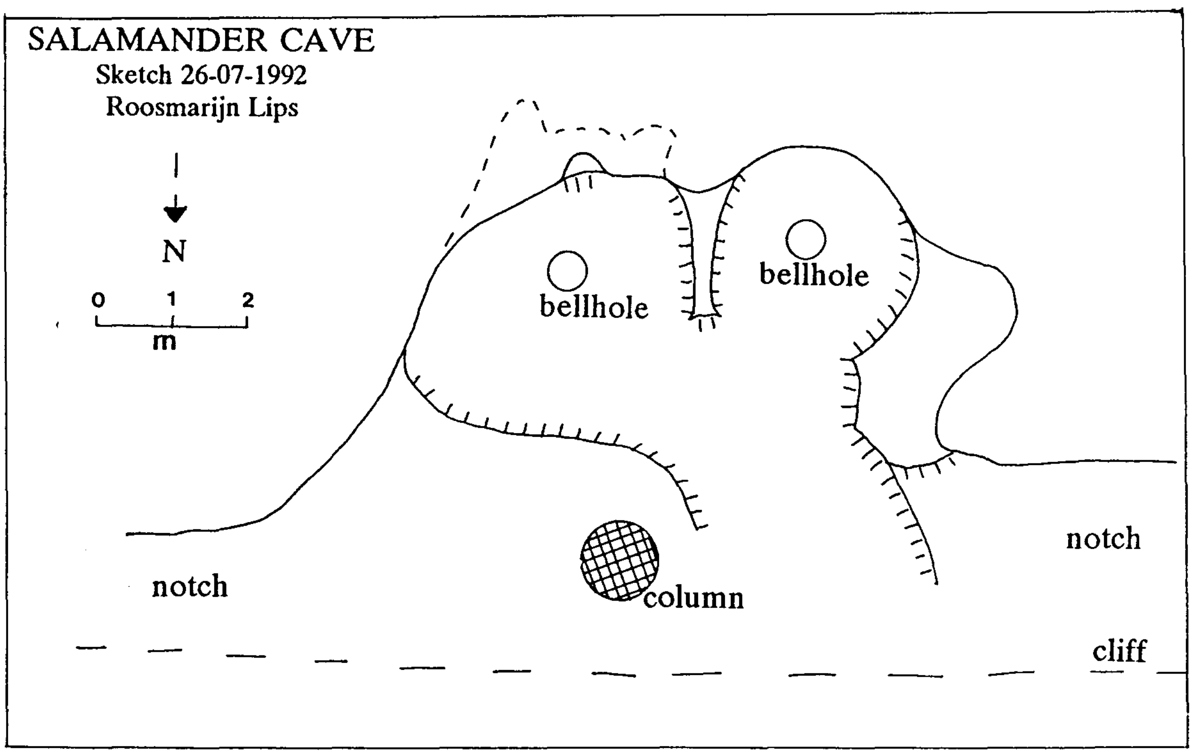

Fig. 1.10. Salamander Cave, Stake Bay.

reflecting the varying importance of the processes involved, related to exposure to wave energy. Assuming a similar wave regime and biota to the present, no abrasion due to the presence of sand and a general erosion rate of 1 mm/a (Trudgill, 1976), a notch of 7 m deep (the maximum extent of the +6.4 m notch on Cayman Brac) could have formed in 7000 years. Of course this is a very rough estimate and only serves to give an idea of the rate of the formation of a notch in geological time.

In the cliff and on a block just east of Stake Bay (Fig. 1.2), there are two notches about 1.5 m apart in elevation. The upper one is more pronounced than the lower and its elevation appears to be closer to the general elevation of +6 m of the Sangamon notch elsewhere. A small cave, Salamander Cave, composed of a chamber of about 9 m wide and 5 m deep (Fig. 1.10) has formed between the two notch elevations (Photo 1.1). Focke (1978) discusses the formation of a double notch (Fig. 1.11) and argues that a double notch is in fact "a single notch with a surf bench growing in the middle" (p. 336). Such features occur in cliffs exposed to very turbulent water where organic accretions are very pronounced in the intertidal zone. However, the location of the Cayman Brac double notch does not suggest a high wave action if the wave direction was northeast as it is at present. Even if the wave direction was slightly different in the past a much wider extent of this double notch feature should be found for Focke's theory to hold here. Another possibility is that the notches are of two different periods and that only at this location (and perhaps some others hidden by vegetation) has the lower notch been preserved. However, this possibility is debatable because the double notch occurs in an

Photo 1.1 The double notch at Salamander Cave

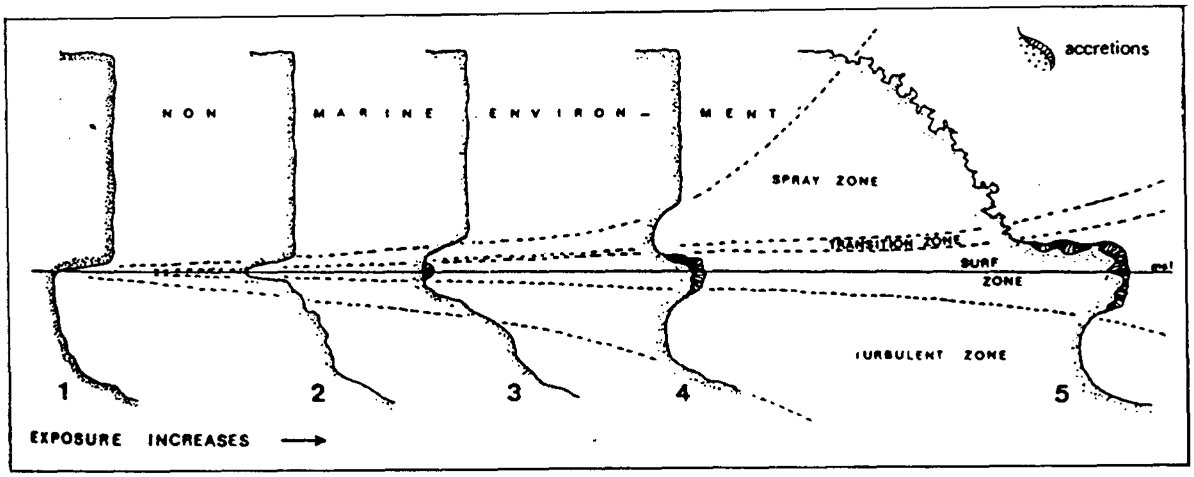

Fig. 1.11. Morphological variations of limestone cliffs as a function of water turbulence (degree of exposure - Focke, 1978, Fig. 2).

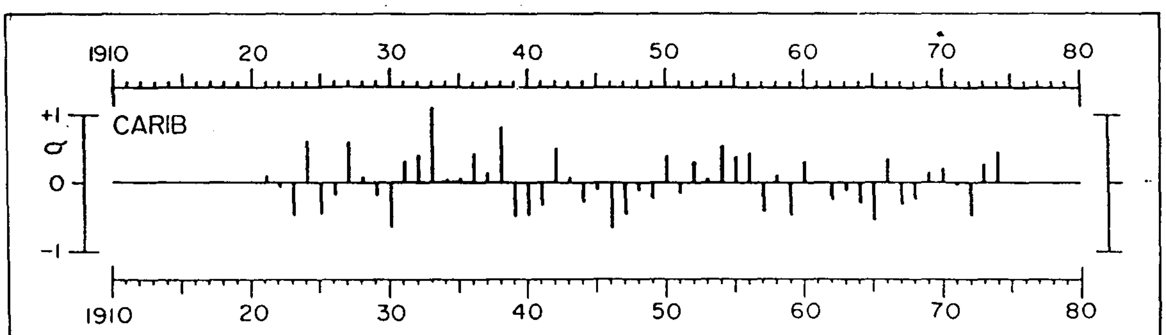

Fig. 1.12. Time series plot of hydrometeorological index (in σ) for the Central American - Caribbean area (Hasenrath, 1985, Fig. 8.7:1).

isolated block on the coastal plain as well and if the double notch has been eroded away by wave action of the sea at all the other places around the cliff why has this easy-to-attack block been unaffected?

1.5 Climate.

The Caribbean region is a large body of water interrupted by islands. The climate of these islands is of predominantly marine type because their size is too small to create meso-scale climatic variations. The mean annual temperature of the Caribbean Sea is 27°C. Annual temperature ranges on the islands are small, varying from about 3°C (26-29°C) in the south to about 9°C (19-28°C) in the north. However, occasional invasions of cold air from the North American continent may cause considerable drops in temperature in the northern parts (Niewolt, 1977).

Climatic variations are reflected primarily in the rainfall activity. Throughout the 20th Century, runs of prevailing wet years have alternated with runs of prevailing dry years (Fig. 1.12) which may have important consequences for the large-scale water budget, the natural vegetation and the land use (Hastenrath, 1985). The Mosquito Control and Research Unit of Cayman Brac maintains eight rain gauges on Cayman Brac and one on Little Cayman. Figure 1.13 shows their location. Note the concentration along the north coast. The longest records have only 16 years of data which is not enough to obtain

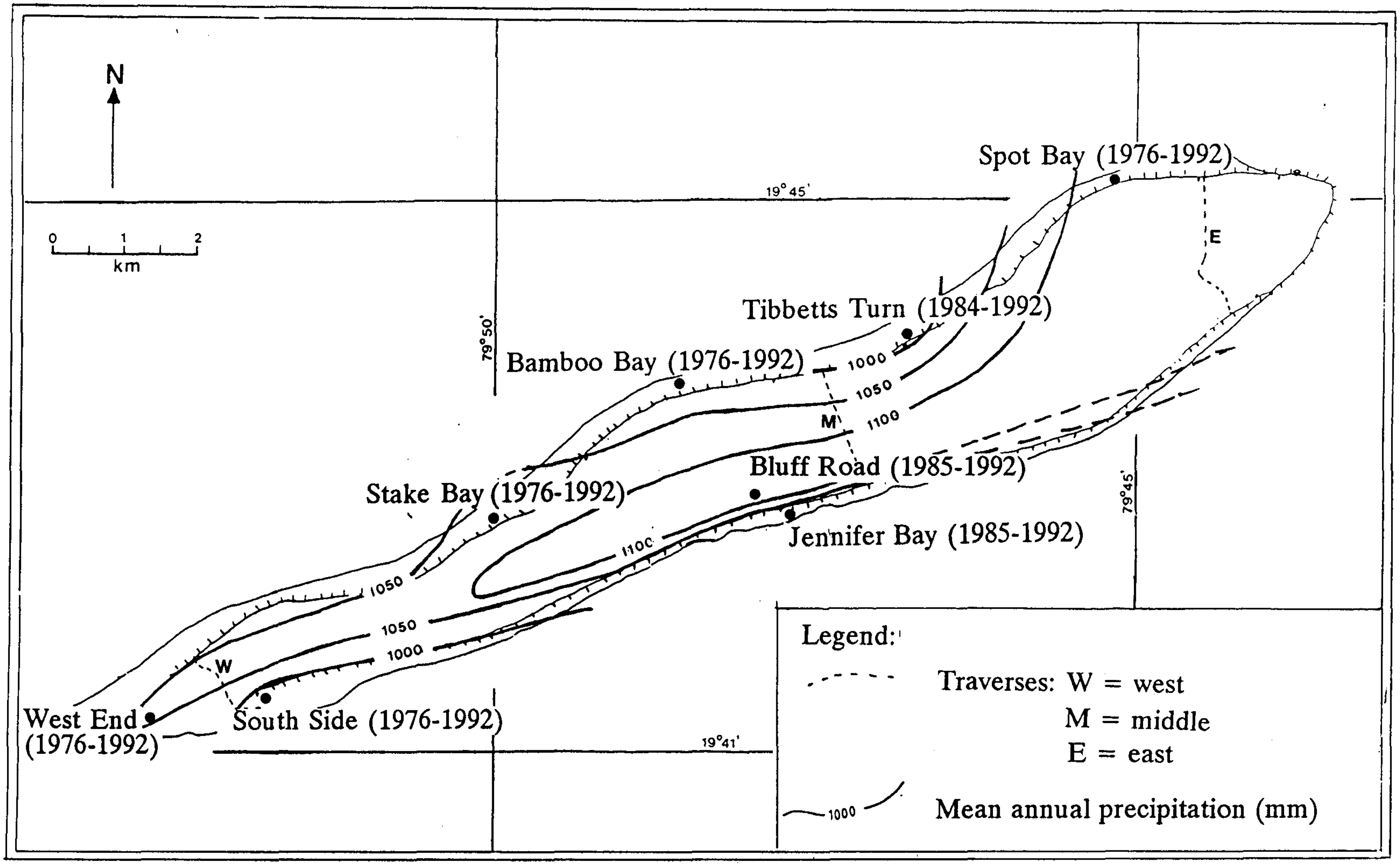

Fig. 1.13. Location of the rain gauges on Cayman Brac.

reliable statistical results (in the tropics at least 30 continuous years of data are needed due to the high interannual variability; Niewolt, 1977). The interannual variability of precipitation on Cayman Brac and on Little Cayman is shown in Figure 1.14a. The rainfall values of Cayman Brac are an average of the observations at the eight stations; although the island is small these average values do not always reflect the situation on the whole island. For instance the rainfall deficit for 1976 and 1977 are due to a dry year at the east end of the island, whereas the west and central sections experienced a slightly wetter than average year (Fig. 1.14b). For other years however all the stations on Cayman Brac and the one on Little Cayman agree in the general dry or wet trend; e.g. 1978, 1979, 1983, 1988 and 1990 were wet years, whereas 1984-1987 were very dry years.

The region experiences the rainy season during the summer months (Fig. 1.15) when the Trade Wind inversion is high, weak or even absent most of the time and therefore permits the formation of rain-bearing clouds (Hastenrath, 1985). An interruption of the rainy season in July (Fig. 1.15) in the western part of the Caribbean region is related to a "temporary strengthening of the subtropical high pressure cell, caused by northerly winds from the North American continent" (Niewolt, 1977, p. 166).

The yearly precipitation averages 1025 mm but varies from 1140 mm in the east and on the plateau in the centre of the island to about 980 mm around the middle of the north coast and the south west coast (Fig. 1.13). This distribution reflects the NE-SW direction of the rain-bringing trade winds.

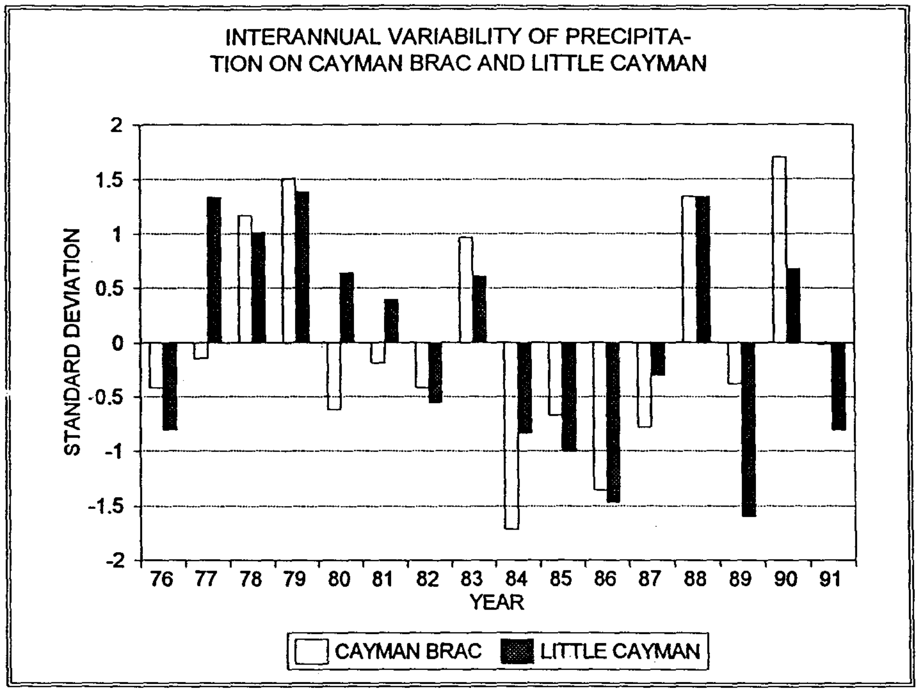

(a)

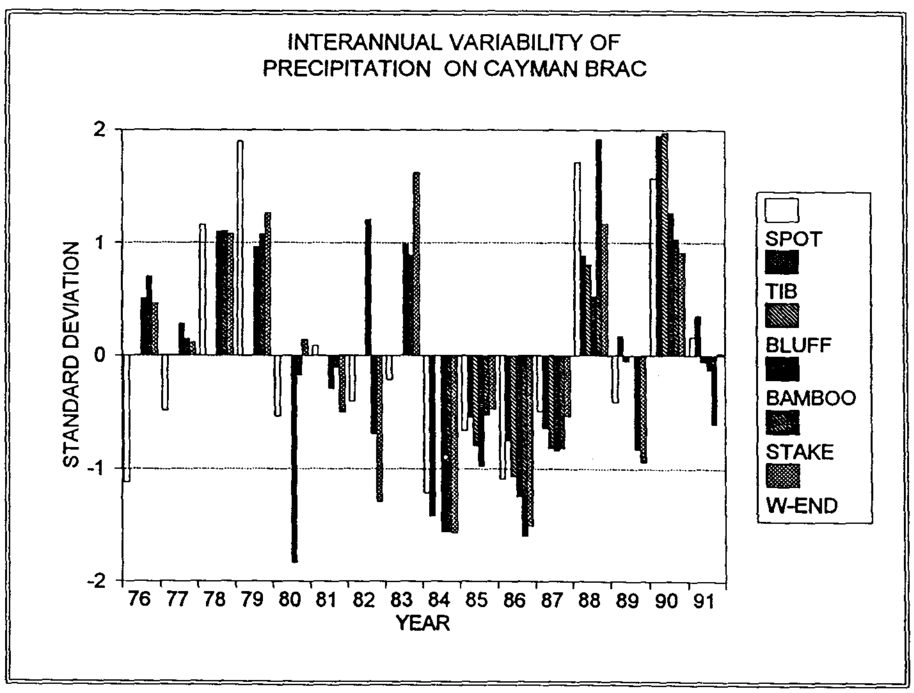

(b)

Fig. 1.14. Interannual variation of precipitation (a) on Cayman Brac and Little Cayman. (b) on Cayman Brac.

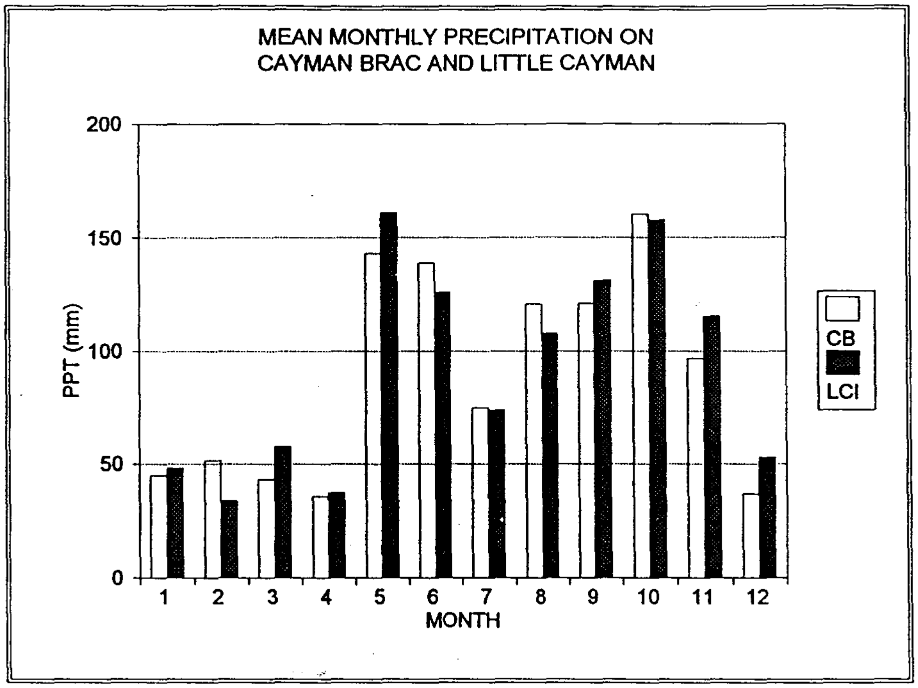

Fig. 1.15. Mean monthly precipitation on Cayman Brac and Little Cayman.

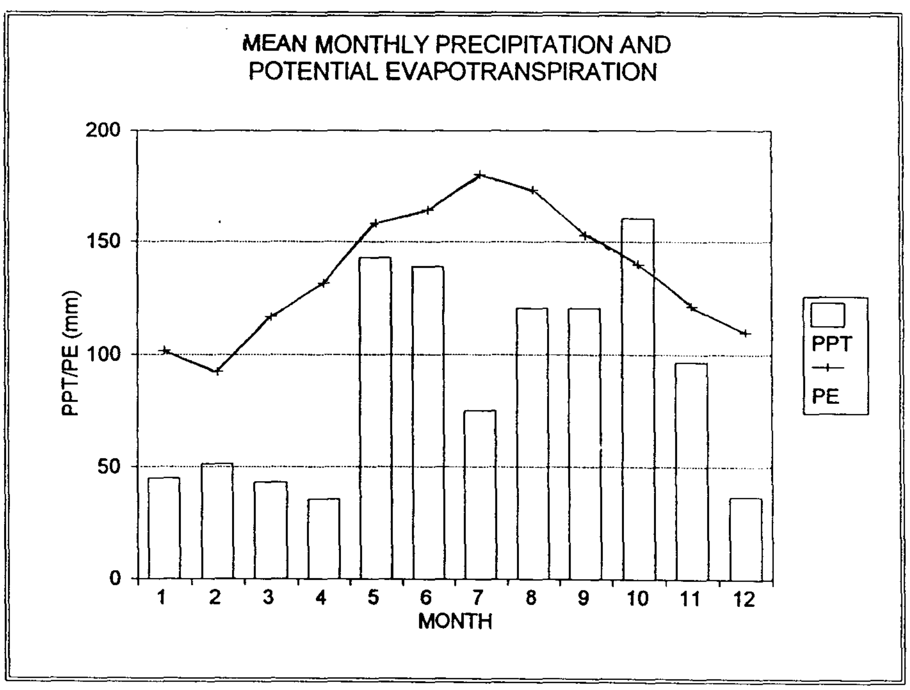

Fig. 1.16. Mean monthly precipitation and evapotranspiration.

The potential evapotranspiration (PE) was calculated according to Thornthwaite (1948) using the temperatures of Montego Bay, Jamaica (1830 N, 07755 S, 8 m above sea level, the closest climatic station for which temperature data were available). Because temperature differences are not very large between this station and Cayman Brac, it is believed that the PE calculated will reflect the PE on the latter within the margins of uncertainty of the method used. Figure 1.16 shows that the monthly PE is greater than the monthly precipitation eleven months of the year. This will tend to greatly limit the water storage on the island, the more so because the rain falls in tropical downpours and therefore could for a great part runoff and not infiltrate at all. The relatively karstified carbonate rocks with not much soil cover on Cayman Brac however may allow the water to infiltrate relatively fast. Evapotranspiration depends on wind speed (among other factors). Thus, the east end of the island is expected to have a higher evapotranspiration and be dryer during dry periods than the west side. This is reflected in a less dense and lower vegetation on the eastern end.

During the period of this study (June 18 to July 27, 1992) only one day (June 22, 1992) of continuous thunderstorms and tropical downpours was observed. Except for a few localised, isolated rain showers of short duration (less than one hour), the rest of the rain fell during the night accompanied by thunder and lightning as may be expected because of the location. In marine and coastal areas the diurnal rainfall regime is caused by "nighttime 'convection', the result of a steepened lapse rate as the upper troposphere is cooled by radiation losses, mainly from the tops of the clouds, while the lower layers of the atmosphere remain warm by close contact with the water surface" (Niewolt, 1977, p. 117). Furthermore only a few overcast days interrupted the sunny six weeks. This observation corresponds with the general trend of the rainy season on this island where July is a relatively dry month (Fig. 1.15).

1.6 Karstic features of the surface.

1.6.1 Phytokarst.

Everywhere along the coast the surface of exposed bedrock is formed of sharp pinnacles separated by pits, known as phytokarst (Photo 1.2). In the intertidal zone, algae (mainly Cyanophyceae or blue-green algae), in their search for protection especially from too strong sunlight, and for nutrients and/or moisture, bore into the rock and so actively erode it but also form a food source for grazing animals. The depth of boring is believed to be a function of light intensity and may reach 800-900 μm into the rock (Trudgill, 1985). Out of the spray zone the rocks are not covered any more with the slippery black/green layer and they have a whiter colour.

On top of the plateau the surface consists mainly of a highly developed phytokarst covered by a dense vegetation through which travelling is hazardous without a machete to cut a trail (Photo 1.3). The phytokarst found on top of the plateau looks like that along the coast and is probably due to a combination of the boring activity of blue-green filamentous algae, rainwater dissolution and mixing corrosion. According to Folk

Photo 1.2 Phytokarst on the coastal platform which consist of the Ironshore Formation and the cliff face of the Bluff Group at Spot Bay.

Photo 1.3 Phytokarst and vegetation on the plateau

et al. (1973) the algal acid attacks by boring and dissolves calcite preferentially over dolomite and even the calcite from among the dolomitised coral septa. Ford (pers. comm.) has however observed the same type of karren surface in Greece far from the sea and without the presence of algae and he believes that dissolution by rainwater may play a more important role than suggested by Folk *et al.* (1973). Another evidence for the contribution of rain water dissolution to the formation of phytokarst is that the same forms have been observed on gypsum and salt surfaces, where there is no algal contribution.

The phytokarst observed on Cayman Brac is much lighter in colour than the black phytokarst described by Folk *et al.* (1973). The black pigment is a survival mechanism of the algae because it screens out sunlight and thus prevents destruction of the chlorophyll (Fritz, 1907 in Folk *et al.* (1973)). Burial and subsequent exposure or native bush fire could cause the death of the algae and thus the disappearance of the black colour (Folk *et al.,* 1973). Another possibility is that the dense vegetation cover on the plateau of Cayman Brac functions as a good enough protection against the sunlight and that the black pigment is not necessary, as has been observed in cave entrances of caves in Sarawak, Borneo (Bull and Laverty, 1982).

1.6.2 Observations on the plateau.

Three traverses were made across the top of the plateau (Fig. 1.13) examining the percentage soil/grass cover versus bare rock, the number of sinkpoints, of plants taller than one meter and the presence of terra rossa/paleosol. The observations were made every one hundred meter on both sides of the trail over an area of 1.5 m by 1.5 m. They represent the features observed in the area beside the trails because the rate of growth of the vegetation in this climate allows any vegetation removed from beside the trail while cutting to grow back very fast.

The width of the island was measured from east to west and the location of each observation is expressed as a percentage of the total distance, the south cliff being 0% and the north cliff 100%.

1.6.2.1 Soil/grass cover

The percentage soil/grass cover and the percentage bare rock in one area always add up to 100%. Figure 1.17 shows that the surface on top of the plateau is not covered by much soil and even where soil present it is not very thick. There is a definite decrease in soil cover (or increase in bare rock surface) from the east end of the island towards the west end (Fig. 1.18), especially on the northern half of the island. Close to cliff edges the percentage of bare rock also seems to be somewhat higher. Both these reductions in soil/grass cover may be due to the reduced water availability. On the north side this may be due to the prevailing wind direction and along the cliff edges due to the increased hydraulic gradient and probably the existence of more jointing owing to the fact that the cliff has lost support on one of its sides and will tend to fall that way. This will not have as much influence on the higher vegetation with its very extensive, deep roots

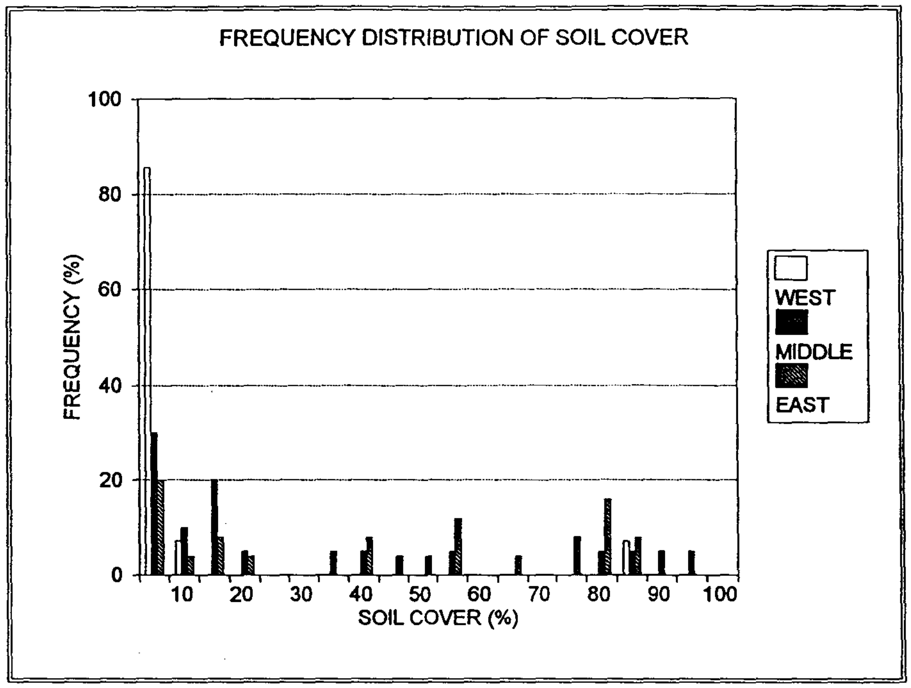

Fig. 1.17. Frequency distribution of soil cover.

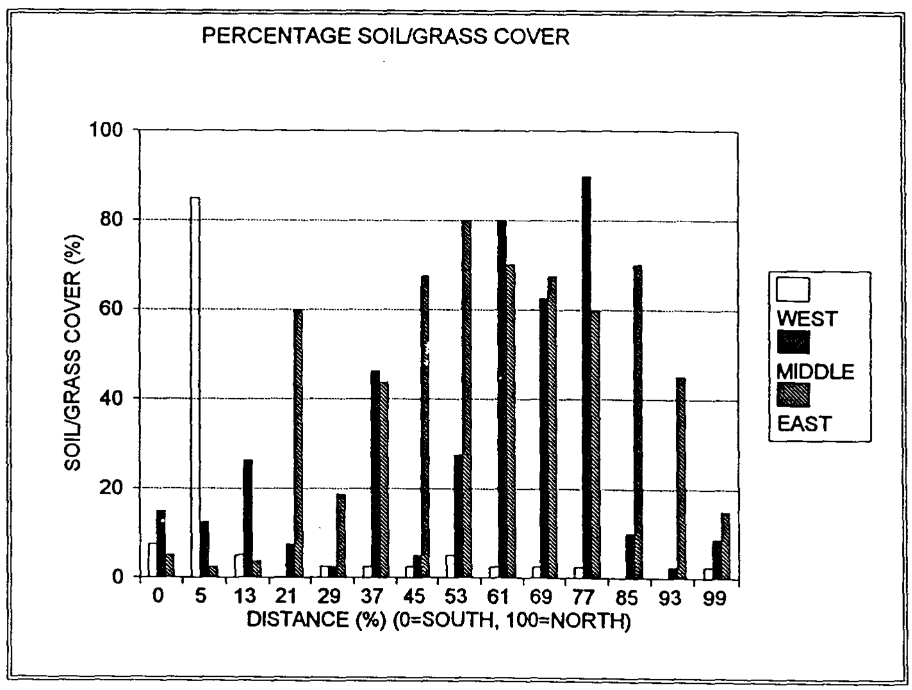

Fig. 1.18. Percentage soil/grass cover.

but could be a serious hindrance for the lower vegetation.

1.6.2.2 Sinkpoints

In this study, a sinkpoint is defined as any depression caused by dissolution where water can infiltrate relatively quickly into the bedrock (note that a crack is not considered a sinkpoint). This very general definition includes many different types of dissolutional forms and was adopted because the purpose was to estimate the number of points of water infiltration on the surface and not to make a detailed study of the morphology of the surface karst. The size of individual sinkpoints varied from a few centimetres to 1.5 m in diameter and their depth from a few centimetres to a few meters. At certain places two or more smaller sinkpoints may have developed into one bigger sinkpoint and they were therefore counted as one. The maximum, as well as the minimum, number of sinkpoints per area seems to be proportionally related to the percentage of bare rock (Fig. 1.19): there are hardly any sinkpoints under 30% bare rock and between 2 to 13 sinkpoints were counted where there is more than 95% bare rock.

In the west the percentage of bare rock is fairly constant as is the number of sinkpoints over the whole width of the island (except close to the south cliff where there might have been an occasional soil patch). In the centre the number of sinkpoints over the width of the island varies a little more but so does the percentage of bare rock and the two seem to be closely related. Finally the east end has a high percentage of bare rock in the southern half where most of the sinkpoints can be found as well. The

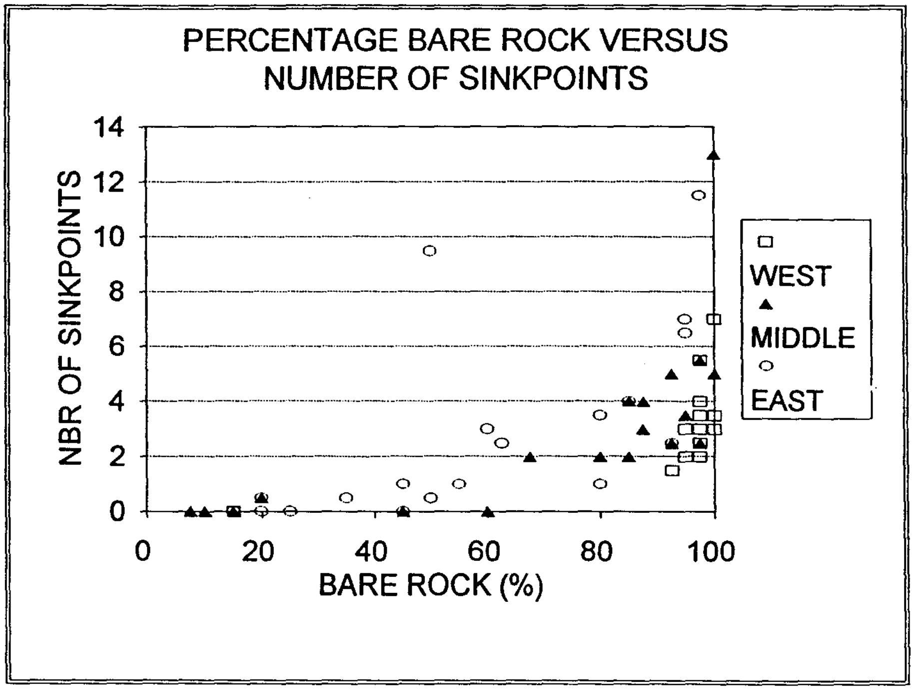

Fig. 1.19. Percentage bare rock and number of sinkpoints.

observed relationship between soil cover and number of sinkpoints is probably due to the fact that the soil fills the sinkpoints and thus the higher the percentage soil cover the greater the number of sinkpoints that could be hidden underneath the soil. Also the soil will be preferentially preserved in the depressions and thus if a piece of bare rock is present this will tend to stick out of the soil and there will be no sinkpoint development on it. The great difference in number of sinkpoints observed when the rock is very bare could be due to the size differences between sinkpoints. It is however clear that if the surface is more than 60 % bare rock sinkpoints are present.

If there are on average three sinkpoints per m^2 of bare rock (seven per 2.25 m^2) or 3×10^6 per km^2, and if this density is taken as an average for the whole plateau surface of 26 km^2 then there are approximately 8×10^7 sinkpoints. Taking into account the size differences of the sinkpoints this number clearly explains why there are no streams on the plateau. According to Stenson (1990) the doline densities of 3×10^5 to 4×10^5 dolines per km^2 he found in gypsum of Nova Scotia, Canada, were the highest densities ever recorded in the karst literature. However, he compared (Stenson, 1990, Fig. 4.7) doline densities in regions occupied by large dolines separated from each other by narrow ridges or towers with the small dolines in his study area. In many, if not all, of the tropical regions mentioned in his study the density recorded may well have been the maximum density of dolines possible in the region. Furthermore, in the tropical regions, smaller sinkpoints are most probably also present but they may not be considered as dolines by the authors in question. The density of sinkpoints calculated above exceeds the values noted by Stenson (1990) by an order of magnitude. Again the difference may probably be found in the different definitions of doline/sinkpoint and also the different areas (tropical versus temperate).

1.6.2.3 Vegetation.

The vegetation on the island was studied because its production of CO_2 might be fundamental to the degree of karst development. Different types of vegetation might have different influences on karst formation. The distinction between high and low vegetation was made by counting the number of plants over one meter tall, high vegetation being trees and bushes with roots that can penetrate very far into the rock in search of water. Therefore, they do not necessarily depend on the moisture retained at the surface in the soil or epikarst layer. Roots were observed in several caves, located a few meters below the surface.

Figure 1.20 shows an increase in number of high plants towards the west. However, the northern half of the eastern traverse passes through former and present pastures and the bush and higher vegetation has widely been cleared. In spite of this human intervention, the area occupied by bushes and trees is less in the east than in the west (Table 1.2). This could be explained by higher evaporation on the windward side of the island and does not seem to be related to the percentage soil cover (Fig. 1.21), which is in agreement with the proposition that these higher plants are not dependent on the soil layer for their water and nutrients.

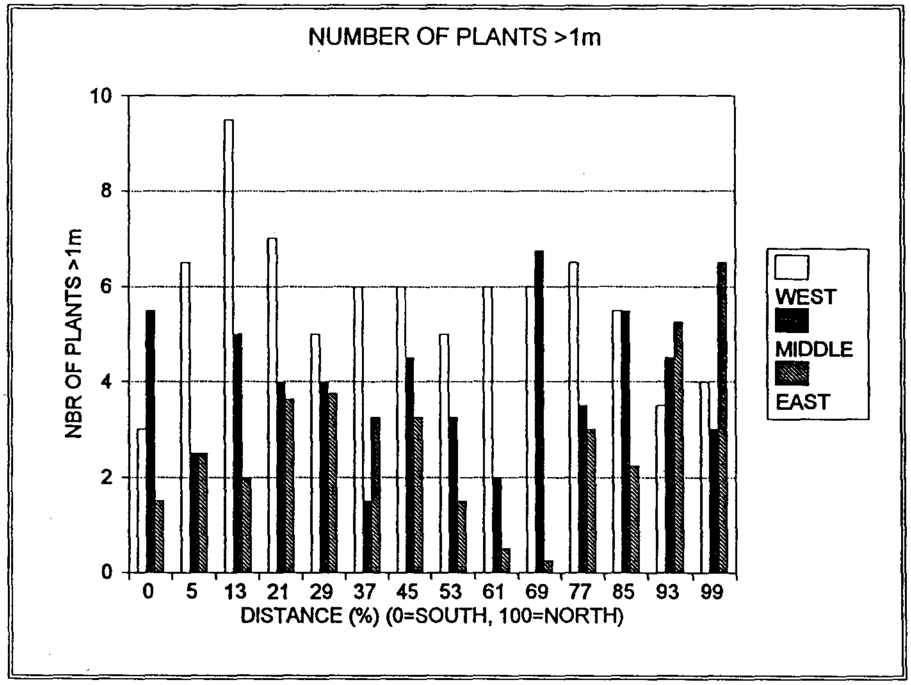

Fig. 1.20. Number of plants taller than one meter.

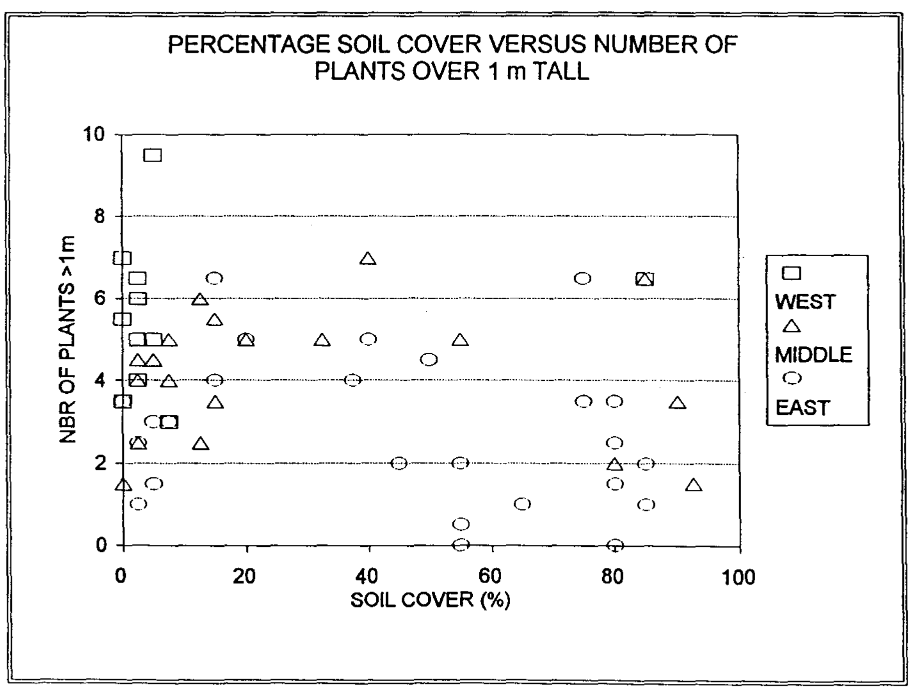

Fig. 1.21. Percentage soil cover and number of plants taller than one meter.

Table 1.2. Charateristics of surface features at three transects across the plateau.

DISTANCE	PHYTOKARST									PASTURE			BUSH			TREES			CACTI			LITTER		
	HIGHLY DEV.			DEVELOPED			POORLY DEV.																	
%	W	M	E	W	M	E	W	M	E	W	M	E	W	M	E	W	M	E	W	M	E	W	M	E
0			X	X	X									X										
5		X	X				X						X	X						X		X		
13		X	X	X									X							X			X	
21	X	X				X						X	X	X	X				X				X	
29	X	X	X										X		X			X			X		X	X
37	X	X				X					X			X	X	X		X	X				X	
45	X	X										X		X	X	X				X			X	
53		X		X								X	X	X		X							X	
61	X										X	X	X									X		
69	X	X										X	X	X								X	X	
77	X					X						X	X	X	X						X		X	
85	X	X										X	X	X	X		X		X				X	
93	X	X				X							X	X	X		X		X	X	X			X
99	X	X				X							X	X	X		X						X	

* SOUTH SIDE IS 0% AND THE NORTH SIDE IS 100%
X = PRESENT
W = WEST, M = MIDDLE, E = EAST

1.6.2.4 Terra Rossa.

Terra rossa (Latin for red earth) is a bright red coloured soil that is found on carbonate rocks in sub-tropical climates. It is the clayey residual deposit (Whitten and Brooks, 1972) of carbonates dissolution and the red colour is due to the presence of iron in the form of Fe_2O_3 and FeOOH from the parent material or from further weathering of liberated Fe silicates (Schroeder, 1984).

On Cayman Brac terra rossa is found in two distinct forms: as an unconsolidated sediment and as a well indurated hard rock. The lithified terra rossa probably represents a paleosol for it is far more widespread and the combination of the two forms is only observed at two points along the northeast side of the island. The unconsolidated form might be the residue of the dissolution of the calcareous cement of the lithified form, or the residue of bedrock dissolution, or both.

To compare the different traverses a relative scale has been made up: 0 = no terra rossa in any form, 1 = sedimentary terra rossa, 2 = both the sedimentary and the lithified form are present, 3 = lithified terra rossa is rare but present and 4 = lithified terra rossa is very common (Fig. 1.22). Terra rossa occurs randomly on the island and that it is found at 2/3 of the stations. Figure 1.23 shows that where soil cover is less than 50% there is no sedimentary terra rossa and that terra rossa is not necessarily present at all places where there is (almost) no soil (especially not along the central traverse).

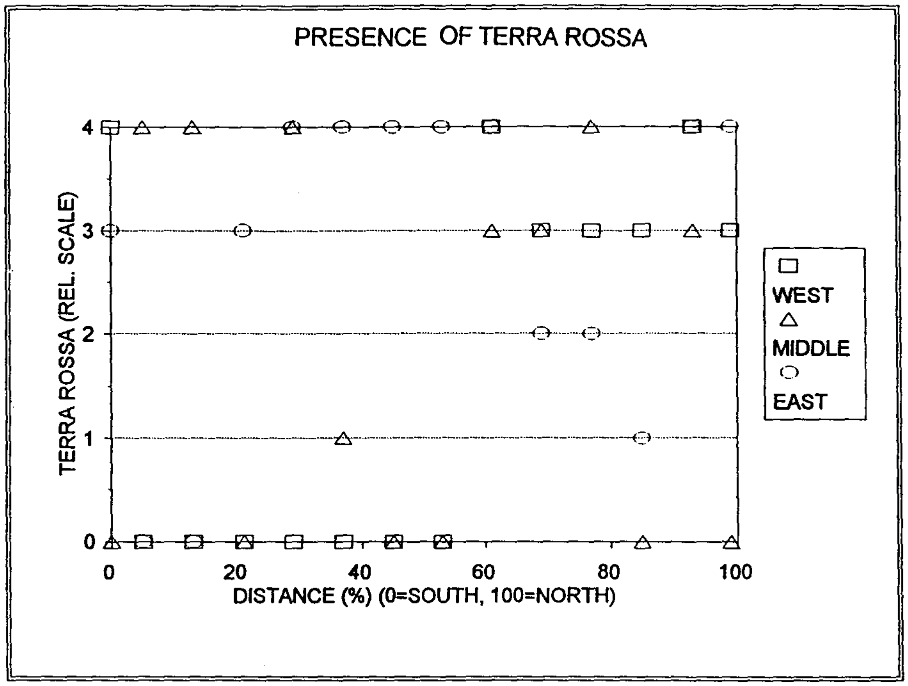

Fig. 1.22. Presence of Terra Rossa.

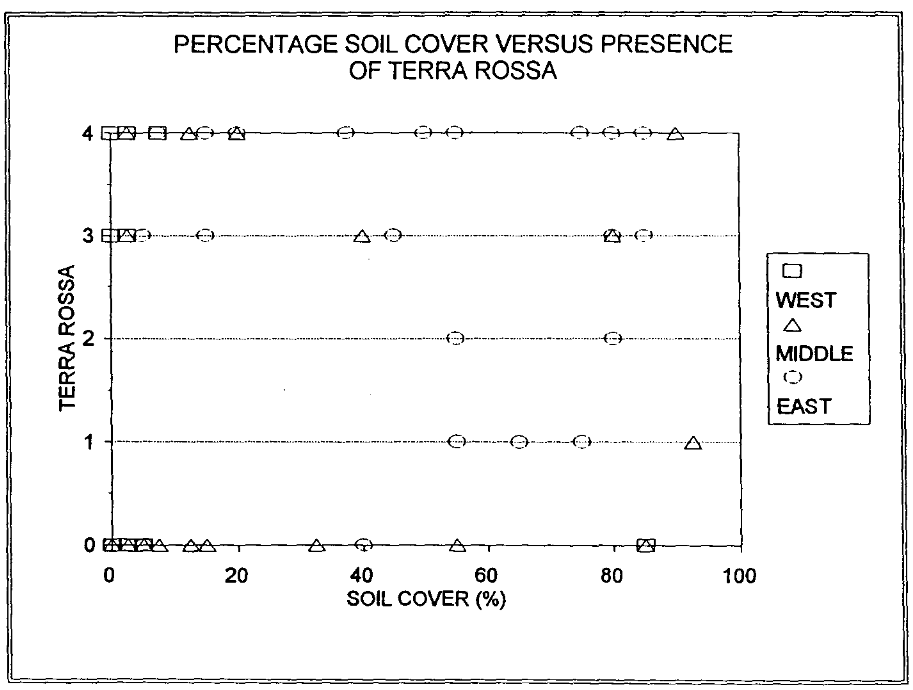

Fig. 1.23. Percentage soil cover and the presence of Terra Rossa.

1.7 Previous work.

The origin of dissolution caves has long since interested geologists and geographers in Europe and North America. However, early theories concerned with this subject were biased towards the regional setting in which the author lived. Hence, Europeans were mainly concerned with vertical shafts and underground rivers and the Americans with dry horizontal cave systems. After the Second World War scientists focused their attention more on fluid mechanics and the chemistry of carbonate rocks than on the geomorphology. For instance, Thrailkill (1968) studied groundwater chemistry and hydrology, while Ford and Ewers (in Ford and Williams, 1989) examined the potential pressure field existing between the input and the output. Dreybrodt (1988) looked at kinetic solutions and Worthington (1991) provided empirical results for a conduit development model. More detailed reviews on speleogenesis are given in e.g. Ford and Williams (1989), White (1988), Jennings (1985) and Watson and White (1985).

1.7.1 Island hydrology and cave development.

Mylroie and Carew (1990) recognised that the models mentioned above do not explain satisfactorily the origin of caves on small oceanic islands. Hence, they proposed a "flank margin model", based on data collected in the Bahamas (small carbonate islands), a region of tectonic stability and slow subsidence.

At this point an overview of the hydrology of small carbonate oceanic islands is in order.

1.7.1.1 Island Hydrology.

On most, especially small, oceanic islands formed of young carbonates runoff is insignificant and there are no streams. Hence, all the rainwater falling on these islands (less evaporation loss) will infiltrate in the ground and form a freshwater lens that floats on top of the heavier saline water. Radial movement of the water towards the sea, (hypersaline) lakes or low lying swampy areas sustain the lens. The shape and thickness of the lens is given approximately by the Badon Ghyben (1889)-Herzberg (1901) relationship expressed as

$$zg\rho_s = (z + h)g\rho_f \tag{1}$$

or

$$z = \frac{\rho_f}{\rho_s - \rho_f} h \tag{2}$$

where z is the depth of the interface below mean sea level, h is the freshwater head above mean sea level, g is the gravity constant, ρ_f is the freshwater density (1.000 kg m^{-3}) and ρ_s is the saline water density (1.025 kg m^{-3}). This principle assumes that the interface between the fresh and saline water is a sharp boundary that is under static conditions. Hence, the interface will be depressed 40 m for each meter of freshwater head above the mean sea level. However, such static conditions do not exist in reality and therefore later adaptations to this general model have been made by Muskat (1937), Hubbert (1940), Glover (1959), Cooper (1959; and verified by field experiments by Kohout (1960)) and Henry (1964). These authors recognised that the interface is more a zone of transition than a sharp boundary and that it does not intersect the water table at the shoreline. The main significance of Henry's work was that it attempted to quantitatively account for hydrodynamic dispersion (or mixing) in that it advanced an advection-dispersion equation for miscible fluids.

Since 1965 many papers concerning freshwater lenses have been published and they can roughly be divided according to focus into five topics (Reilly and Goodman, 1985, p. 139):

1. applications using two-dimensional cross-section analysis where the vertical gradients play an important role in establishing the relationship between the two fluids;
2. applications using two-dimensional areal analysis. Caution is needed with this approach because it does not consider density effects which are indispensable in determining the exact equilibrium positions of the two fluids;
3. applications using three-dimensional analysis;
4. upconing applications using cylindrical coordinate systems;
5. comments on advances in numerical methods and field studies.

Reilly and Goodman (1985) give an extensive review of the work that has been done in freshwater lens analysis.

1.7.1.2 The freshwater lens.

The shape and extent of a freshwater lens depends on five main factors: 1. precipitation; 2. porosity and permeability of the bedrock; 3. the shape and 4. the topography of the island; 5. sea level fluctuations due to e.g. tides, atmospheric pressure and salinity of the sea water.

Precipitation is the only source of freshwater on a small oceanic island and thus the amount of precipitation determines the amount of freshwater that will contribute to the formation of the freshwater lens. However, water loss by evapotranspiration may be very important and, in the Bahamas, it is estimated to be more than 75 % of the annual precipitation (Tarbox, 1986). Runoff is only significant in areas rendered impervious by development. According to Henry (1964) the depth of the interface below mean sea level is proportional to the square root of the rate of uniform vertical recharge per unit area (Fig. 1.24).

The *permeability* of the aquifer is inversely proportional to the depth of the interface because the higher the permeability the easier the water moves through the rock and thus the shorter will be the residence time of the water in the freshwater lens and the faster the discharge of the water at the shore. In highly permeable aquifers the freshwater tends to form a thin layer atop of the saline water or tends to mix with the saline water to form a brackish layer. On the other hand, in aquifers of low permeability a thick, stable lens with a thin mixing zone will more likely develop. Secondary porosity in the

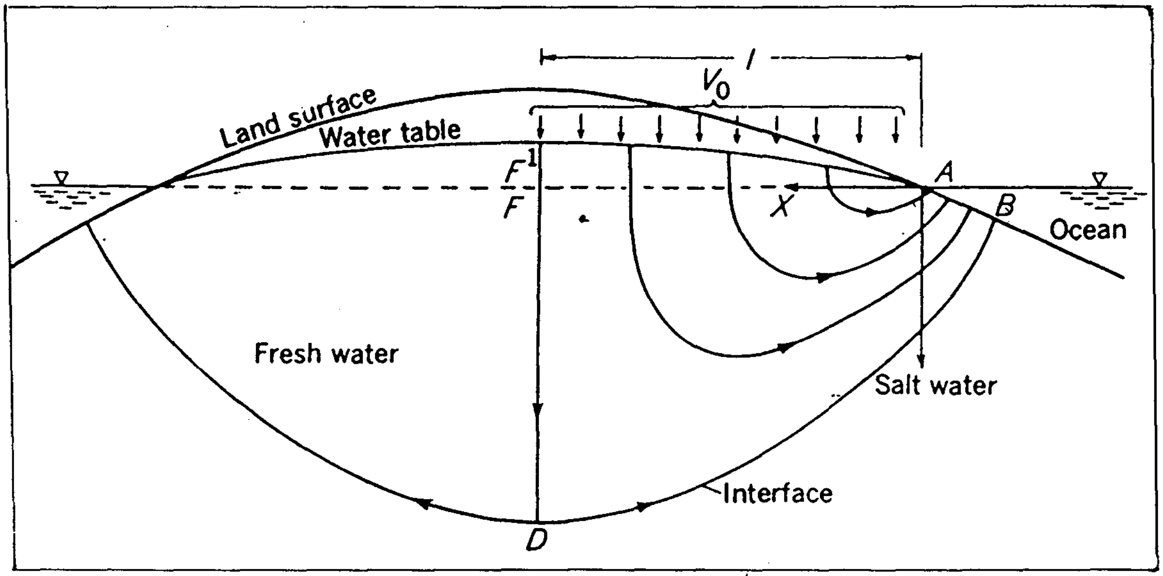

Fig. 1.24. Schematic sketch of the flow pattern beneath an oceanic island receiving uniform discharge (not to scale - Henry, 1964, Fig. 32 A).

V_o = uniform discharge
l = half width of the island
AB = outflow seepage face
BD = interface separating the static salt water from the flowing fresh water.
DF' = line of symmetry
F'A = water table at which V_o enters the zone of saturation

form of joints, fissures, solution conduits and caverns provides direct hydraulic connection between the aquifer and the ocean, defines the shape and extent of the lens, allows for rapid recharge of rainwater into the aquifer, increases mixing possibilities of water from different hydrochemical zones and facilitates mixing dissolution (Ng *et al.*, 1992).

The *size* and *shape* of the island determines the direction and extent of the freshwater lens. If the island is long and narrow, for example, then the lens should be long and narrow too. However, it could happen that the island is so narrow that the formation of a freshwater lens is impossible because the freshwater will mix with the saline water as a result of tidal movements or low precipitation rates. On the other hand, on large islands thick freshwater lenses with thin mixing zones may exist in bedrock of high permeability (Tarbox, 1986). Although Cayman Brac is elongated, it might be that the width, especially in the east, is large enough to support a distinct, though thin, fresh water lens. Depending on the other factors involved, it might also be that there are several small lenses of varying thickness.

The *topography* of the island plays an important role as well in that the thickest lenses are often found underneath the highest parts of an island. The higher the surface the further will be the distance between the surface and the water table. More water will be able to percolate to the water table due to less water loss by evapotranspiration in the surface layer. Also the longer the flow path, the longer water will take to reach the water table and the more continuous will be the recharge of the freshwater lens. Because the water table will be relatively stable under these conditions there will be reduced movement of the interface too, and therefore less mixing between the fresh and saline water (*op. cit*). If there are low lying areas or (hypersaline) lakes, the freshwater will discharge into these swamps or lakes and the extent of the lens will thus be reduced.

Sea level fluctuations occur as a result of tides, atmospheric pressure or temperature and salinity of the sea water (Vacher, 1978). Because the aquifers are hydraulically linked to the sea, these fluctuations must occur also in the water table. However, the amplitude of the fluctuations will decrease inland as a function of the period of oscillation and the permeability of the bedrock. The longer the period of oscillation and the more permeable the bedrock is, the further a wave can penetrate inland (*op. cit*). Sea level fluctuations due to changes in atmospheric pressure have longer periods of oscillation than tidal fluctuations and will thus be less dampened than the tidal fluctuations. Vacher (1978) noticed that on Bermuda the atmospheric pressure-induced sea level fluctuations play a more important role in the day-to-day fluctuations of the water table than do the tidal oscillations. He also emphasised that a drop in atmospheric pressure often heralds the arrival of rain and that the rise of the water table may mistakenly be interpreted as being the result of the infiltration of the rainwater. According to Wheatcraft and Buddemeier (1981) the fluctuations are in a vertical plane and not horizontal and they induce the mixing of the fresh and the saline water. The freshwater lenses on the atoll islands studied by the above authors were limited in size and extent and responded more quickly to withdrawal of the water as well as to recharge of freshwater in a vertical coupled system than in a horizontally controlled Badon Ghyben-Herzberg lens.

1.7.1.3 Halocline or mixing zone.

The interface between fresh and saline water is not a sharp boundary but a diffused zone. According to the Badon Ghyben-Herzberg principle, the interface lies, under static conditions, 40 m below mean sea level for each meter of the water table above mean sea level (a depth ratio of 1:40). Bugg and Lloyd (1976) found that the base of the freshwater lens as defined by the boundary of 500 ppm chloride on Grand Cayman is more accurately represented by a depth ratio of 1:20 and that the base of the halocline is at a depth ratio of 1:50. The measured centre of the halocline was found at a depth ratio of 1:40, which is thus similar to the ratio under static conditions. Numerous studies (Mather, 1975; Bugg and Lloyd, 1976; Wheatcraft and Buddemeier, 1981; Tarbox, 1986; Budd and Vacher, 1991; Ng *et al.*, 1992) have tried to determine the thickness of the freshwater lens, the position of the halocline and/or the sustainable yield of the lens[1] and the pumping rates for the wells because every change in the seaward discharge will modify the position and thickness of the halocline. When the seaward discharge is completely cut off the freshwater lens will be replaced by the halocline.

---

[1] Sustainable yield is "the total volume of potable groundwater that the lens is capable of providing over an indefinite period without fear of contamination of the underlying saline groundwater" (Mather, 1975, p. 142)

The process of mixing of waters with different chemical compositions or concentrations is of the greatest importance for the dissolution of carbonate rocks. Bögli (1964 *in* Bögli, 1980) introduced the idea that if two saturated waters equilibrated to different partial CO_2 pressures mix, the resulting water may be undersaturated with respect to calcite due to the non-linear relationship between CO_2 concentration and calcite solubility. He called this process mischungskorrosion (mixing corrosion). Runnels (1969) applied this idea to non-linear relationships between calcite solubility and other chemical variables (such as salinity, pressure, pH, content of dissolved organics, temperature and ionic strength). Plummer (1975) and Wigley and Plummer (1976) developed computer models which allow the prediction of geochemical environments favourable for calcite dissolution or precipitation as a result of the mixing of natural waters. While Plummer (1975) only considered a closed system scenario, Wigley and Plummer (1976) discussed the mixing in a closed and open system.

Back *et al.* (1986) combined the use of a computerized geochemical model (PHREEQE) with water samples taken in the field. They calculated the saturation index (SI) of aragonite as a result of the simple mixing of the two end-member waters (the fresh ground water in the region and the Caribbean sea water) in a closed system and then plotted the position of the SI of aragonite of water samples of the fresh, brackish and saline water inside a cave. From the difference in the calculated SI and the obtained SI the influence of other variables may be determined.

Observations made by divers in blue holes and submerged caves have clearly demonstrated the existence of a halocline (Smart, 1984; Palmer *et al.*, 1986). Water chemistry studies of blue holes on Andros Island, Bahamas, by Smart *et al.* (1988) show a clear association between waters undersaturated with respect to calcite and the halocline. Divers also revealed the existence of a sulphurous zone within or underneath the halocline due to the very limited diffusion of oxygen through the halocline (Smart, 1984; Palmer *et al.*, 1986). The sulfate reducing bacteria living in this zone form dense bacterial plates in narrow zones strictly defined by the optimal living conditions (Smart, 1984). Bacteria are not only present in the water but also on walls where they form bacterial mats beneath which the limestone is extremely weak and friable (*op. cit*). Smart *et al.* (1988) found in the lower 2-3 m of the halocline of Evelyn Green's Blue Hole precipitation of FeS_2 as a black crust on the rock wall. They concluded that calcite and aragonite undersaturation may be due to changes in P_{CO2}: maximum values are found in the upper part of the halocline and decrease with depth resulting from a decrease in aerobic bacterial production of CO_2. The presence of bacteria in the water and their production of acids may play a very important role in the dissolution of carbonate rocks in the mixing zone. Because of their very small size and the fact that they can live in the dark under anaerobic conditions, they might be more wide spread than was originally believed (Wicks, personal communications 1993).

1.7.1.4 Models for dissolution cave development on small oceanic islands.

The mixing of saturated waters with different chemistries may occur at or close to the water table where infiltration water reaches laterally flowing or static groundwater and at the halocline where the freshwater mixes with the underlying saline water. Therefore it is at these zones that the dissolution of carbonate rocks is expected to be concentrated. At the point of discharge (usually along the coast) the water table meets the halocline and there will thus be a mixing of three different waters which might be even more favourable for the dissolution of carbonate rocks. The flank margin model for dissolution cave development (Mylroie and Carew, 1990) is based on this last assumption. Also along the coast the mixing zone will be wider as a result of the greater influence of sea level fluctuations due to e.g. tides.

The flank margin model was developed based on observations made in caves on the Bahamas islands, especially on San Salvador Island. The islands lie in a tectonically stable region that is subsiding at a rate of 2-3 m/100 ka (McNeill *et al.*, 1988). The islands consist of Pleistocene eolian (dune) ridges of up to 60 m high surrounded by low-lying areas. The caves that are nowadays situated about 6 m above mean sea level were formed when sea level was higher than at present. During these sea level high stands only the ridges stood above the sea and the freshwater lenses in these ridges were of very limited extent and thickness. Therefore it is believed that the formation of the caves took place during a maximum time span of 25,000 year (the estimated time that sea level was higher than at present during the past 150,000 years, the age of the rocks in which the caves are found) in small freshwater lenses as a result of mixing of the freshwater and the saline water, especially at the point of discharge of the brackish water along the coast under the margin of the ridges. Due to inhomogeneities in the bedrock, the flow of the fresh/brackish water is concentrated along preferential flow paths. Discharge will thus be at certain points and not along the entire length of the coast, which enhances the formation of dissolution pockets separated from each other by areas where discharge does not take place. Enlargement of the initial dissolution pockets form bigger chambers that are filled with brackish water and that develop headward because the saline water will be able to penetrate further inland due to the presence of the chambers and enlarged joints. Dissolution of the carbonate rock along the flow paths leading towards the chambers result in the formation of radiating passages leading towards the interior where they end abruptly or pinch out. The chambers are round or oval, oriented parallel to the trend of the ridges. In the caves thin wall-partitions and isolated bedrock pillars are often found. After drainage of the caves due to the fall of the sea level, speleothems may develop. Surface erosion caused the retreat of the margin of the ridges and in many cases the opening of the caves. If the sea level rises again water will occupy the caves again and cave development will continue. Dissolution of the speleothems formed during the dry period may also take place (Mylroie and Carew, 1990).

Ollier (1975) described six types of caves on the Trobriand Islands, a group of five small coral islands 200 km off the northeast coast of Papua:

1. *straight caves*: their linear plan view indicates presumably preferential erosion along joints. Although Ollier describes them as being stream

passages or having evidence that they were stream passages in the past, this is not evident from the descriptions he gives of some of these caves. The water in them does not seem to flow like a stream, but it is stagnant in the form of a lake.

2. *collapsed tunnels* are short and wide tunnels that have been modified by collapse. They are often perpendicular to the shoreline but never reach it. All described tunnels have water.
3. *cenotes* are collapse dolines with water at the bottom.
4. *phreatic caves*. The most typical examples are the ones that "consist of large chambers connected by narrow passages" (p. 178). They have large (up to one meter in diameter) symmetrical scallops and well developed phreatic spongework in the walls and bellholes in the roof.
5. *sea caves* are small and are often mere notches cut into the cliff faces. Phreatic caves that have been interrupted and modified by wave action are also considered as sea caves.
6. *other caves*. Under this category Ollier places all the caves that have been modified by collapse in such a way that their original form is no longer recognisable.

Although Ollier never mentioned the word mixing corrosion, the concept is implied in his writing: "There is no reason why brackish water should not attack limestone to form caves as long as there is some mechanism for occasionally changing the local physicochemical conditions. The changes in salinity after rain would probably be sufficient to do this" (p. 185). He further divided the caves into three groups: vadose, water table and phreatic caves (Fig. 1.25). As to the location of the phreatic caves Ollier wrote (p. 189) "Cave formation is most likely to occur where the flow lines converge, and this situation - behind the shoreline and below the level of the cliffs - is precisely where the largest phreatic caves are found". Ollier never proposed a cave formation mechanism other than the existing ones based on continental settings but he did discuss why these theories did not completely apply to coral island speleogenesis.

At present, the flank margin model appears to be the most comprehensive model that has been advanced. However, it is qualitative, i.e. it gives an explanation for the location and morphology of the caves together with a plausible dissolution mechanism, but it makes no quantitative predictions concerning the rate of dissolution, of formation of the initial pockets and of the extension inland, nor does it say if and how the presence of the caves influences the extent and shape of the fresh water lens and/or of the mixing zone.

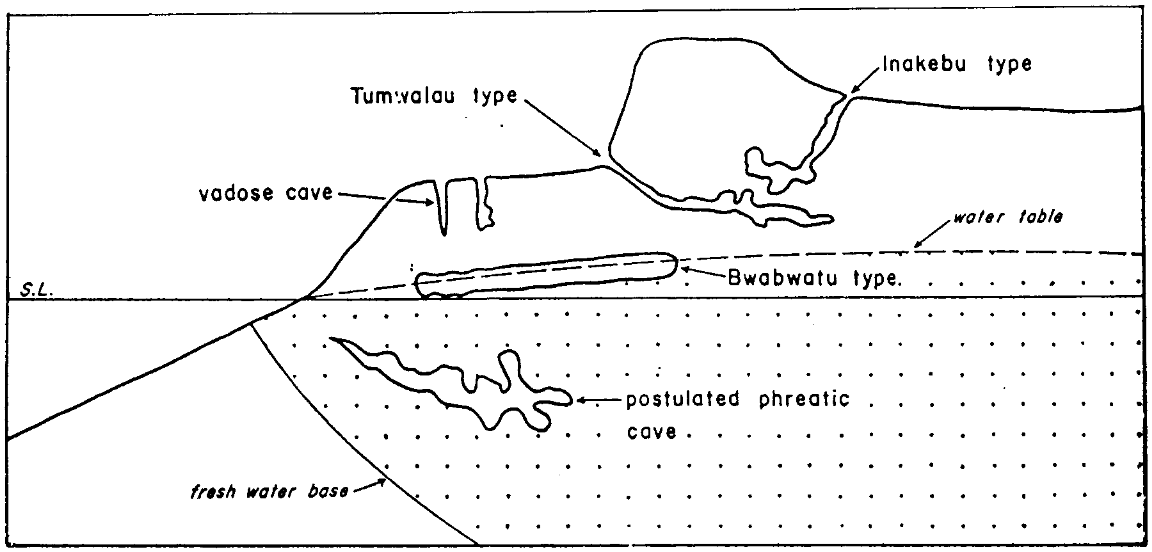

Fig. 1.25. Relationship of type caves to topography and hydrological zones (Ollier, 1975, Fig. 17).

CHAPTER TWO

CAVES

2.1 Introduction

In this study a cave is defined as a natural underground space which is large enough for human entry. This is a anthropocentric definition and is not based on the natural processes responsible for the cavity (Ford and Williams, 1989).

Cave openings are visible over the entire length of the cliff at different elevations above the notch. Although the dense vegetation on the plateau may hide cave openings from view, it is believed that there are not many caves here. The openings encountered during the traverses were very small and only one cave could be entered. On the coastal platform formed by the Ironshore Formation, no caves were found. However, under water caves exist according to reports from some divers (personal communications).

The caves described in this study are some of the largest found on the island. Their length varies from about 5 m to 450 m and they are situated between 1 and 23 m above the notch, which is itself approximately 6.4 m above present sea level (Woodroffe *et al.*, 1983). The caves have been separated into two groups, the notch caves which have their entrance one to two meter above the notch and the higher caves, having their entrance more than two meter above the notch. In total there are at least 75 caves of enterable size on Cayman Brac according to a treasure hunter who has visited them all (personal communications).

There are more openings visible in the south cliff than in the north cliff due to the absence of private property in front of the cliff, the nearness of the road to the cliff and the more open vegetation. At some places the openings are concentrated at certain elevations but due to the dense vegetation and the westward dip of the cliff it is very difficult to follow these elevations over longer distances or to be sure that elevations at different sites are similar. The unconformity separating the Brac and the Cayman formations, appears to form a constraint to the vertical development of those caves formed below it (Photo 2.1).

2.2 The description of the caves

2.2.1 Notch caves

2.2.1.1 Rebecca's Cave (Figs. 1.2 and 2.1).

Rebecca's Cave is the most westerly cave on the south side. It is located at the end of a long gravel road just east of Salt Water Pond in the partly dolomitised limestone of the Pedro Castle Formation. The cliff here is at its lowest point and it is actually more like a step at the base of a more gradual slope. The entrance consists of a 3 m long and 1 m wide passage; the first 2 m are straight and unroofed and the last part turns to the NE and has more rounded forms. A large chamber follows, with one

Photo 2.1 The Pollard Bay Caves in the Brac Formation are limited in their vertical extent by the unconformity separation the Brac and the Cayman formations

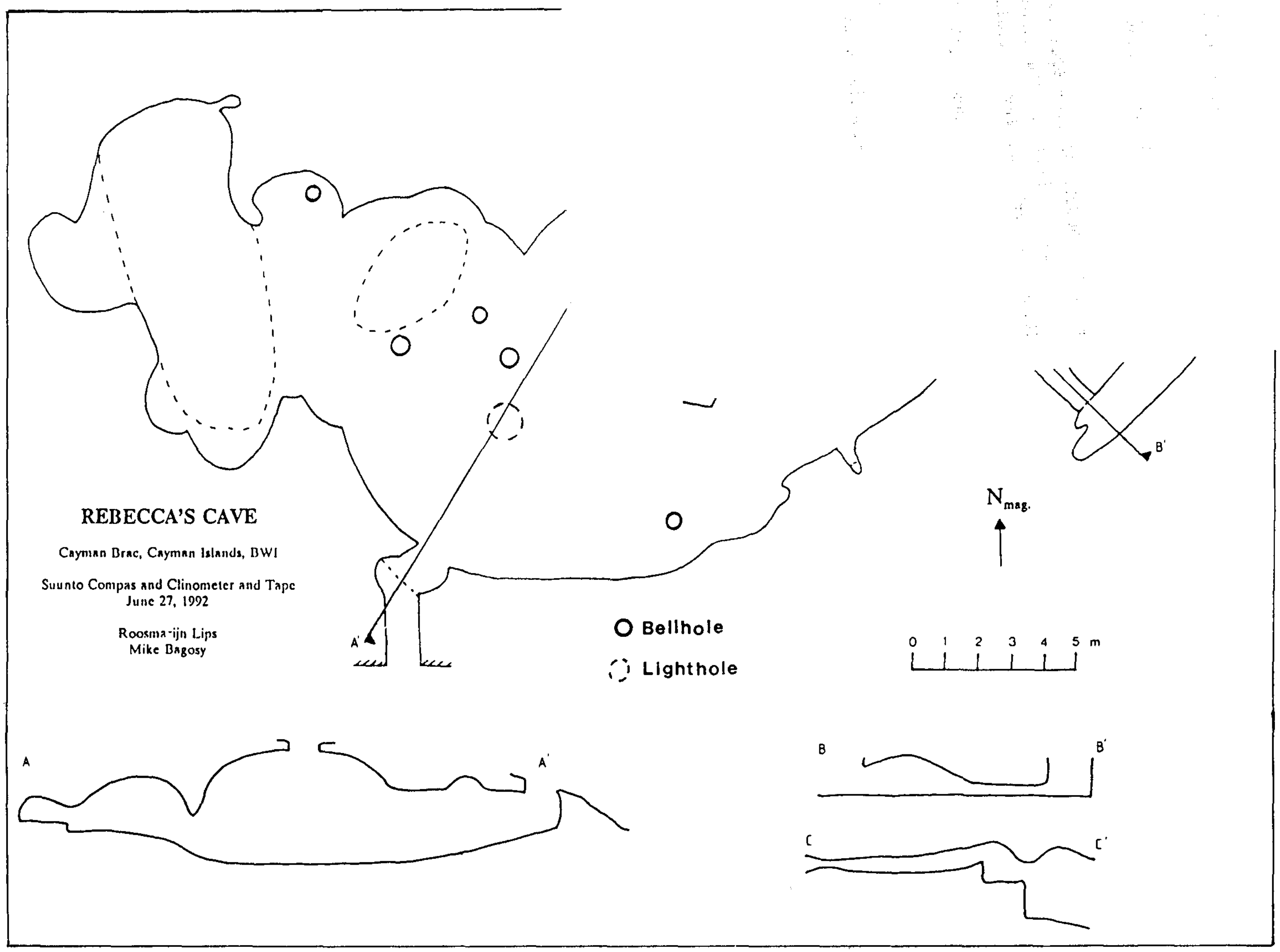

Fig. 2.1. Rebecca's Cave.

accessible side passage, directed NE, at the east end (Fig. 2.1). Some passages that are too tight to go through, go off to the NE and NW. At two third of the way a small side passage leads to an unroofed passage of 7 m long (Fig. 2.1). Three meter to the NE in the prolongation of this latter passage is a small cave consisting of one big room in which speleothems are present. Speleothems are also visible in the walls and ceilings of the northern half of the side passages.

The big chamber is elongated along an E-W axis and is 13 m at its maximum wide, 18 m long and 3 m high. The first thing that catches the eye is the small grave of the one year old Rebecca who was one of the victims of the 1932 hurricane. The eastern part of the chamber has only one small (1.2 m in diameter) skylight whereas the ceiling of the western end has completely collapsed. The middle part is the narrowest and the lowest section of the room. Here is a skylight of 3.5 m by 2.5 m which shows a rock thickness of 1.5 m between the ceiling and the surface. In the eastern wall, a section of the northern wall and some patches of the ceiling flowstone remains and other speleothems are visible. Between the skylight in the middle of the room and the one at the western end, some globular speleothems ("popcorn"; probably formed due to evaporation of the seepage water) and recent stalactites can be seen. The floor of the eastern section consists of sediment and in the western section of collapse blocks and a little bit of soil. The southern wall east of the entrance passage, displays a form of speleothem resembling weathered cauliflower and appears to have been formed underneath the sediment cover.

There are seven cylindrical holes of circular cross-section (bellholes) in this cave, six of which are in the big chamber. The circular skylight in the big chamber is most likely a bellhole which has been intercepted by the erosion at the surface. The diameter of the bellholes does not vary much (0.4 m to 0.6 m) and their depth is between about 0.4 m and 1.5 m.

On the surface north of the cave there are more pits and crevices. Unfortunately, the dense vegetation inhibits easy penetration.

2.2.1.2 Bats Cave (Figs. 1.2 and 2.2).

Bats Cave is situated on the south side of the island about 500 m east of Rebecca's Cave in the dolostone of the Cayman Formation. It has a very big entrance porch which can be seen from the road. Five entrances leave this porch, two leading to a small cave and the other three to a main cave. There are breakdown blocks and inactive stalactites in some parts of the porch and on the approach to it from the road. These give the impression that the cave was much bigger and that the entrance porch was once a large chamber off which the present main cave and the small side cave extended deeper into the cliff. All the entrances are situated between one and two meters above the notch which can be seen about every where. This may indicate that the cave predates the notch and that the cave has been opened up by the sea at the relative sea level high stand that cut the notch or during an earlier period of relative sea level high stand.

The plateau lies about six meters above the notch and thus about four to five

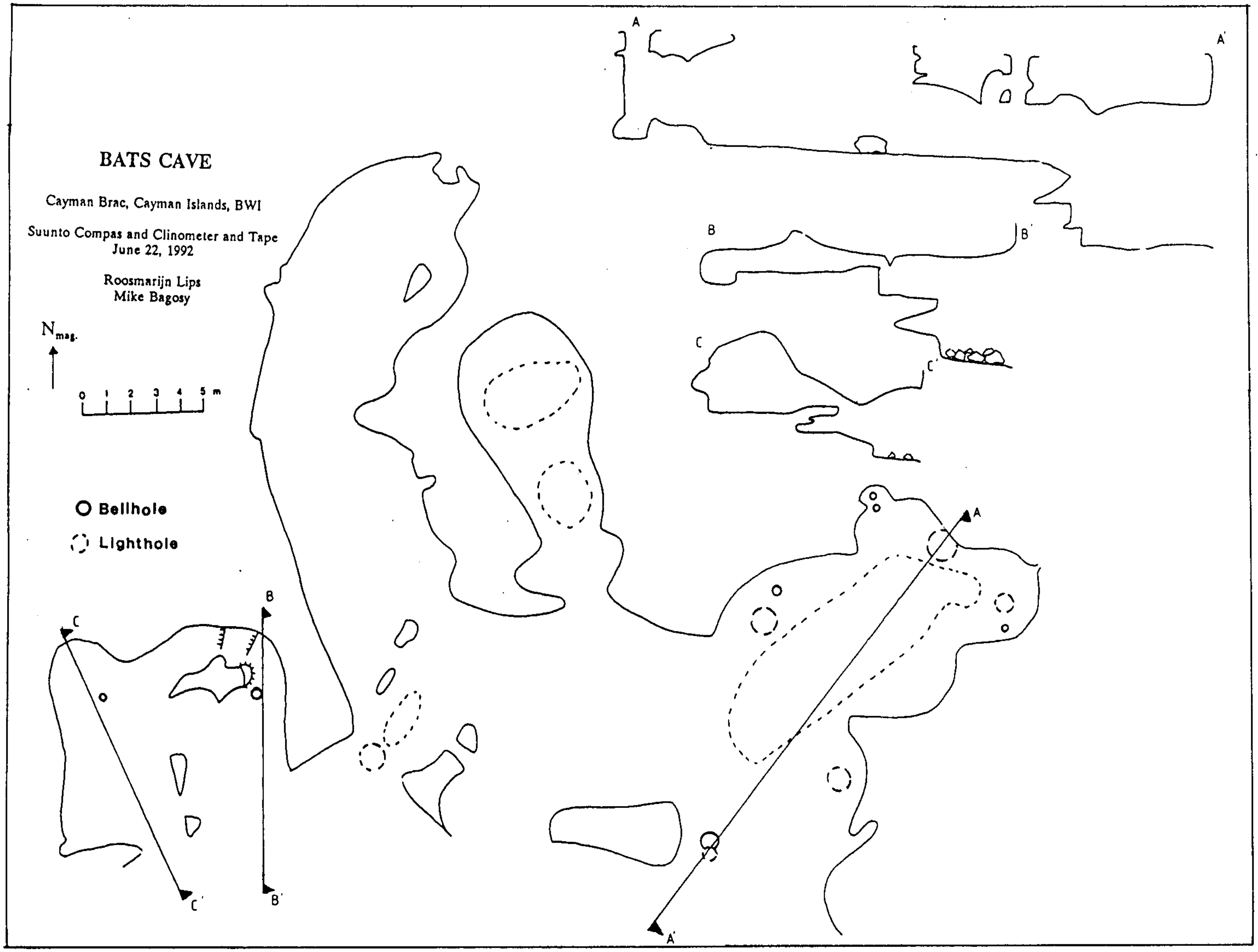

Fig. 2.2. Bats Cave.

meters above the cave floor. The thickness of the roof varies between one-and-a-half to two meters. There are seven bellholes and six round and four irregular shaped skylights (Fig. 2.2). The round skylights are believed to be bellholes intercepted by surface erosion while the irregular ones are due to ceiling collapse.

The small cave consists of a chamber, 9 m by 9 m, with a low (1 m) eastern half and a high (3.5 m) western part. A short passage leads around a bedrock block of 3.5 m long and 1.5 m wide in the north-east corner of the room. The floor in the eastern half consist of infilled rimstone pools whereas the floor on the western side is covered with sand-sized sediment. Inactive, partially dissolved dripstone is present only at the eastern entrance of the small cave. In contrast, the flowstone along the eastern wall appears to be actively growing. Breccia is found in the northern wall of this cave and on one spot old flowstone is also visible in this wall, just underneath a line of breccia.

The three entrances of the main part of Bats Cave lead to a large passage parallel to the cliff, from which three lesser passages lead further into the cliff. The western most passage, named Bats Passage (because a bat colony occupies the northern half of it), is the only one that still has a completely intact ceiling, without any bellholes. This passage first leads NNW and then NNE. It is about 5.5 m wide, 25 m long and 3 to 4 m high. The floor is covered with reddish sand-sized sediment. The passage is comparatively free of speleothems. Some old flowstone can be seen in both walls in the southern half and there is breccia in the northern wall. In the northern half of Bats Passage (the part occupied by the bats) there is a lot of the reddish crust formed on the

the main entrance there is a skylight, 0.6 m in diameter, connected to a bellhole with a diameter of 0.5 m. The wall and floor just east of the entrance are covered with inactive flowstone. The wall in between the entrances is full of different types of speleothem, in particular flowstone.

2.2.1.3 Great Cave (Figs. 1.2 and 2.3).

Great Cave is situated in the dolostone of the Brac Formation in the cliff at the south-east end of the island, where the road along the south side ends. Blocks fallen off the cliff face have formed a coarse talus that has to be scaled to enter the cave. Above the entrance the shift of a further big block is visible; more breakdown is imminent. From a room 13 m long, 11 m wide and 3.5 m high, two passages continue to the west (A and B), sub-parallel to each other and one passage to the east (C). A and B are connected by a passage (D) that lies 2.5 m above the floor and contains different types of speleothems (see 4.1 Types of speleothems). Below this passage there are a few small passages which appear to be a continuation of the entrance room.

Passage A goes due West and ends after 16 m with an opening too small to go through. It has three side passages, the first of which leads 5 m to the SSE and lies 2.5 m lower than A. The second side passage trends 2.5 m to the SE and the last one goes 1.7 m up into a small room, consisting of two lobes. The long axis of this room is sub-parallel to A. The eastern lobe is semi-circular with a diameter of 2.2 m and a height of 1 m. The western lobe is roughly square with a maximum width of 2.3 m and a height

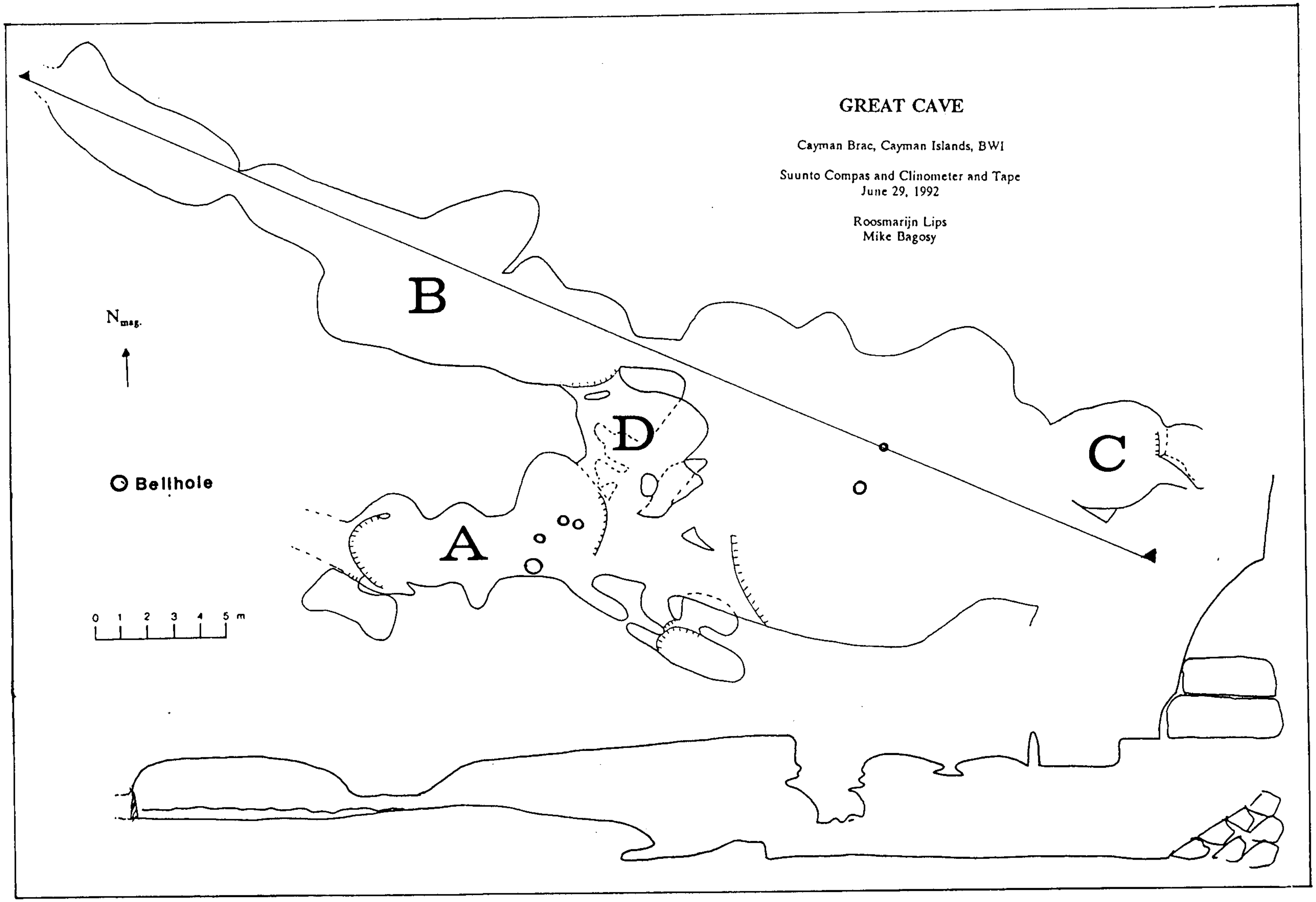

Fig. 2.3. Great Cave.

of 1 m as well.

Passage B leads approximately WNW and terminates, after 27 m, in an opening too small to go through. This passage has no side passages. The first 3 m are only about 1.5 m high while the next 12 m narrow down from a height of 4.5 m to a height of 1.5 m. A small opening leads into a 2 m high room containing a lake. The water is 0.1 to 0.4 m deep and reddish-brown in colour with a foul odour. Black sediment is present on the bottom of the lake. A reddish crust is present almost everywhere on the walls and ceiling. There are helictites, flowstone and remnants of partially dissolved speleothems. A rim 0.5 cm wide along the wall just under the water level suggests that the water level may have remained constant for some time.

The eastern passage is short and resembles a room with a diameter of about 4 m. At the end a small room is situated at 1.5 m above it. The southern side of C consists of big blocks that have been cemented together. These blocks are probably part of the cliff face breakdown.

One peculiarity of this cave is that in many places the bedrock seems to consist of a mixture of caymanite, calcite and original bedrock (Photo 2.2). This "mixture rock" is also found in the caves along the beach of Pollard Bay, east of Great Cave.

2.2.1.4 The caves along the beach of Pollard Bay (Figs. 1.2 and 2.4).

There are a string of short caves along the beach of Pollard Bay between Great Cave and at least the eastern end of the beach. In the west the caves are very close to each other, almost joined together, while towards the east they are spaced further from each other (a few meters). The caves appear to have been formed along three different levels, but not all these levels are present in each cave. The caves do not go further than 15 m inside the cliff. All the caves have similar characteristics: a wide entrance room with some pockets to the side; a low ceiling (approximately 1 m high) with a few parts where it is high enough to stand. There are no true bellholes but there are some irregular pockets in some ceilings. They have irregular walls and ceilings due to the presence of "mixture rock", porous bedrock (with lots of fossils), popcorn speleothems and algae on top of the speleothems, that are no longer growing but do not seem to be much dissolved either. There is also older speleothem (stalactites, stalagmites and mainly flowstone) in almost all of them. The floors are irregular and consist of sand-sized sediment lying on "old" gours, flowstone or bedrock. Often, a crust may be seen on the walls and ceilings.

The majority of the caves are situated below an unconformity which is visible in the cliff. The passages just underneath it all seem to terminate at this unconformity. As a result they often have flat roofs. The few caves that are above the unconformity are inaccessible. Hence, it was not possible to examine them in more detail.

The notch here is mainly hidden behind blocks fallen off the cliff face. Blocks are also present at the entrances of the caves. In the notch inactive speleothem columns

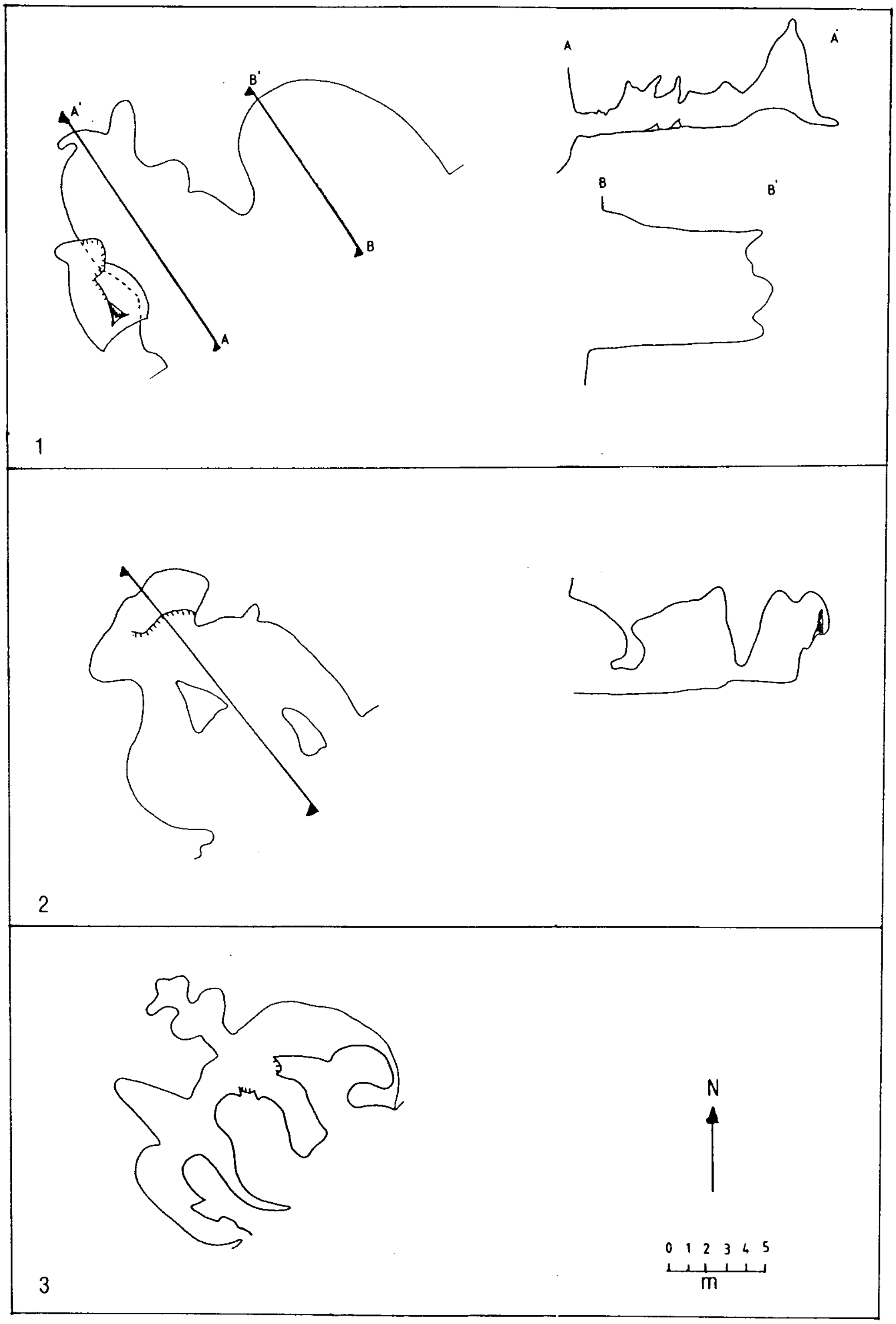

Fig. 2.4. Pollard Bay Caves.

with a diameter of approximately 0.2 m are present.

In the past, these caves might have been part of one big system or they might always have been separate as at present. The different levels could represent one or more formation stages, depending on the number and mode of sea level fluctuations responsible for their formation: a gradual change from high to low sea level (or vice versa) might have had the same result as a number of more abrupt fluctuations between high and low stages.

2.2.1.5 Hospital Cave (Figs. 1.2 and 2.5).

Hospital Cave is located on the north side of the island in the dolostone of the Cayman Formation, about 500 m east of the hospital. The cave floor is 1.1 m above the notch; wooden stairs lead to it. East of the main entrance and slightly higher are two smaller entrances and four meters west of it is a big joint going sub-perpendicular into the cliff.

The main entrance, 3.5 m wide and 3 m high, leads into a large chamber 4.5 m high, 10 m wide and 5 m long. Seventeen of the 21 bellholes in the cave occur in this entrance chamber, the others are at 1.5 m (three examples) and 9 m (one) further into the cave. Reddish crust and bats can be seen in many of them. The walls in this chamber are overgrown with algae and are pocked, thereby obscuring any remains of speleothem or other important features that might be present. Speleothems are rare except on the

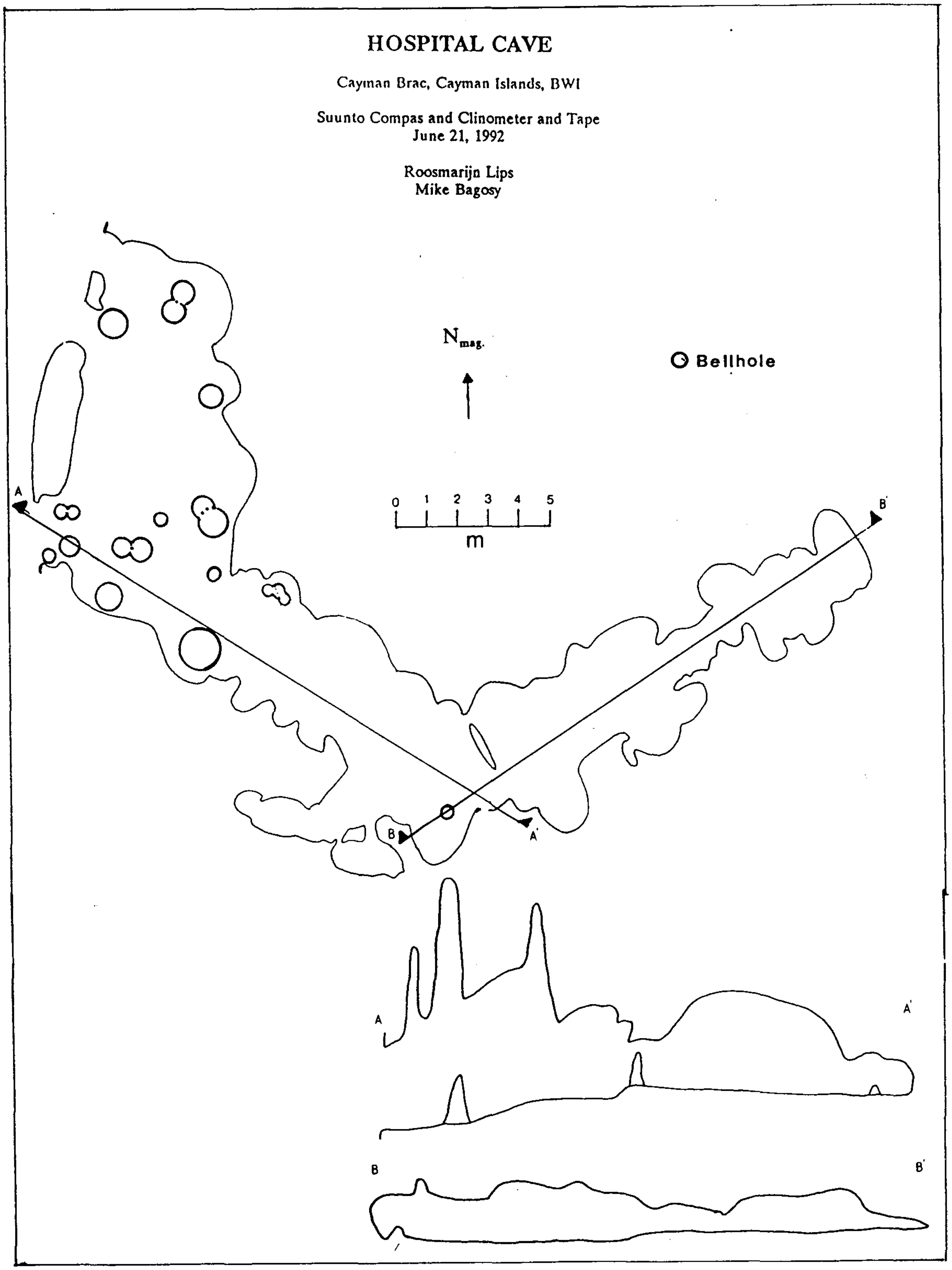

Fig. 2.5. Hospital Cave.

floor where a thin layer of flowstone exists which is broken up in some places and reveals bedrock or sandy sediment with pieces of rock in it.

The cave continues to the southeast through a 5 m wide and 2.5 m high opening in front of the main entrance. A step leads up into a short, low passage, in the middle of which stands a stalagmite 1 m high and 0.5 m in diameter which has been dissolved at many places. A smaller room follows, From this a short passage leads to the south and terminates in another passage aligned along a joint 300°E, which can be seen in the ceiling. The cave continues to the NE with a passage changing from 3 m wide and 1.5 m high to about 2 m wide with a maximum height of 1 m. At the end of the wider part there is an alcove in the east wall of 1 m deep and 3 m long with columns, stalagmites and gours.

All the walls and ceiling are rounded and often scallop-shaped. In many places remains of what appears to be flowstone and/or breccia are present. Except for the alcove there are not many speleothems, especially not actively growing ones.

2.2.1.6 Cross Island Road Cave (Figs. 1.2 and 2.6).

This cave is located in the cliff on the north side, just east of the road that leads across the middle of the island. It is developed in the dolostone of the Cayman Formation. There are three entrances, two smaller ones (one is 3.2 m by 1.2 m and the other 1.6 m in diameter) which are about 6.5 m above the notch and a main entrance (4 m by 2 m) whose floor has collapsed and is covered with junk (trash lumber, steel

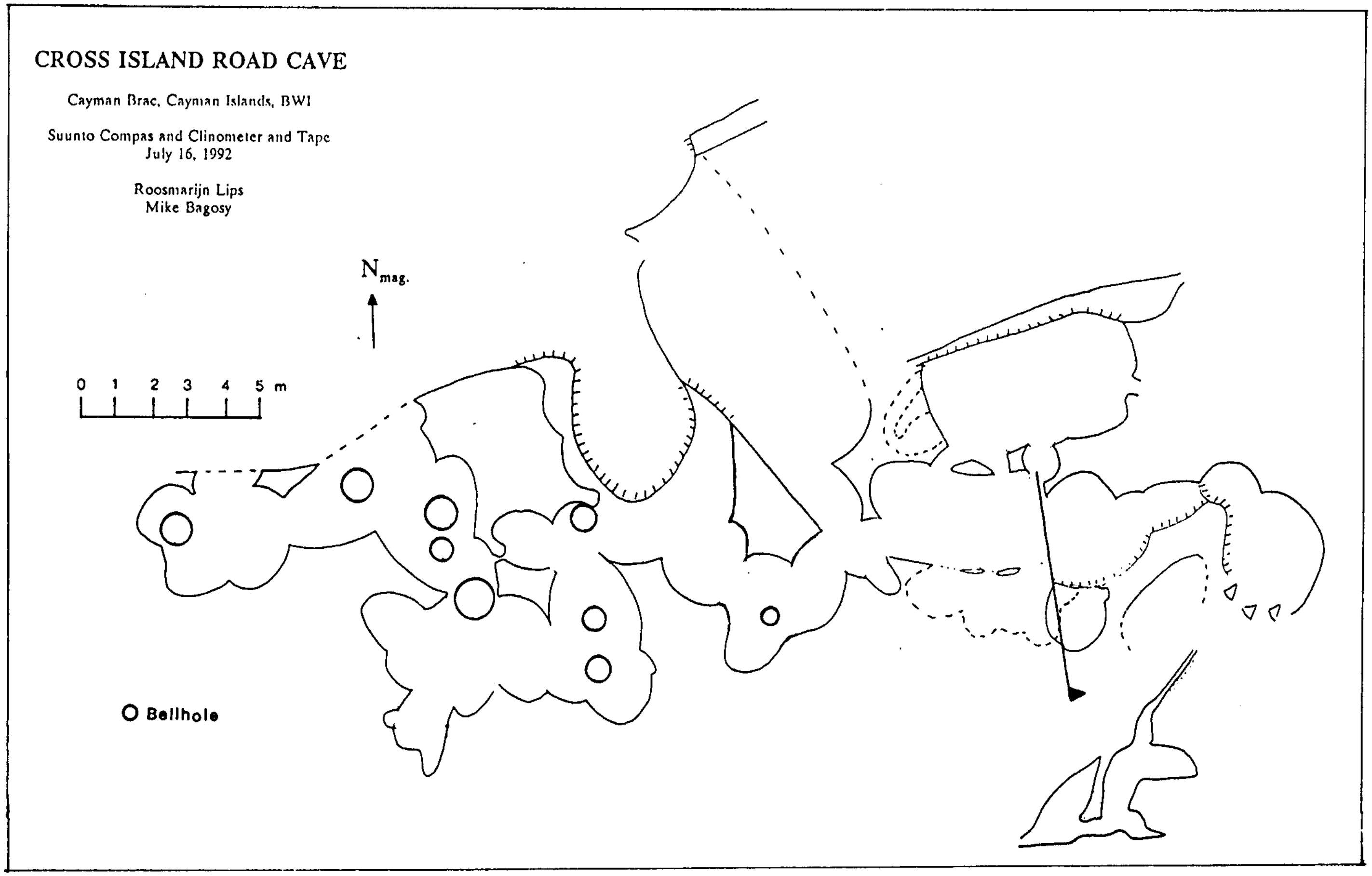

Fig. 2.6. Cross Island Road Cave.

cables, plastic, etc.) which makes it impossible to determine its former height above the notch.

A large joint (or perhaps a lithologic contact that has sprung open) bearing 135°E with a dip of 40°E goes straight into the cliff and plays an important role in the structure of the cave. All the entrances are located underneath the joint and the ceiling of the main entrance is determined by it. The whole western part of the cave lies beneath the joint and appears to be morphologically different from the eastern part which lies above the joint. The western part of the cave consists of a string of rounded "rooms", intersecting each other and thus forming steps in the floor and ridges in the ceiling. Bellholes are abundant and they only occur in the western section, underneath the joint. The joint can only be seen in two bellholes.

The eastern part is reached by two openings of less than 1 m in diameter. The northern wall here is sloping upward along the joint and in the southern wall three small openings lead to an approximately 1 m high, 6 m long and 3.5 m wide chamber. A joint going ENE-WSW forms the south side of this chamber. This part of the cave is much richer in speleothems; the whole sloping wall is covered with flowstone as is the floor of the southern chamber. The floor in the rest of this part consist of sand-sized sediment with gravel while the floor in the western part is mainly made of bedrock.

The eastern side of the entrance hall shows a crack at floor level, which leads to a low "room" that can also be entered a little further inside the cave. This "room" gets too low to continue and is furthermore half filled with junk.

Although the map does not show it very clearly, a difference exists in the field between the east and the west side of the cave. Not only in the amount of speleothem but also in the morphology of the two parts: the western part consist of rounded pockets connected to each other while the majority of the walls in the western part are straight and sloping due to joints.

2.2.2 Higher caves

2.2.2.1 Tibbetts Turn Cave (Figs. 1.2 and 2.7).

Tibbetts Turn Cave is located on the north side of the island in the dolostone of the Cayman Formation about two kilometres east of Cross Island Road Cave. The road leading to the cave is the first road on the right after the Z-turn (Tibbetts Turn) in the highway coming from the west. The entrance is almost at the top of the cliff and a foot path leads to it.

Through the only entrance (0.5 m high and 1.5 m wide) a small room of about 5.5 m in diameter is reached off of which there are two rounded rooms of 3 m in diameter, one to the north-east and the other to the south-west. Through the southeastern corner of the entrance room a large chamber (16 m by 6 m) is reached. In the middle of the chamber the ceiling has collapsed and a large block separates the chamber in two. The large block is covered with small stalagmites but the ceiling above it is free of any speleothems. The ceiling of the western part of the chamber is full of partially dissolved stalactites and some columns. The southern wall appears to consist partially of

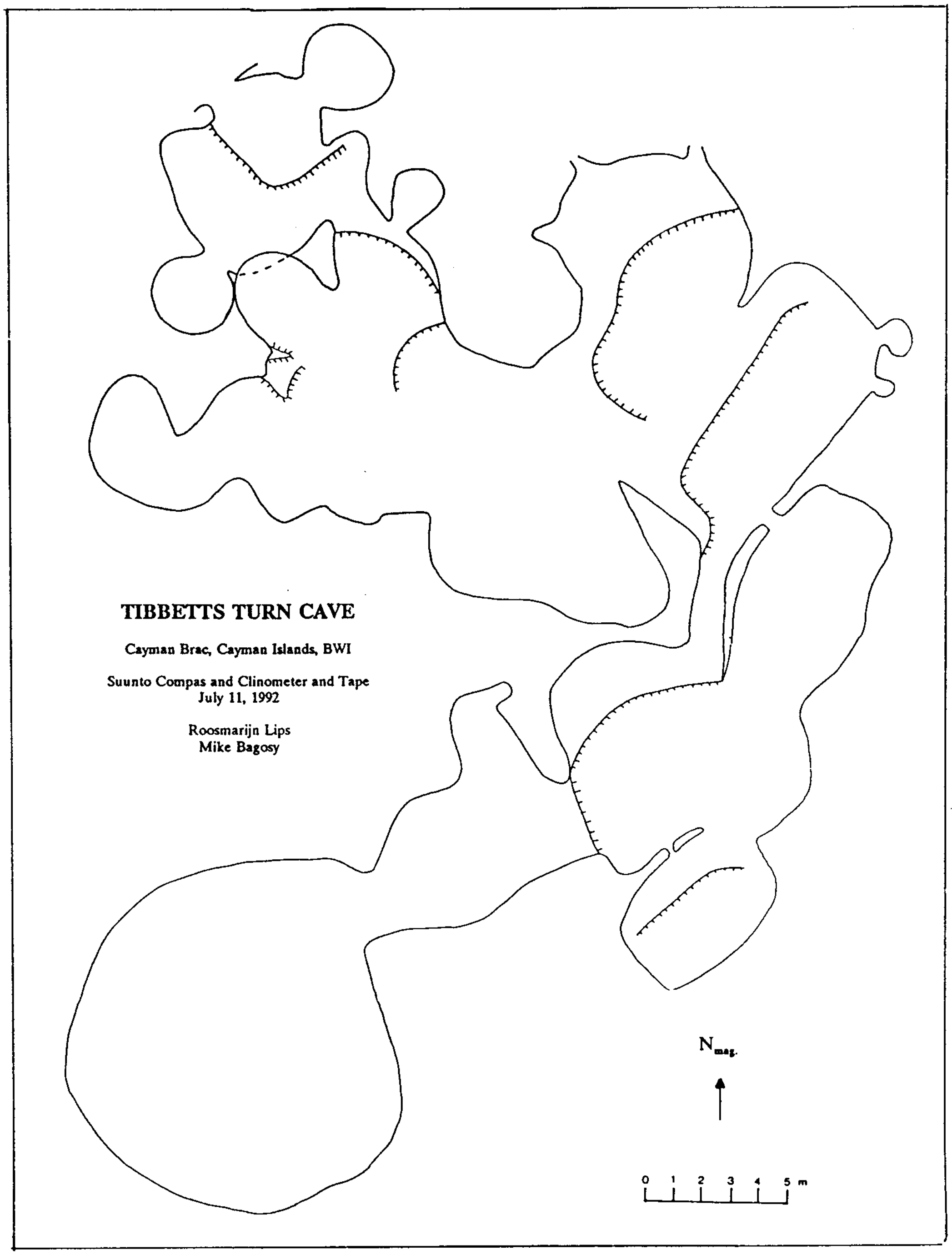

Fig. 2.7. Tibbetts Turn Cave.

breakdown blocks which have been cemented together by a layer of flowstone and through which space can be seen on the other side. In front of the wall a row of columns accompanied by some stalactites is formed. The floor of this chamber consist of gours and sediment in the western and northern half and of only sediment in the rest of it. In the east a smaller room (7 m in diameter) goes to the north. The floor is covered with breakdown blocks that are partly cemented together by flowstone. There are two columns here that have been broken at different height off the floor; one at 82 cm and the other at 22 cm. The columns might have been broken when the ceiling in the large chamber collapsed.

The cave continues to the south. An elongated room can be reached through a small opening or from the south. The floor is covered with flowstone and a sand to gravel sized sediment. The walls are also covered with flowstone and some stalactites with eccentrics and some columns decorate the room. The room enlarges towards the south where the floor consist of dry gours. A row of columns separate the two parts. Along the walls flowstone floors have formed. Some small dissolution gullies have developed on the flowstone floor on the northwestern side by aggressive water coming out of a centimetric opening in the flowstone floor. The flowstone floor along the eastern wall continues into another room (4 m by 5.5 m) which ends with a row of columns along the south-western and north-eastern walls. A row of stalactites is formed over the entire width of the room parallel to the southeastern wall.

The floor of the next passage consists also of dry gours and flowstone, covered with a brownish sand-sized sediment. Partially dissolved stalactites hang from the ceiling along the southern wall. This passage leads to a large southern chamber. This chamber is filled with partially dissolved dripstone and a floor covered with flowstone and partially dissolved stalactites in the southern half. A row of columns separates the two parts of the chamber. The floor of the southern half consist of sand-sized sediment and along the southern wall there is a dry rimstone dam.

In many parts of the cave the bedrock appears to be very coral rich (Fig. 2.7). It is more porous than the rest of the bedrock but no morphological differences have been observed between the parts of the cave with and without this type of bedrock.

2.2.2.2 Peter's Cave (Figs. 1.2 and 2.8).

Peter's Cave is located on the north-eastern side of the island at the end of Light House Road in Spot Bay. It has developed in the dolostone of the Cayman Formation. The main entrance is about 23 m above the notch (29 m above mean sea level) and a second important entrance lies ~ 10 m lower and ~ 25 m westward. It is the highest cave known on the island.

The cave has several levels but only the upper one is well developed. It consist of two main passages that are parallel to the cliff and separated by what seems to be, at places, a relatively thin bedrock partition. However, the first one is reached by the main entrance while the second one can only be reached via the lower levels. At two places light and/or sound contact could be established between the two passages through

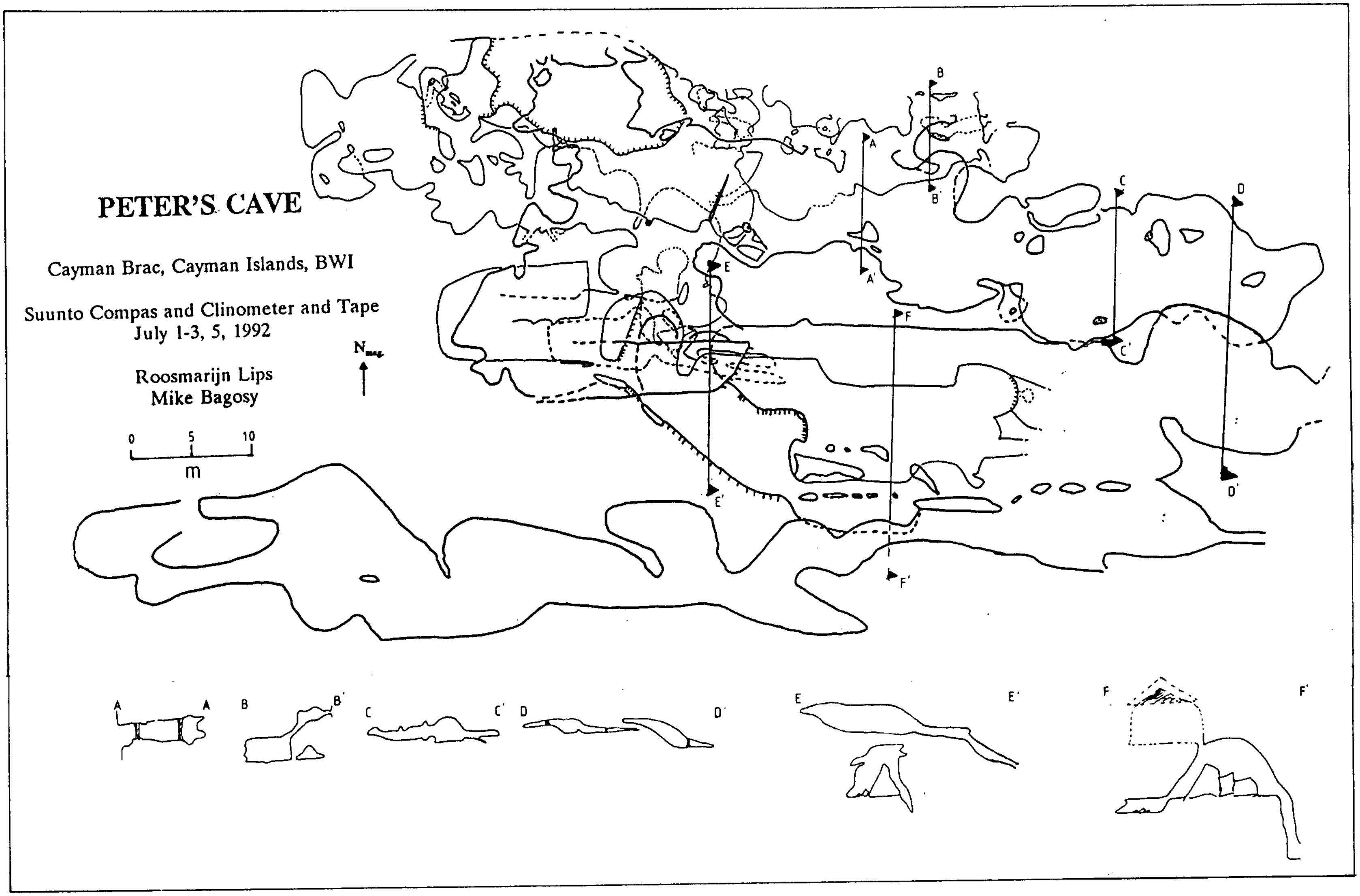

Fig. 2.8. Peter's Cave.

openings that were too small to pass through. In general these two main passages descend stepwise inland (Fig. 2.8). Their floor consist of flowstone that appears to have been formed later than the majority of the other speleothems and that has "drowned" the bases of all the partially dissolved columns and stalagmites. The first main passage has been used as a hurricane refuge and the islanders have put beach sand on the floor to level it.

The lower levels are all in the western half of the cave. This part is different from the eastern half in that it appears to have undergone extensive breakdown, sliding and shifting of large bedrock slabs. The eastern half is much more stable and only minor breakdown occurred in the second main passage. The different levels are partially caused by dissolution, partially by breakdown.

The eastern end of the first main passage appears to have insufficient air circulation causing an increased CO_2 content. This result in yawning, slowed reactions and a headache when visiting it. After heavy rain a temporary lake is formed here along the south-eastern wall. In the northwestern side of the first main passage, several small openings show daylight but none is big enough to be used as entrance.

About 10 m west of the main entrance a crack in the floor leads to a lower level that is in contact with the second entrance. This part of the cave consists of a large room that is complicated by breakdown in its eastern part; close to the crack there are two openings that lead to another section of the cave trending east. Daylight enters through some small openings situated below the main entrance and in the western part of it there is a third entrance which is much smaller than the two previously mentioned ones. The continuation of the cave to the east is blocked by a speleothem column.

The second entrance (14 m wide by 3 m high) is much larger than the main entrance (3 m wide and 1 m high). It opens up into a large chamber of which the floor is littered with large breakdown blocks on which stalagmites have formed. The cave continues through a few constricted openings in the southwestern corner of this chamber. The next part of the cave is quite confusing because there are many openings in between the blocks through which one can continue. Sometimes the blocks are covered by a thin layer of flowstone, sometimes by a crust, resembling gypsum crusts (see 4.4.1.4.). Towards the south-east the breakdown blocks are replaced by a flowstone floor. This is were another tight passage is reached. It can best be described as a sandwich made of two parallel slabs which left just enough space to squeeze through. At the end another room is entered by a tight opening. In the south-eastern corner of this room another complicated part is reached that descends into an elongated small room where the floor is covered with "moonmilk" (see 4.1.5). In the north-eastern corner a much more spacious part is entered. It appears to be the western extension of the second main passage. Towards the west this part end in large breakdown blocks. Here, it is possible to climb up into a space formed by two slabs and which has a tiny opening at the highest point which is in contact with the first main passage. Along the south side of this passage the floor and ceiling drop off into a low passage that due to time limitations was not examined further.

In the east the second main passage is reached by climbing a large pile of big breakdown blocks. At the foot of this pile the lower passage continues for another 20 m. Over the length of this lower passage there is a pile of breakdown blocks along the middle. There is some speleothem along the walls.

The second main passage is wider than the first one and it is filled with partially dissolved speleothems in the eastern half where it ends in a small breakdown. The southern wall consist of bedrock partitions at the top of a slope which leads down to a third main passage that continues towards the west. It contains a lot of moonmilk and ends in the west with a "room" of which the floor is covered with broken speleothem. Along the western wall of this "room" a flowstone floor leads another 15 m further west until it turns east and gets too tight to continue.

2.2.2.3 Little Cayman Brac Cave (Fig. 1.2 and 2.9)

This cave is the furthest north-east situated cave on the island that can be reached. It is developed in the limestone of the Brac Formation about 12.5 m above mean sea level (6.5 m above the notch). The cliff in which the cave is formed descends straight down into the sea and the spray of the breaking waves can be felt at the entrance.

The cave consist of a number of passages sub-parallel to each other that appear to have formed along pre-existing vertical joints in the bedrock that are still visible in the ceiling (Fig. 2.9). The cliff face in between the different entrances shows remains of speleothem and rounded forms suggesting that there was once a passage here

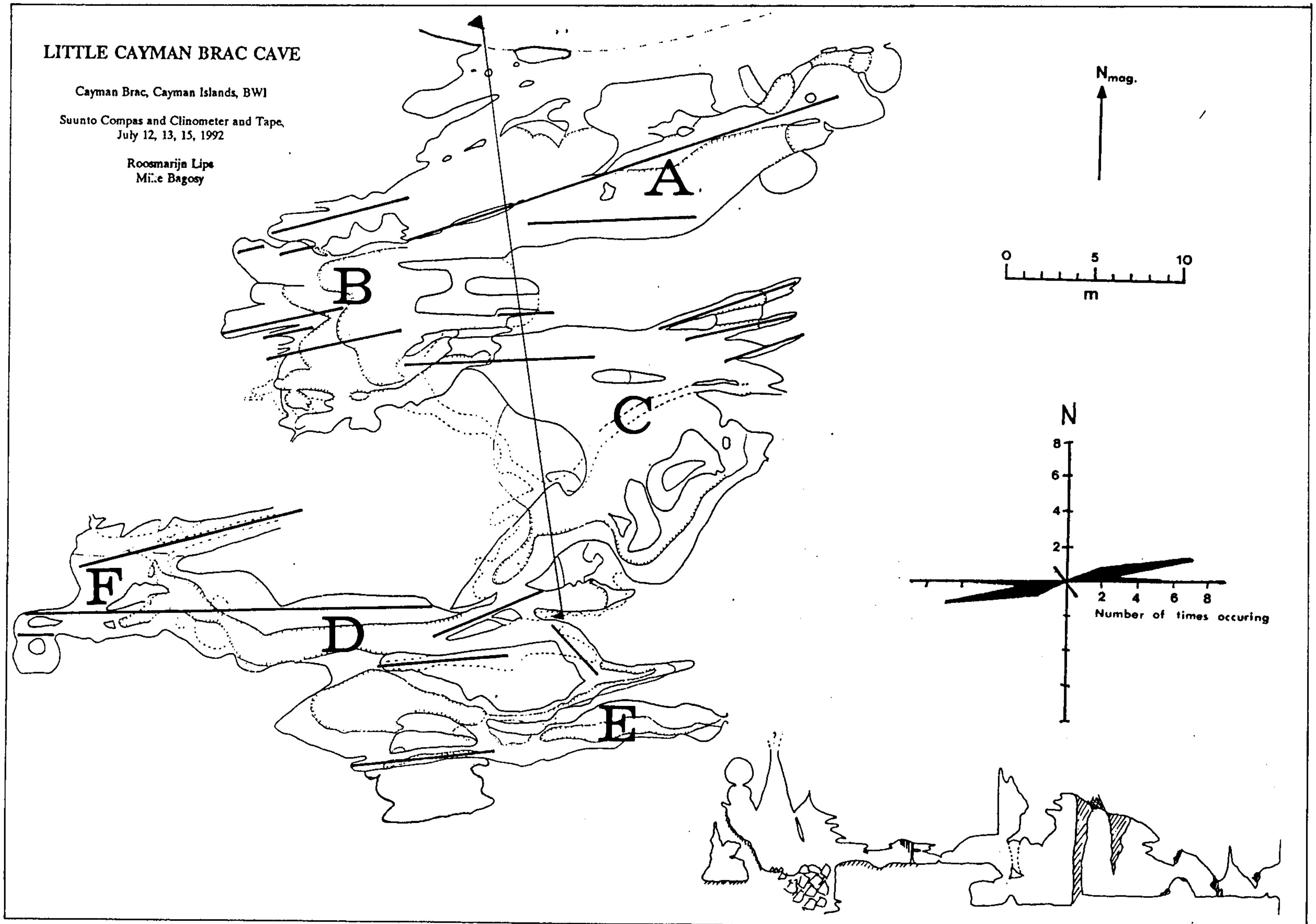

Fig. 2.9. Little Cayman Brac Cave.

as well. The western entrance might be the remains of this passage that disappeared as a result of cliff erosion.

Room B and C are formed at the intersection of two or more joint directions. In B only minor breakdown has taken place but C is dominated by it. The eastern wall of C contains much caymanite that was more resistant than the bedrock, creating a solutional "boneyard" (i.e. "interconnected, nontubular, solution cavities of varied size and irregular geometry arranged in an apparently random, three-dimensional, maze-like pattern" (Hill, 1987, p. 22). Above the breakdown pile in C the joint in the ceiling widens, giving access to a higher level.

Some of the joint surfaces contain scallops which do not show any systematic asymmetry, and thus no indication of water flow directions. They are probably formed by very slow flowing or stagnant water. The scallops become smaller towards the top, where the distance between the two walls also becomes smaller. In part C is a dome-shaped stalagmite accompanied by some small stalactites from which water always drips relatively fast. This was the only place inside the cave where water kept dripping fast enough to take water samples even when it had not rained for days.

The decimetric to metric pockets in the walls of part D also give the impression of a boneyard. This part of the cave is relatively free of speleothems, except along parts of the walls.

The speleothems appear to become increasingly active further inside the cave. The ones in part A and B are all partially dissolved (except for the flowstone floor) while the majority in part E are still wet.

On some walls, especially in the southern part, there is a brownish crust of which the content and origin are unknown. Along the walls and bedrock pillars of the most southern part of the cave it forms a line about 40 cm off the floor. It might have formed as the result of a chemical reaction between the bedrock and a sediment cover that once was that deep, or due to precipitation out off stagnant water.

2.3 Cave geometry.

A basic premise of the flank margin model (Mylroie and Carew, 1990) is that halocline caves form from the coast inland. If this assertion is true then a decrease in cave volume would be expected inland. To test this hypothesis, the plan area and the volume of the studied caves were determined. The area of the cave calculated from the cave plan as the product of the length and the breath is the plan area. To represent the evolution of the plan area from the coast inland, a standard length interval of one meter was chosen (Fig. 2.10). The plan area can thus be calculated as

$$C_i = \sum_{j=1}^{n} A_{P_j} \qquad (1)$$

where C_i is the area of the interval i meters from the cliff face of cave C. The quantity

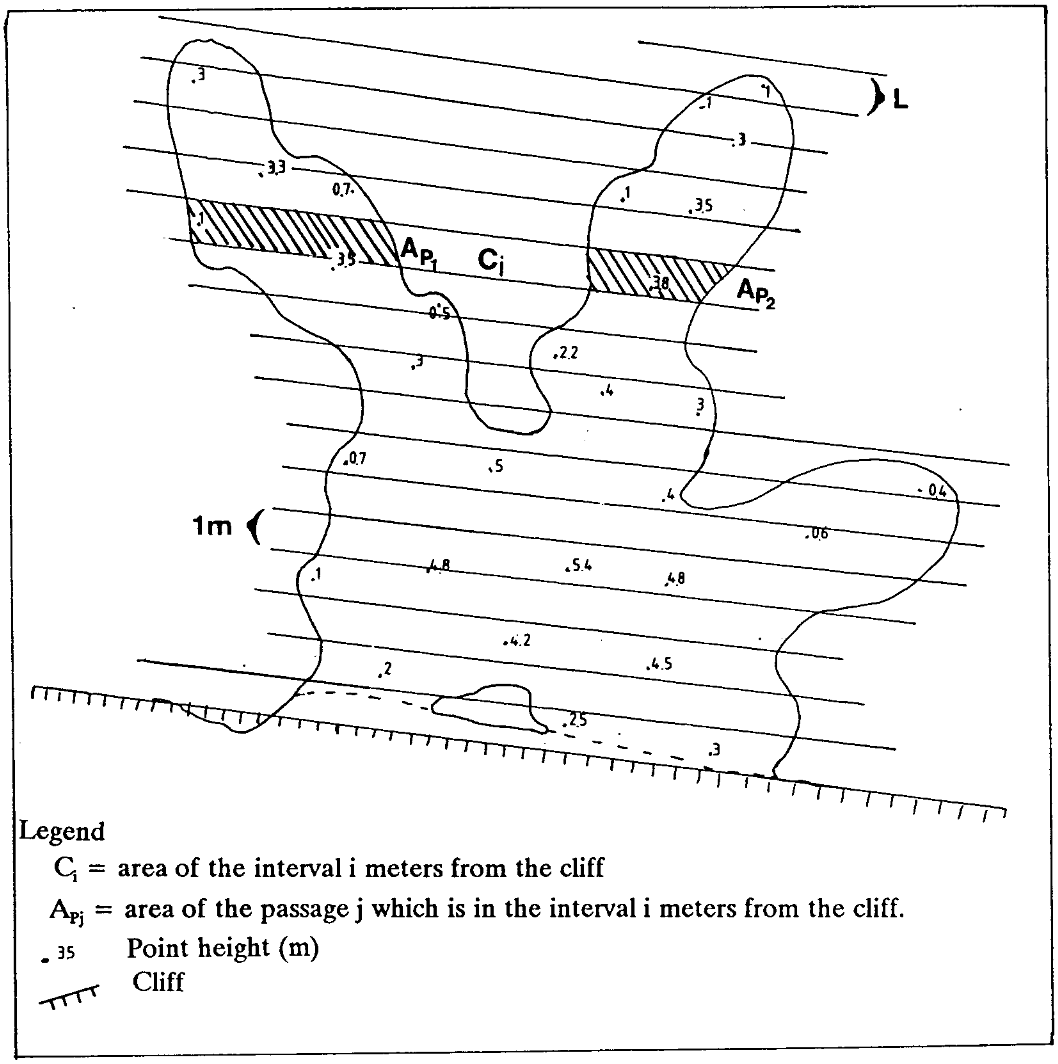

Fig. 2.10. Schematic representation of cave geometric parameters.

on the right hand side of equation (1) is the sum of the areas of the n passages of C which are in the interval i m from the cliff face. The total area is then

$$A_C = \sum_{i=1}^{L} C_i \tag{2}$$

where A_C is the total area of cave C and L is the furthest interval distance of C from the cliff face. The volume of each interval i is obtained as the sum of the product of the area and the average height of the n passages that are in this interval. Total volume is then obtained in a similar manner as the total area.

Figure 2.11 presents the plots of the relationship between area and volume. The close agreement between the variables suggests that it might be possible to infer one from the other. If the relationship is linearised by taking the natural logs of the area and volume, it may be described by a simple regression equation such as

$$V_C = a + b\ A_C \tag{3}$$

where V_C is the log normal of the volume of cave C, A_C is the log normal of the area of C and a and b are the equation parameters. This implies that volumes of caves on Cayman Brac may be estimated from published cave maps (Fig. 2.12).

The outliers in the Figure 2.11 are the first and/or the last meter or meters.

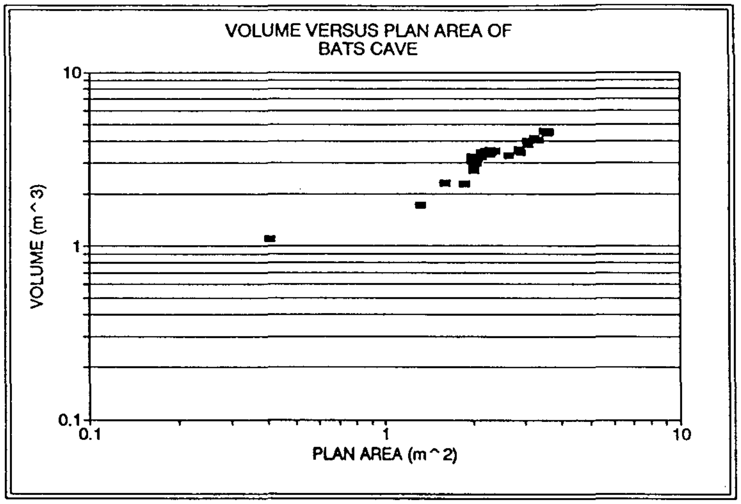

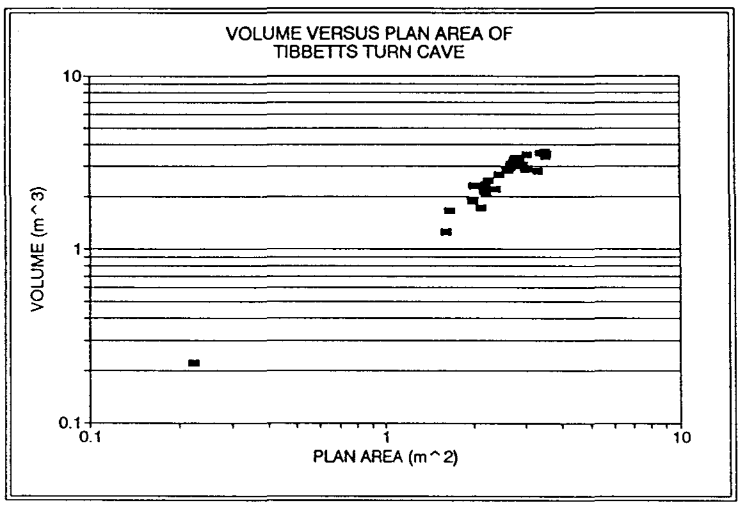

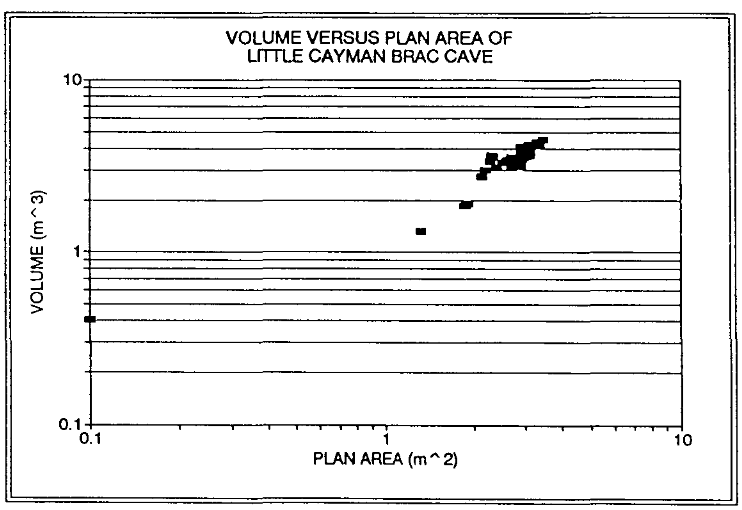

Fig. 2.11. Relationship between area and volume of the caves.

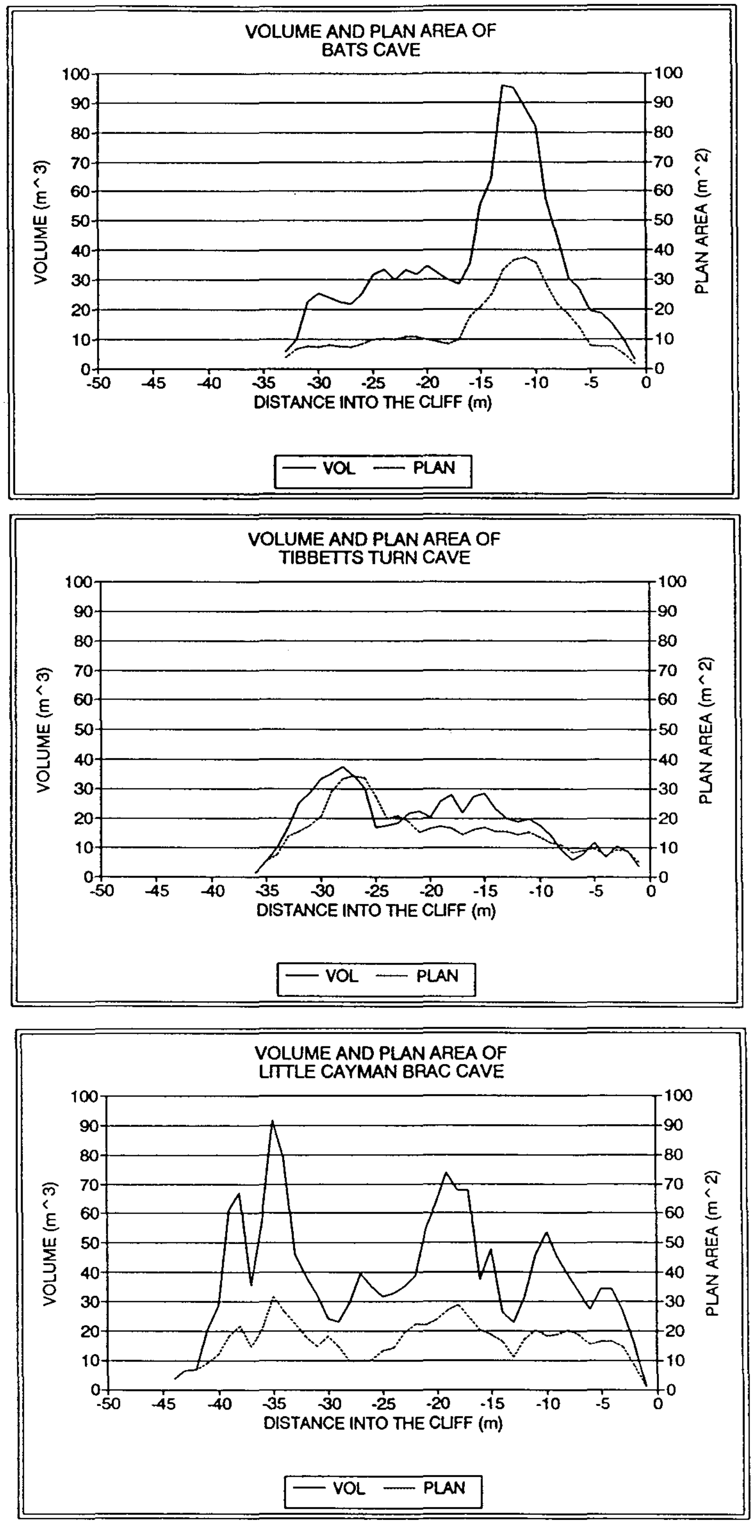

Fig. 2.12. Area and volume of the caves.

Due to the shape of the caves and their angle with the cliff face, the first meter interval was often only partially inside the cave (Fig. 2.10). The last meter interval was not always complete either and so the area and the volume in this interval were often much less. It is now possible to use the outliers as a measure of where to start and end the individual caves.

Figure 2.13 shows the cumulative volumes of the notch caves and the higher caves. There is a difference between the notch caves and the higher caves. The notch caves exhibit a greater variation in volume within short distance than the higher caves. They generally have a rapid increase in volume within the first few meters after which the volume increases more slowly. As can be seen from the cave maps this pattern is due to the presence of a large chamber close to the cliff and smaller passages going inland. The more gradual decrease in volume changes from cave to cave, depending on the number and size of the side passages. The higher caves show a much more gradual increase in volume over the entire length. Tibbetts Turn Cave appears to be the opposite of the notch caves: smallest volume closest to the cliff face and the largest volume furthest inland. The slight sinuosity of Peter's Cave and Little Cayman Brac Cave indicate zones of lesser and greater volume parallel to the cliff, which can be seen from the cave maps as big passages parallel to the cliff.

It therefore appears that the cave volume can be used to group caves into different types, linked to different formation processes.

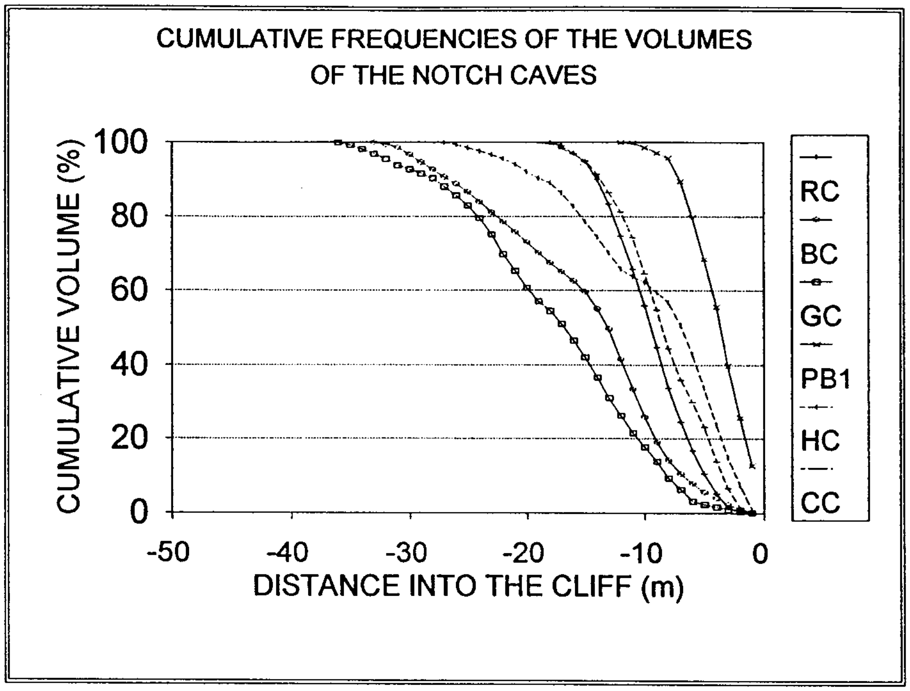

(a)

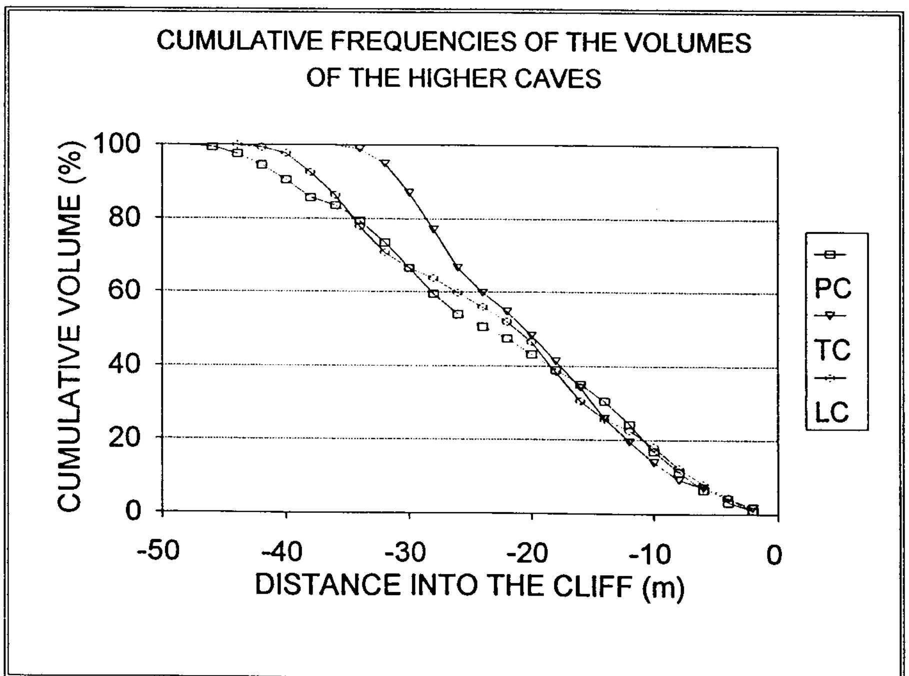

(b)

Fig. 2.13. Cumulative volume curves of (a) notch caves and (b) higher caves.

2.4 Direction of cave development.

The directions in which passages develop could give some information about the mechanism behind the development; e.g. passages could develop along joints or specific flow directions.

Figure 2.14 shows Cayman Brac and the directions in which the caves developed. The notch caves and Tibbetts Turn Cave appear to have developed in all directions while the two other higher caves have passages more parallel to the cliff. This is also clear from Figure 2.15, which shows the total length of passages in the different directions for all the caves on the north and the south side. The cliff along the south side of the island is relatively parallel to the direction of the long axis of the island (67 °E) while the cliff along the north side appears to follow this direction stepwise (Fig. 2.14). The longest lengths sub-parallel to the cliff belong to Little Cayman Brac Cave (towards the west) and Peter's Cave (towards the east).

All notch caves and Tibbetts Turn Cave appear to have developed in all directions, with a slight preference towards the N-NE. All the passages of Peter's Cave are (sub)parallel to the cliff (90 °E) but no joints are visible in the ceilings. On the other hand, the passages of Little Cayman Brac Cave are (sub)parallel to the cliff and also follow a joint pattern (Fig. 2.9). This is the only cave in which joints are actually visible inside the cave and which determine the direction of the passages.

Little Cayman Brac Cave developed along a vertical joint pattern sub-parallel

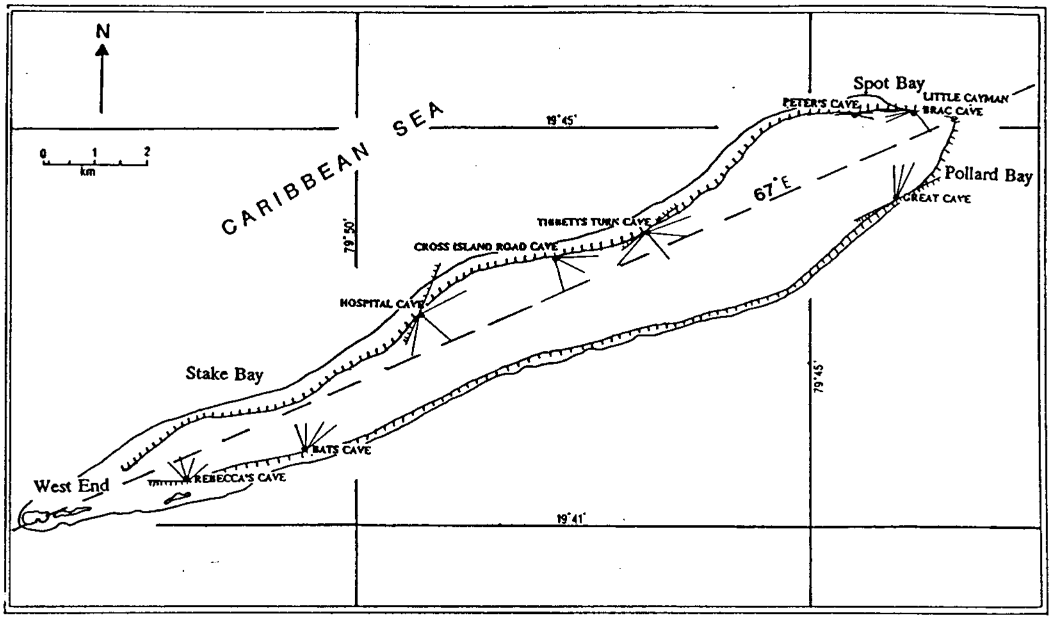

Fig. 2.14. Directions of cave development on Cayman Brac.

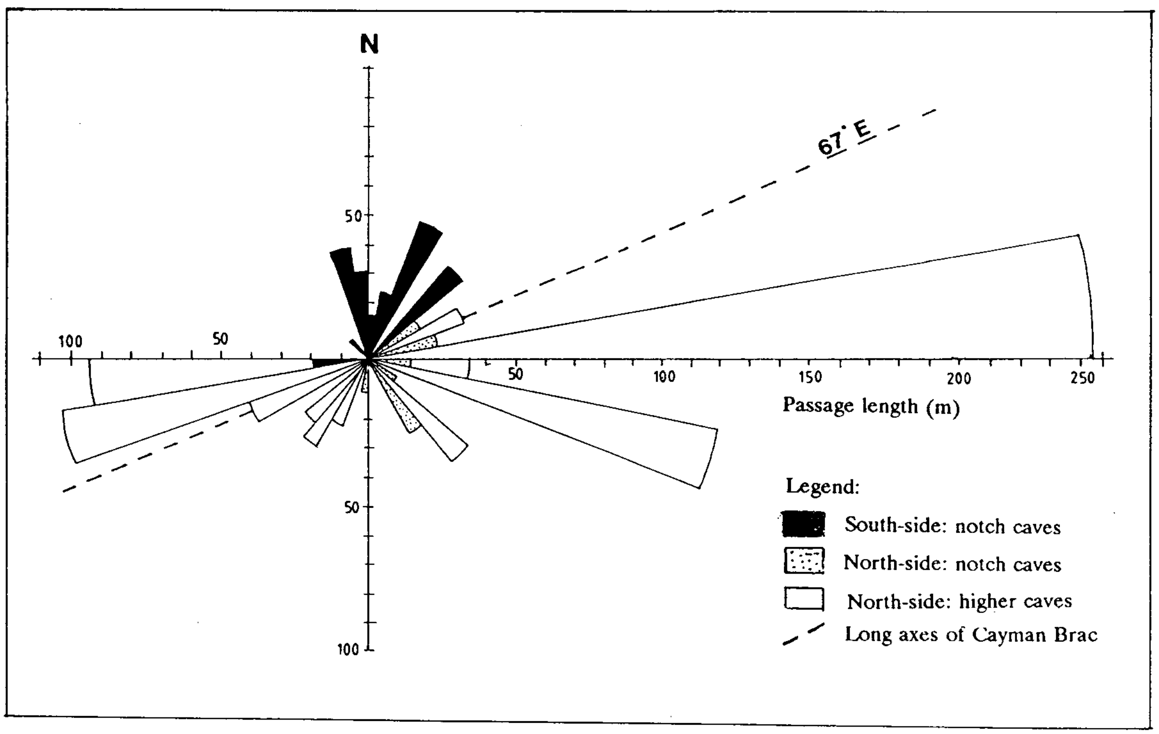

Fig. 2.15. Total length of cave passages in each direction.

to the cliff. These joints most probably are formed as the result of the lack of support for the rocks on the sea side; i.e. stress release joints. There are no vertical joints in Peter's Cave but it is possible that there is some kind of horizontal structure, that is also responsible for the stepwise lowering of the passages from the entrance further inside the cave (Fig. 2.8). The notch caves and Tibbetts Turn Cave are likely formed by a process that acts in all directions, e.g. dissolution in a phreatic zone.

2.5 Bellholes

Bellholes are circular tubes or saucer-shaped indentations in the ceiling which have a vertical long axis and a variable depth (Wilford, 1966). They develop with apparent disregard of any structural features in the bedrock. Sometimes two or more bellholes merge to become one (e.g. in Hospital Cave). The bellholes observed on Cayman Brac had smooth walls without any grooves suggesting that they are not formed by aggressive water running down their sides in streams.

2.5.1 Depth and diameter

The diameter of the bellholes in all the caves ranges from 0.15 to 1.4 m and the depth from 0.3 to 5.5 m. However, these ranges vary in the individual caves; e.g. the bellholes in Peter's Cave are shallow (up to 1 m) while the ones in Hospital Cave are deep (up to 5.5 m). Figure 2.16 shows that there is no linear relationship between the diameter and the depth of the bellholes found on Cayman Brac. There is only one cave,

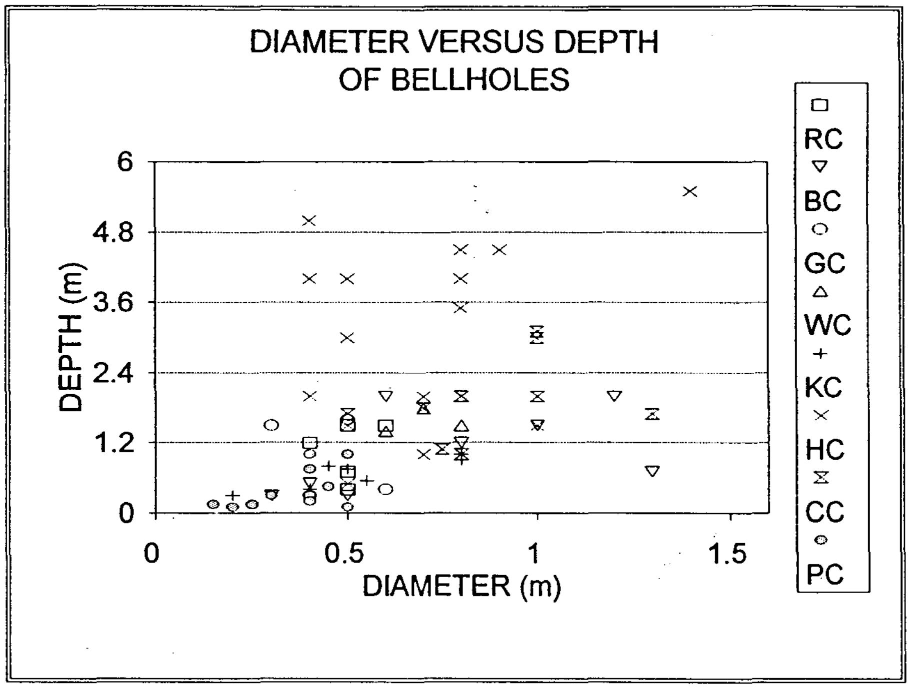

Fig. 2.16. Diameter and depth of bellholes.

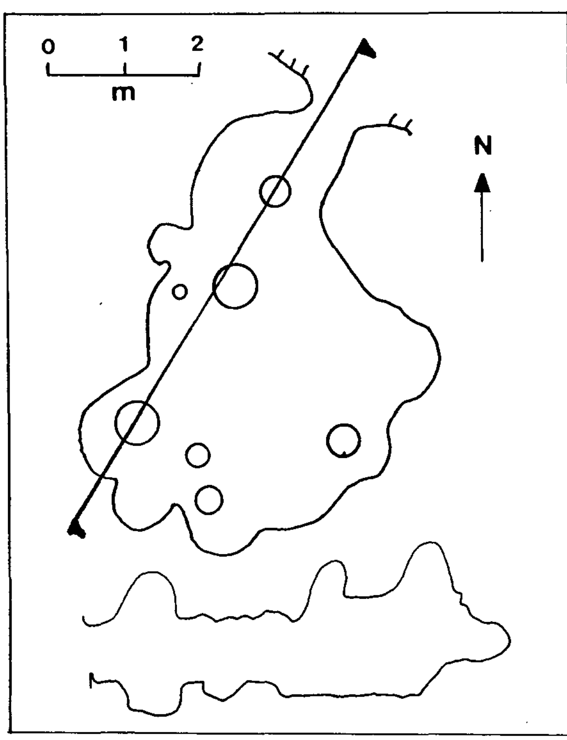

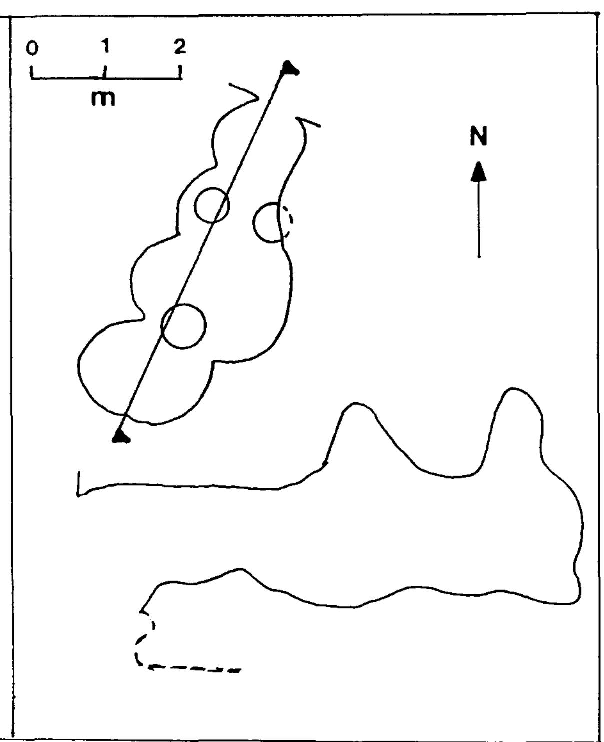

Fig. 2.17a. Climb in Cave.

Fig. 2.17b. Walk in Cave.

Climb In Cave, Stake Bay (Fig. 2.17a), in which there appears to be some relationship (Fig. 2.18). This relationship, however, is not dependent on the distance from the entrance (Fig. 2.18).

2.5.2 Distribution

The majority of the bellholes are found in the notch caves (including in two small notch caves in Stake Bay (Climb In Cave and Walk In Cave (Figs. 2.17)). Only in the ceiling of the first main passage of Peter's Cave there are some relatively small ones.

In Hospital Cave the bellholes are clearly concentrated close to the entrance (Fig. 2.5). In Cross Island Road Cave bellholes are only found in the western section, under the joint. Beside the few small bellholes there are circular skylights in Bats Cave that resemble bellholes. It is believed that these skylights are bellholes that have been intersected by surface erosion. The same appears to be true for the small circular skylight in Rebecca's Cave. The two bellholes in the large chamber in Great Cave have small diameters (30 and 50 cm) but great depths (~ 1.5 m). Of the other four clustered in the southern passage three have the same measurements: 40 cm in diameter and 30 cm deep.

2.5.3 Origin

Bellholes have been observed in caves in the humid tropics (e.g. Belize: Miller, 1981; Trobriand Islands: Ollier, 1975; Sarawak: Wilford, 1966; Trinidad: King-

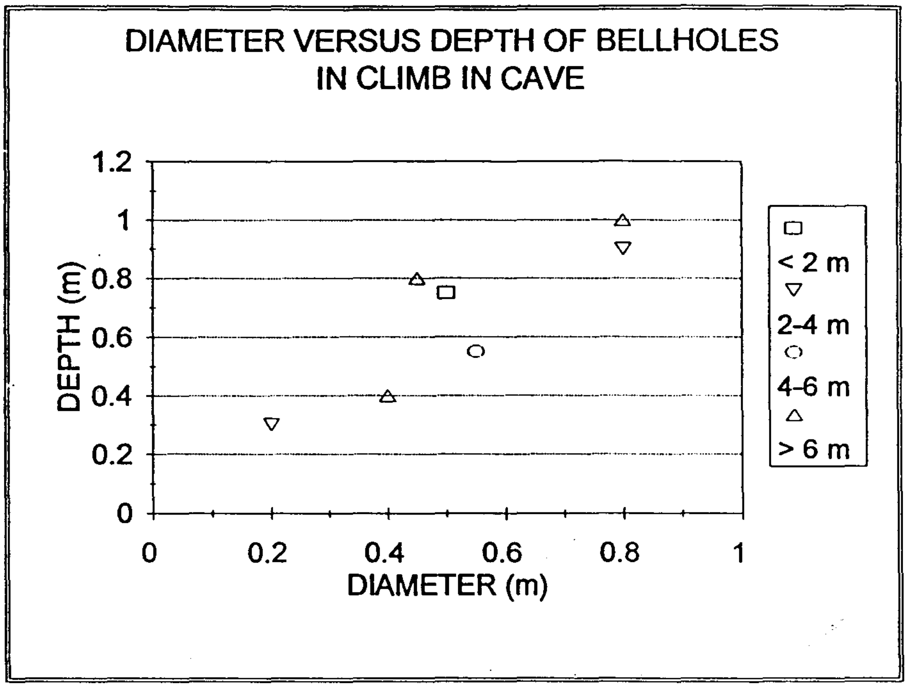

Fig. 2.18. Diameter and depth of bellholes in Climb in Cave in relation to the distance inside the cave.

Webster and Kenny, 1958). It is still unknown how bellholes develop. King-Webster and Kenny (1958) believed that they were excavated by the claws of generations of roosting bats. Bats tend to search for an indentation in the ceiling to sleep during the day. The jostling for the central position could cause, over time, erosion of soft granular rock. Enlargement of the deepening indentation is the result of bats climbing up to the top when the cavity becomes too deep to fly directly into it. This theory appears to be a little far fetched; how come all these bellholes have a circular section? How does clustering develop? Why are they distributed at random in certain caves and in clusters in others?

Miller (1981) also believed that bats must play some important role in the formation of bellholes because he observed bellholes only where there were bats. He suggested that their urine might be the acting parameter. In this case, there is a chick and egg problem: did the bellholes form as a result of the presence of the bats or did the bats come to the bellholes because they are ideal roosting places? On Cayman Brac bats were observed in some bellholes but Bat Passage, Bats Cave, where a bat colony has sought refuge, does not have any bellholes.

A third possibility is that bellholes are dissolution features. Wilford (1966) suggest that they are formed in the same manner as potholes, i.e. they are "produced by eddies in fairly fast flowing water, the turbulence locally increasing the potential aggressiveness of the water" (p. 180). However, Wilford also mentioned locations of bellholes where there could never have been fast flowing water and thus questioned his own suggestion. According to Ollier (1975) bellholes are formed in the phreatic zone where dissolution can occur equally well in all directions. The question of why they are clustered in one cave and randomly distributed in another still remains unanswered. Finally, Ford and Williams (1989) proposed that bellholes "may be vadose or floodwater forms of biogenic origin" (p. 298).

None of these theories describes satisfactorily the formation of bellholes. The dissolution theories appear to be more plausible than the ones involving bats, but not all questions are answered yet. The biggest problem is that these bellholes form in bedrock without fractures or apparent feedwater point inputs. This suggest that whatever causes these bellholes to form comes from inside the cave. This idea is supported by the fact that bellholes form in caves with different bedrock thickness above them; e.g. bedrock thickness above Great Cave is about 25 m while at Rebecca's Cave it is less than 2 m.

2.6 Clastic sediment and bedrock analysis.

2.6.1 Methods.

2.6.1.1 Insoluble residue

The insoluble residue of both bedrock and sediment was measured. The procedure used for both was the same except that the samples for bedrock were about 50 gr and for sediment about 10 gr. The bedrock samples consisted of several small pieces (from which the weathered surface was removed) to increase the surface area exposed to acid.

Samples were dried in an oven before weighing and then placed in 150 ml beakers. 9N HCl was added to the samples until they were barely covered. To prevent loss of sample by too vigorous effervescence watchglasses were placed over the beakers and distilled water was added when needed to dilute the acid and reduce the effervescence. When all reaction had ceased the solutions were passed through filter papers of known weight. The procedure was repeated until there was no more reaction between the sample and new acid added to it. Filter papers with the insoluble residues were dried in an oven before being weighed. The insoluble residue was calculated as weight percentage of the dried sample before dissolution.

The following sections describe the procedures/techniques of analysis of the clastic sediment samples.

2.6.1.2 Organic matter.

About 10 gr of sediment was dried, weighed and placed in small porcelain cups of known weight, and put in a Muffle Furnace at 450 °C for 30 minutes after which they were weighed again. The amount lost, being the amount of organic matter, was calculated as weight percentage of the dried sample before heating.

2.6.1.3 Colour.

The wet and dry colour of the sediment samples as well as the dry colour of the insoluble residue were described using the Munsell Colour Chart and the Munsell notation.

2.6.1.4 Grain size.

A sample of approximately 100 gr of sediment was dried and weighed. A set of 13 sieves of mesh sizes every half ϕ between -2 and 4 ϕ ($\phi = \log_2 d$ (d = diameter in mm)) were arranged in downward decreasing mesh size ending with a pan. The sample was added and the sieves mechanically vibrated for 15 minutes. The weight of the sediment retained on each sieve and in the pan were measured and calculated as weight percentage of the total sample. The loss of sediment during the procedure was less than 3% of the total weight. The sediment with grain size greater than -2 ϕ was manually sieved through sieves with mesh sizes -4, -3.67, -3.25, -3 and -2.5. The Wentworth scale was used for the description of the grain sizes (Fig. 2.19).

2.6.1.5 Statistical methods of grain size analysis.

For each sample the cumulative percentage of each grain size was calculated and cumulative curves were drawn. From these curves the grain size at 5%, 16%, 25%, 50%, 84% and 95% were read. If the curve did not represent the 84% and/or the 95% then the grain size was estimated by a straight line extrapolation of the curve. These grain sizes were used to calculate mean grain size, standard deviation (degree of sorting), skewness and kurtosis.

The formulae and classifications of Folk and Ward (1957) were used: -

Mean size: $$\frac{\phi 16 + \phi 50 + \phi 84}{3}$$

	WENTWORTH GRAIN SIZE SCALE	$\phi = -\log_2 d$	dimension (d in mm)
GRAVEL	Boulder	-12 - -8	4096 - 256
	Cobble	-8 - -6	256 - 64
	Pebble	-6 - -2	64 - 4
	Granule	-2 - -1	4 - 2
SAND	Very coarse sand	-1 - 0	2 - 1
	Coarse sand	0 - 1	1 - 0.5
	Medium sand	1 - 2	0.5 - 0.25
	Fine sand	2 - 3	0.25 - 0.125
	Very fine sand	3 - 4	0.125 - 0.0625
MUD	Coarse silt	4 - 5	0.0625 - 0.031
	Medium silt	5 - 6	0.031 - 0.156
	Fine silt	6 - 7	0.0156 - 0.0078
	Very fine silt	7 - 8	0.0078 - 0.0039
	Clay	> 8	< 0.0039

Fig. 2.19. Wentworth scale for grain sizes.

Standard deviation: $$\frac{\phi 84 - \phi 16}{4} + \frac{\phi 95 - \phi 5}{6.6}$$

The standard deviation (σ) may vary between 0 and ∞ and the proposed classification is:

	$\sigma < 0.35$	very well sorted
$0.35 <$	$\sigma < 0.50$	well sorted
$0.50 <$	$\sigma < 1.00$	moderately sorted
$1.00 <$	$\sigma < 2.00$	poorly sorted
$2.00 <$	$\sigma < 4.00$	very poorly sorted
	$\sigma > 4.00$	extremely poorly sorted.

Skewness is calculated as;

Skewness: $$\frac{\phi 84 + \phi 16 - 2(\phi 50)}{2(\phi 84 - \phi 16)} + \frac{\phi 95 + \phi 5 - 2(\phi 50)}{2(\phi 95 - \phi 5)}$$

The values for skewness (Sk) vary between -1 and 1 and are categorised as follows:

$-1.0 <$	$Sk < -0.3$	very negative-skewed
$-0.3 <$	$Sk < -0.1$	negative-skewed
$-0.1 <$	$Sk < 0.1$	near symmetrical
$0.1 <$	$Sk < 0.3$	positive-skewed
$0.3 <$	$Sk < 1.0$	very positive-skewed.

Kurtosis:

$$\frac{\phi 95 - \phi 5}{2.44(\phi 75 - \phi 25)}$$

This index may have values varying from 0.41 to ∞ but usually varies between 0.50 and 8.00 (Pissart, unpublished). The classification is

0.41 < K < 0.67 very platykurtic

0.67 < K < 0.90 platykurtic

0.90 < K < 1.11 mesokurtic

1.11 < K < 1.50 leptokurtic

1.50 < K < 3.00 very leptokurtic

K > 3.00 extremely leptokurtic.

2.6.1.6 Mineral composition.

The mineral composition of the insoluble residues of five cave sediment samples (one from the south side and four from the north side) was determined by X-ray fluorescence (McMaster X-ray Diffraction Laboratory, J. McAndrew).

2.6.2 Results and Interpretations.

2.6.2.1 Insoluble residue.

<u>2.6.2.1.1 Bedrock</u>

As reported above, Little Cayman Brac Cave (LC) and Great Cave (GC) are situated in the Brac Formation, LC in the limestone on the north side and GC in the dolostone on the south side. Rebecca's Cave is developed in the partly dolomitised limestone of the Pedro Castle Formation. The remaining caves are formed in the dolostone of the Cayman Formation.

All the rocks, whether limestone or dolostone, are very pure with less than 3 % insoluble residue (Table 2.1). This purity can be attributed to the location of the island, far from any mainland or shelves where rivers might bring clays and sands into the ocean. The only way that insoluble impurities can reach the island is by wind or by precipitation from the sea water, e.g. silica skeletons.

2.6.2.1.2 Sediment.

The insoluble residues of the clastic sediment samples vary from 2 to 25 % (Table 2.1). The sediments consist therefore largely of carbonate particles, such as shells and pieces of bedrock, which can be confirmed by visual observation of the sediments.

2.6.2.2 Loss on ignition.

The loss on ignition determines the loss of organic matter in the sediment because at a temperature of 450 °C organic matter will burn. The majority of the sediments have between 3 and 8 % of organic matter (Table 2.1). Exceptions are Hospital Cave with 11% and Pollard Bay Cave 2 and Bats Cave with almost 25 %. In the last two caves the presence of bats is probably responsible for these high organic values. In Hospital Cave it is not clear why there is so much. One explanation could be

Table 2.1 Result of bedrock and sediment analysis

	BEDROCK	SEDIMENT							
Cave	Insoluble residue (wgt %)	Insoluble residue (wgt %)	Lost on ignition (%wgt)	Colour Wet	Munsell value Wet	Colour Dry	Munsell value Dry	Colour Insoluble residue	Munsell value Insoluble residue
Pollard Bay Cave 3		29.80	7.69	brown - dark brown	7.5 YR 4/4	light gray	10 YR 7/2	very pale brown	10 YR 8/3
Pollard Bay Cave 2		24.81	23.42	dark redish brown	5 YR 3-2/2	grayish brown	10 YR 5/2	black	10 YR 2/1
Great Cave	1.07	4.82	6.30	yellowish brown	10 YR 5/4	very pale brown	10 YR 8/4	brown/dark brown	10 YR 4/3
Bats Cave	1.73	20.73	24.94	dark redish brown	5 YR 2/2	brown - dark brown	10 YR 4/3	dark brown	7.5 YR 3/2
Rebecca's Cave	0.86	10.64	6.55	strong brown	7.5 YR 5/6	very pale brown	10 YR 7/4	dark yellowish brown	10 YR 3/4
Little Cayman Brac Cave	2.36	5.15	6.07	dark brown-dark yellowish brow	10 YR 3/3-4	light gray	10 YR 7/2	very dark brown	10 YR 2/2
Peter's Cave 1st main passag	2.95	15.47	4.59	redish brown- yellowish brown	5 YR 4/4-6	strong brown	7.5 YR 5/6	strong brown	7.5 YR 5/6
Peter's Cave 2nd main passa	2.47	2.06	3.09	yellowish brown	10 YR 5/6	very pale brown	10 YR 7/3	dark yellowish brown	10 YR 4/4
Tibbetts Turn Cave	2.26	27.93	4.63	dark red	2.5 YR 3/6	yellowish red	5 YR 5/8	yellowish red	5 YR 5/6
Cross Island Road Cave	1.58	15.37	3.23	strong brown	7.5 YR 5/6	very pale brown	10 YR 7/4	yellowish red	5 YR 5/6
Hospital Cave	2.38	12.86	11.15	strong brown	7.5 YR 5/6	very pale brown	10 YR 7/4	white	10 YR 8/2

the presence of land crabs, which were observed at the site where the sediment sample was collected. Land crabs, hermit crabs and bats were on the other hand also seen or heard in many other caves where the percentage of organics was not as high. Another possibility is that more organics are brought in from the plateau above by infiltration water or blown in by wind.

2.6.2.3 Colour.

Table 2.1 shows the wet and dry colour of the sediments and the dry colour of the insoluble residues. Three main colour groups can be observed:

1. dark colours indicating the presence of organic matter,
2. reddish colours indicating the presence of iron and
3. light greyish colours indicating the dominance of bedrock and shelf particles.

The sediments may be divided into four groups according to the change in colour between the wet and dry conditions. PB2 and BC go from dark reddish brown to brown, suggesting a high content of organics and presence of iron. In the second group consisting of PC1 and TC, iron is clearly present because the samples change from reddish brown to yellowish red. PB3 and LC change from dark brown to pale brown, while the remainder of the caves, belonging to the fourth group, are characterised by a colour change from strong brown to pale brown. The last two groups probably contain quite some bedrock particles, calcareous dust and/or silicates.

The dry colour of the insoluble residues of PB3, PC1, TC and HC are similar to the dry sediment colours. The reddish colour thus persist in PC1 and TC. The iron in these samples most likely comes from patches of terra rossa on the surface. On the other hand, the insoluble residues of GC, RC, LC, PC2 and CC show more similarities with the yellowish brown colour of the wet sediment samples. The insoluble residues of PB2 and BC had a darker and less reddish colour than the wet sediment samples, strengthening the idea that they contain a lot of organics, probably due to the presence of bats and other animals.

2.6.2.4 Grain size analysis.

The results of the sieving are represented as cumulative curves in Figure 2.20 and as histograms in Figure 2.21. Table 2.2 summarises the results of the statistical analysis.

The sediments are in general very poorly sorted with medium sand as the mean as well as the modal grain size. Both fine and coarser particles are present and their relative amount varies from cave to cave (Fig. 2.21). The poor sorting is due to the fact that the weathering products (which are the dominant components of the sediments) have not been transported by water or wind after deposition.

The sediments do not form thick layers inside the caves and in many places they are quasi absent. Care was taken to ensure that the samples were collected from parts of the caves that were relatively unfrequented by visitors. This means that they

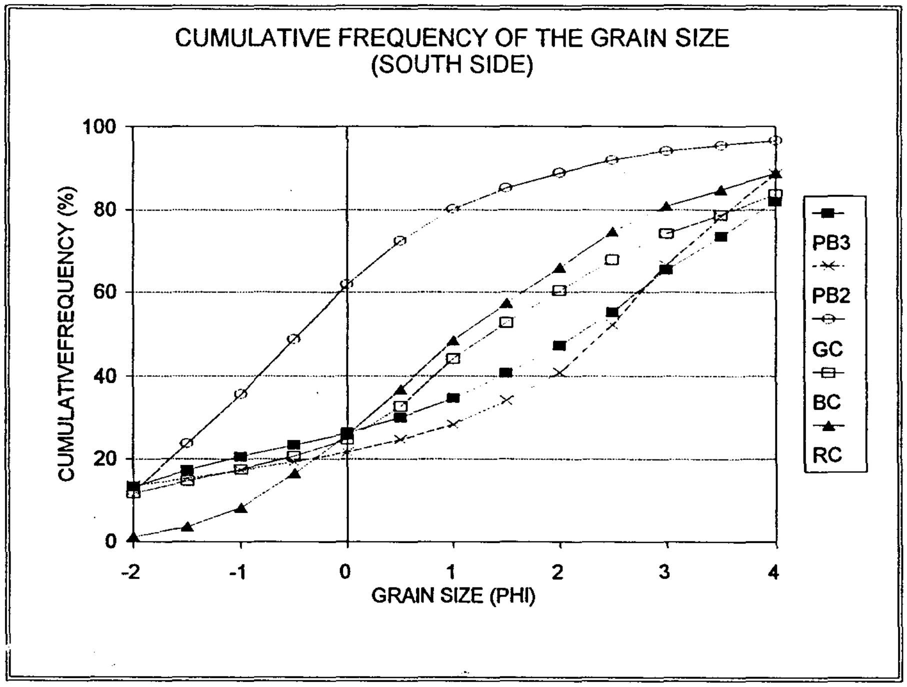

(a)

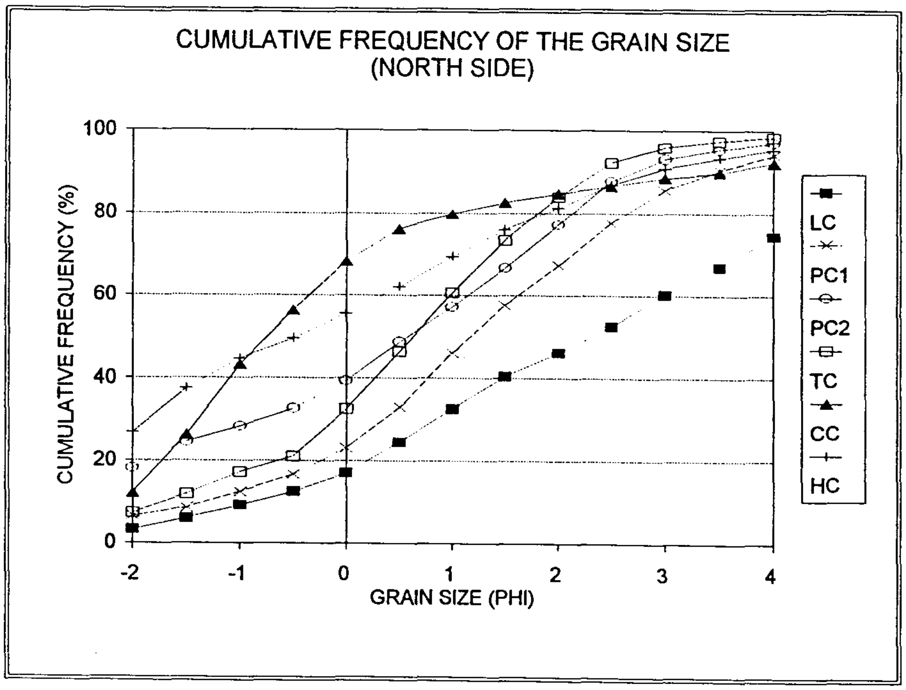

(b)

Fig. 2.20. Cumulative grain size curves of caves on (a) the south side and (b) the north side.

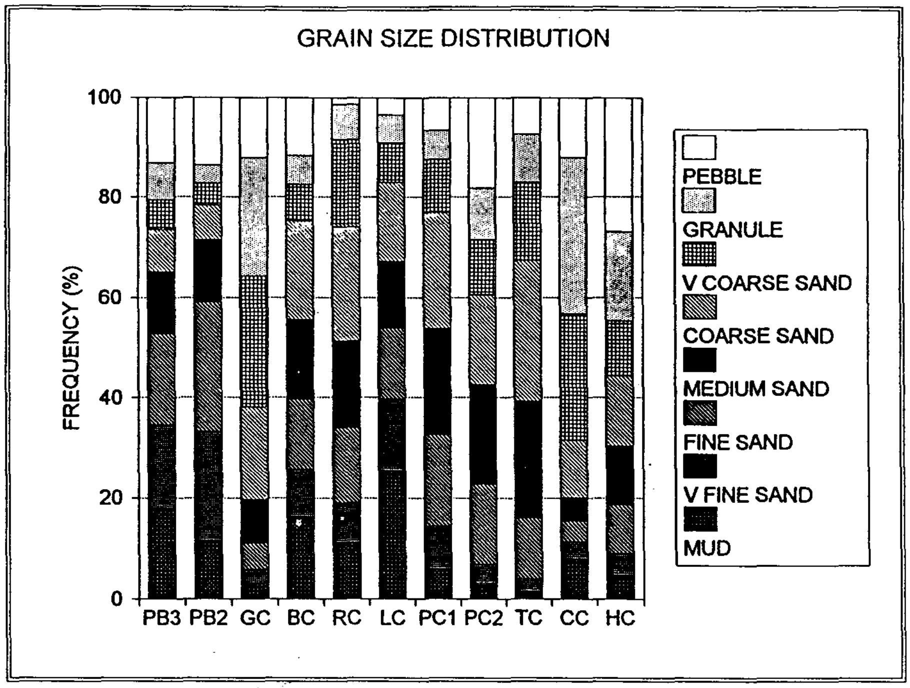

Fig. 2.21. Grain size per size class.

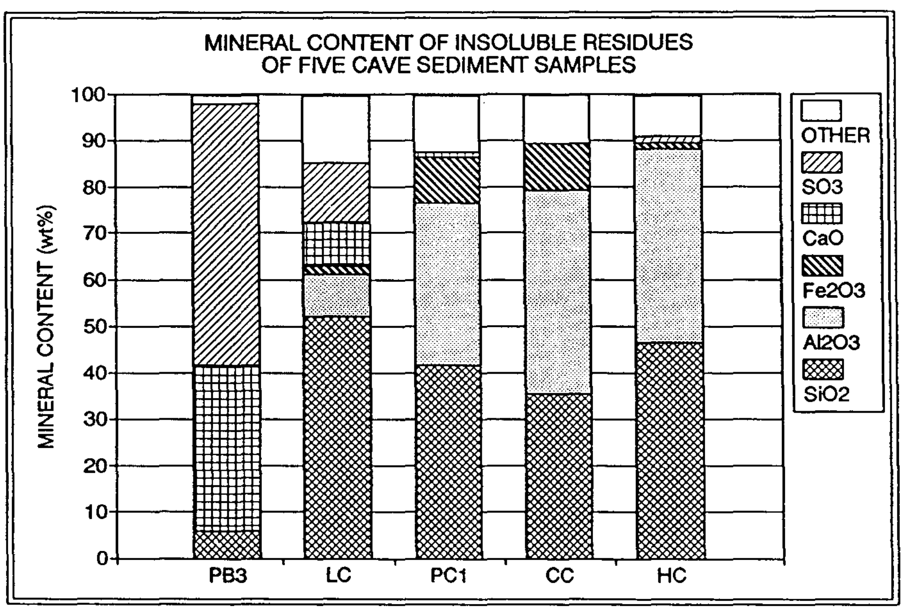

Fig. 2.22. Principle mineral composition of insoluble residues of five cave sediment samples.

Table 2.2 Grain size analysis

CAVE	MEDIAN	MODE phi	MEAN phi		STANDARD DEVIATION (SORTING) phi		SKEWNESS		KURTOSIS	
Pollard Bay Cave 2	2.20	3 /-1.5	1.52	MS	2.77	VP	-0.37	VNA	0.93	MK
Pollard Bay Cave 3	2.60	3	1.68	MS	2.50	VP	-0.56	VNA	1.20	VLK
Great Cave	0.45	-0.5/0	-0.02	VCS/CS	1.67	P	-0.21	NA	1.18	LK
Bats Cave	1.35	1	1.37	MS	2.60	VP	-0.04	S	1.14	LK
Rebecca's Cave	1.10	1	1.32	MS	1.90	P	0.18	PA	0.97	MK
Little Cayman Brac Cave	2.30	none	2.27	FS	2.27	VP	-0.06	S	0.85	PK
Peter's Cave 1st main passage	1.20	1	1.17	MS	2.07	VP	-0.05	S	1.44	LK
Peter's Cave 2nd main passage	0.55	2/2.5/-2.5	0.25	CS	2.05	VP	-0.15	PA	0.68	PK
Tibbetts Turn Cave	0.60	1	0.50	CS	1.65	P	-0.15	PA	1.28	LK
Cross Island Road Cave	-0.75	-1	-0.27	VCS	2.02	VP	0.44	VPA	1.50	VLK
Hospital Cave	-0.45	-2.5 /1	-0.27	VCS	2.26	VP	0.19	PA	0.81	PK

Mean	Standard deviation	Skewness	Kurtosis
V=very	V=very	V=very	V=very
M=medium	P=poor	N=negative	P=platy
C=coarse		P=positive	M=meso
F=fine		A=asymmetric	L=lepto
S=sand		S=symmetric	K=kurtic

were often located close to the walls where you might expect a higher proportion of coarser particles (pebble size) fallen off the wall as a result of mechanical breakdown. This does not, however, seem to influence the grain size at 5% cumulative frequency (Fig. 2.20).

2.6.2.5 Mineral composition.

The mineral composition of the insoluble residue of five cave sediment samples are represented in Figure 2.22 and Table 2.3. PB3 on the south side consist mainly of gypsum ($CaSO_4$). LC contains some gypsum as well but its main component is sand (SiO_2). The other three samples (PC1, CC and HC) consist of clay minerals (alumino-silicates) and PC1 and CC also have a considerable amount (10%) of iron.

2.6.2.6 Conclusion.

The sediments are mainly formed from the particles that are liberated as a result of the dissolution of the lime mud in between the grains of the bedrock. The bedrock over the whole island consist basically of allochthonous limestones with less than 10 % of the components being greater than 2 mm in diameter, which is reflected in the dominant grain sizes of the sediments (Fig. 2.21). The coarsest particles appear to be bigger pieces of bedrock and pieces of shells. That most of the sediment consist of bedrock particles is confirmed by the high percentage that is soluble and the grain size of insoluble residues.

Table 2.3 Principal mineral content of the insoluble residues of five cave sediment samples

	PB3		LC		PC1		CC		HC	
	wgt% of IR*	wgt% of TS**	wgt% of IR	wgt% of TS	wgt% of IR	wgt% of TS	wgt% of IR	wgt% of TS	wgt% of IR	wgt% of TS
SiO2	5.9	1.2	52.0	2.0	41.7	5.3	35.4	4.4	46.4	2.3
Al2O3	0.8	0.1	9.1	0.3	34.8	4.5	43.9	5.4	41.8	2.1
Fe2O3	<50ppm	0.0	2.0	0.1	10.1	1.3	10.2	1.3	1.5	0.1
P2O5	0.4	0.1	4.8	0.2	3.7	0.5	1.9	0.2	1.2	0.1
K2O	0.0	0.0	1.5	0.1	2.5	0.3	1.9	0.2	1.8	0.1
MgO	0.1	0.0	0.6	0.0	2.4	0.3	2.3	0.3	1.1	0.1
CaO	35.8	7.1	9.4	0.4	1.1	0.1	0.8	0.1	1.0	0.0
TiO2	0.0	0.0	1.3	0.0	2.1	0.3	1.7	0.2	2.2	0.1
SO3	56.3	11.2	13.1	0.5	0.2	0.0	0.2	0.0	1.5	0.1
Cl	0.3	0.1	2.4	0.1	0.2	0.0	0.9	0.1	0.5	0.0
F	0.3	0.1	1.3	0.0	0.6	0.1	0.3	0.0	0.5	0.0
TOTAL %	99.9	19.9	97.5	3.7	99.4	12.7	99.4	12.2	99.4	5.0
IR (%)		19.89		3.78		12.8		12.3		5.04

* IR = Insoluble residue

** TS = total sediment sample

Organic matter is in general not very abundant except in caves inhabited by bats and probably other animals, like different types of crabs and small mammals.

Colour determinations suggests that iron must be present in the majority of the sediments in greater or lesser amount. The iron rich material came probably from the terra rossa at the surface and was transported into the cave by seepage water. Only the insoluble residues of two samples (TC and CC) were clearly red which might indicate that these sediments contain a greater amount of iron than the other ones. However, determination of the mineral composition of the insoluble residues of LB3, LC, PC1, CC and HC show that PC1 has as much iron as CC. The difference in colour between the two insoluble residues might be due to different minerals containing the same ions.

The two most eastern caves, Little Cayman Brac Cave and Pollard Bay Cave 3, are the only ones that are not protected from the direct influence of the sea winds. Sea spray carried by these winds is therefore blown into the caves. This is reflected in the mineral composition of the insoluble residues of the sediments: SO_4 in both caves and chlorine and fluorine in Little Cayman Brac Cave. Furthermore Pollard Bay Cave 3 has a large opening about 3 m above the notch. During heavy storms and hurricanes the water might actually be swept into the cave or at least there will be a much higher input of sea spray. Little Cayman Brac Cave is about 12 m above the notch, hence water cannot enter the cave during heavy storms and hurricanes but there could be more sea salt been blown into it.

Peter's Cave is much higher in the cliff, has a small entrance and the coastal platform is vegetated, which together decreases the amount of sea salt blown into the cave. The other two caves, Cross Island Road Cave and Hospital Cave, are hidden behind vegetation. The insoluble residues of the sediments of all three caves consist mainly of clay minerals (alumino-silicates). The clay minerals as well as the silicates in Little Cayman Brac Cave, are the impurities of the bedrock that remained after dissolution. Some of this material may also have been brought in by infiltration water or fallen in from the surface.

CHAPTER THREE

WATER CHEMISTRY ANALYSIS

The degree of saturation with respect to calcite and dolomite of the waters occurring inside and outside the caves is of importance in understanding past and present dissolution processes. Therefore, it was decided to measure the pH, temperature, conductivity, alkalinity and total and calcium hardness of the waters.

3.1 Methods.

pH was measured with a Cole-Palmer ATC pH-meter which has a resolution and accuracy of 0.01 pH. The pH-meter was standardised against two buffers (pH = 4.00 and pH = 7.00) before each series of measurements. The temperature was taken with a Cole-Palmer dual-sensor digital thermometer, having a resolution of 0.1 °C and an accuracy of $\pm$ 1.0 °C in the range of -10 to 50 °C. A WSI (model number 33) S-C-T meter was used to measure the conductivity. The conductivity measurements were all converted to specific conductivity at 25°C using the function

$$Spc(25°) = 1.81\ Spc(T)\ e^{-0.023T}$$

where Spc (T) is the measured conductivity at T°C, T is the temperature in °C and the equation ranges from 0 to 40°C (White, 1988). The different types of hardness were measured using a Hach Digital Titrator (model number 16900-01).

During the 6 week period of this study only one day of heavy rain was experienced. The rest of the rain fell in the form of light rain showers mainly during the night. Only the heavy rainy day caused visibly more drip sites inside the caves. In general the caves are quite dry and there are not many drip sites, especially not those that have a fast enough drip to collect water for analysis in a relatively short time. Because of this lack of water in combination with the fact that the chemicals for the Hach titration kit arrived only two weeks before the end of the study period, there are not enough data for statistically valuable interpretations. However, some interesting trends appear and the data will therefore be presented as a matter of information.

The saturation indices of calcite and dolomite, the partial pressure of CO_2 with which the water was in equilibrium and the ion balance error were calculated using WCHEM3, a computer program developed by T. Wigley and modified by J. Drake.

pH, temperature and conductivity of 69 samples were measured. These were distributed as follows: 51 samples from 6 caves (6 from Hospital Cave, 16 from Bats Cave, 3 from Rebecca's Cave, 7 from Little Cayman Brac Cave, 15 from Peter's Cave and 4 from Great Cave), 4 rainwater samples, 8 samples of tap water which comes from a brackish well on the northeast side of the island, 5 seawater samples and one sample of a hypersaline lake on the south side of the island.

3.2 Results and interpretation.

3.2.1 pH, temperature and specific conductivity.

3.2.1.1 pH.

The pH of the different water types is quite distinct (Fig. 3.1; Table 3.1). The rainwater has a pH between 6 and 7, well water between 7 and 7.5, sea water between 8 and 8.5 and cave waters between 7.5 and 9. The sea waters have a much higher conductivity than the cave waters and can so be distinguished from them. The pH of the rainwater is somewhat high but still within or close to the values of 5.6 to 6.4 of "normal" rainwater (Ford and Williams, 1989). The pH of the well water seems to be in between the values of rainwater and sea water. This might be explained by the fact that the brackish well water is believed to be a mixture of the two mentioned waters. The pH of sea water is in general 8.1 to 8.3 and only exceeds the value of 8.4 in tidal pools, lagoons and estuaries (Bearman, 1989). Two of the sea water samples exceed 8.4 although they have not been taken from either of the three environments. Table 3.1 shows that neither the salinity nor the temperature seems to have had any influence in these high pH-values because the salinity of one sample is very low and the temperature is not different from other samples with lower pH values. The pH values of the cave water samples are typical for carbonate regions. The values of the individual caves are not constant or even grouped together. This is due to the fact that they represent samples of different types of water taken at different dates, occurring at different distances in the cave and at different depths under the surface.

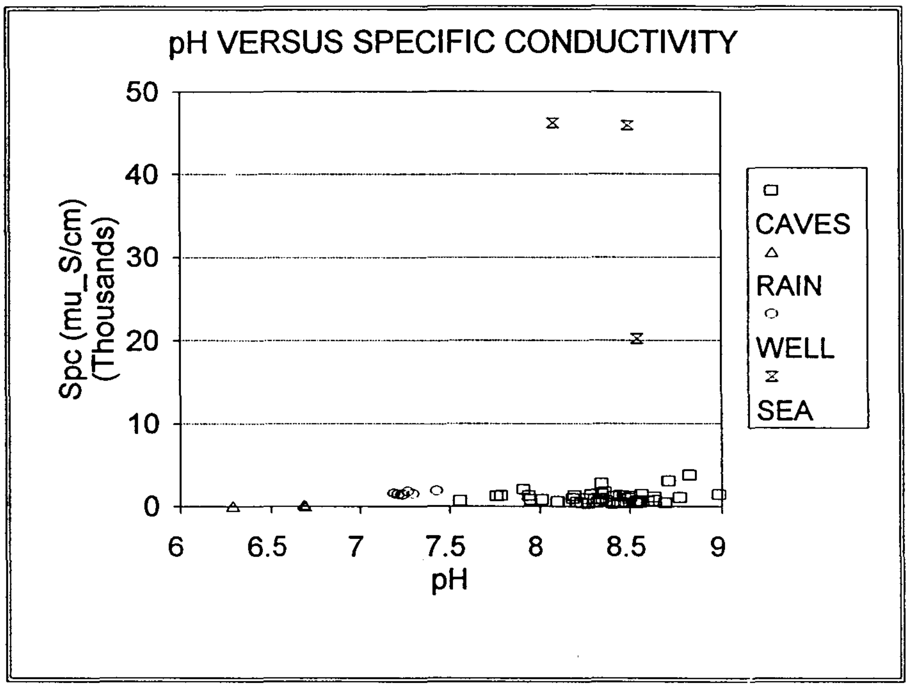

Fig. 3.1a. pH and specific conductivity on Cayman Brac.

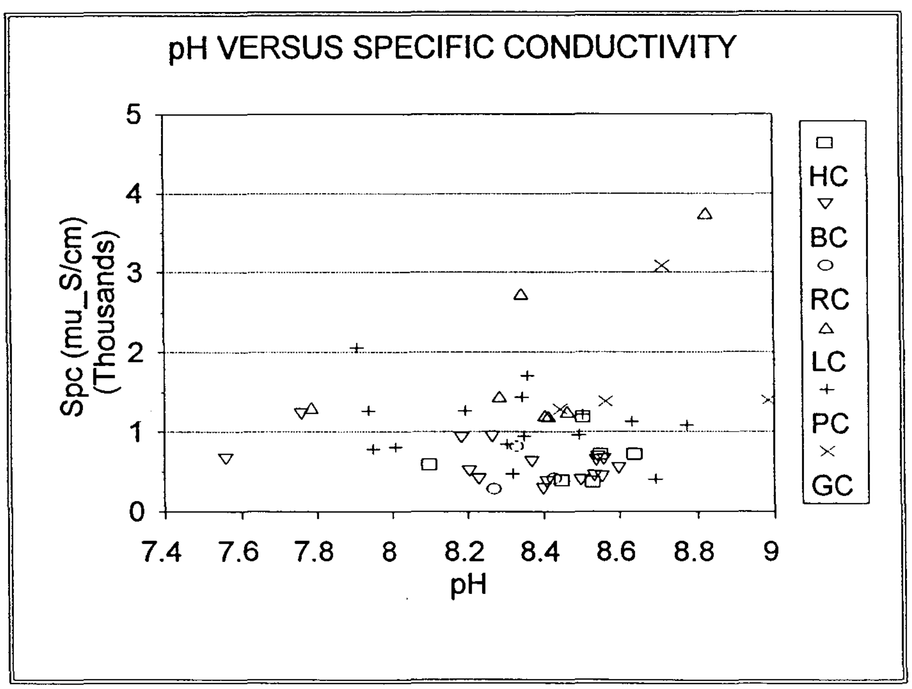

Fig. 3.1b. pH and specific conductivity of cave waters.

Table 3.1 pH, Temperature and Specific conductivity.

Sample site	Distance from the entrance (m)	Spc (25 C) (muS/cm)	pH	Temp. (C)
RC	19	291	8.27	26.4
RC	14	414	8.43	26.7
RC	11	820	8.33	26.7
BC	porch: 5	926	8.19	25.3
BC	1	394	8.50	25.1
BC	13	626	8.37	25.7
BC	19	684	8.55	25.2
		656	8.56	25.4
BC	cliff	287	8.40	23.9
BC	0	645	8.54	24.4
		541	8.60	24.5
BC	notch	375	8.41	25.2
		409	8.23	25.4
BC	0	435	8.56	25.3
BC	notch	507	8.21	25.6
BC	pool: 0	1231	7.76	26.9
		664	7.56	27.3
BC	porch: 1.5	447	8.54	25.8
BC	6	944	8.27	25.5
GC	16	1284	8.45	25.9
GC	5	1908	-	25.9
		-	8.83	26.1
GC	7	2016	-	26.0
		3086	8.72	26.0
GC	17	1706	-	26.0
GC	25	1821	-	25.9
GC	19	1696	-	25.9
GC	28	1543	-	26.0
GC	Lake: 40	1384	8.57	26.3
GC	Pool: 35	1393	8.99	26.0
HC	1	457	-	27.9
HC	5	794	-	26.7
		394	8.45	26.5
HC	10	594	8.10	26.2
		1190	8.51	25.7
		723	8.55	25.9
		723	8.64	25.9
HC	1	377	8.53	26.4

Sample site	Distance from the entrance (m)	Spc (25 C) (muS/cm)	pH	Temp. (C)	Salinity (permill)
PC	1.5	785	7.95	26.6	
PC	5	2062	7.91	26.6	
PC	10	1270	7.94	26.4	
PC	33	946	8.35	27.1	
PC	10	808	8.01	26.7	
PC	35	1130	8.64	27.5	
		1216	8.51	27.0	
		1085	8.78	25.9	
PC	2	844	8.31	26.1	
PC	3	1706	8.36	25.0	
PC	5	1266	8.20	26.1	
PC	10	406	8.70	26.2	
PC	35	476	8.32	27.1	
PC	35	960	8.50	28.1	
PC	8	1438	8.35	25.4	
LC	0	2730	8.35	26.7	
LC	20	1247	8.47	25.9	
LC	23	1306	7.79	25.6	
		1443	8.29	26.0	
LC	25	1207	8.41	26.0	
LC	3	3748	8.83	26.4	
LC	18	1194	8.42	26.0	
Rain		10	6.29	23.9	
		3	6.70	27.6	
		178	6.69	25.7	
		234	-	25.9	
Well		1346	7.23	30.5	
		1446	7.21	27.4	
		1442	7.24	27.5	
		1505	7.19	28.5	
		1477	7.30	31.9	
		1538	7.19	29.5	
		1781	7.27	28.6	
		1840	7.43	29.7	
Sea		> 50,000	8.09	26.6	31.5
		20157	8.55	29.6	27.0
		> 50,000	8.14	29.3	29.5
		46197	8.08	27.8	29.0
		45918	8.50	29.5	30.0
Lake		> 50,000	8.83	33.6	>40

3.2.1.2 Temperature.

The temperature of all the water samples ranges from about 24 to 32 °C while the cave water temperature varies between about 24 and 28 °C. The temperature of both well and sea water varies with the time of sampling due to solar heating.

The water temperature, as was the case for the pH, differs from cave to cave and within each cave: in Great Cave the temperature varies only 0.4 °C while in Bats Cave there is a range of 3.4 °C and in Peter's Cave of 3.1 °C. The thicker layer of bedrock overlaying Great Cave increases the time the water needs to reach the cave and thus the time available to the water to attain thermal equilibrium with the bedrock. The temperature at all different sites in the cave will therefore be more constant in comparison to the water temperature of the different sites in Bats Cave or Peter's Cave. One of the samples in Great Cave is from a lake in which the water has had enough time to come into equilibrium with the air and the temperature of approximately 26 °C can thus be considered as the general temperature of the bedrock and the cave air. About 26 °C is also encountered in Little Cayman Brac Cave where two sites with warmer water were located close to the entrance while the five sites with water of about 26 °C are all further inside. In general the temperature inside a cave away from the entrance does not vary more than one °C and is close to the mean annual temperature (Ford and Williams, 1989) which in this case will be about 26 °C. The mean annual temperature at Montigo Bay, Jamaica (the closest available meterological station for a continuous temperature record), is 26.3 °C which agrees with the 26 °C observed inside the caves.

3.2.1.3 Specific conductivity.

Specific conductivity (Spc) reflects the total ion concentration in a solution and is therefore used as an estimate of the total dissolved solids concentration (Foster *et al.*, 1982). The high salinity of the sea (between 27 and 31.5 ‰) and lake (>40 ‰ (the upper limit of the meter)) water will therefore cause high Spc values. As a matter of fact the conductivity of two of the sea water samples and the lake water sample exceeded the upper limit of 50,000 $\mu S\ cm^{-1}$ of the conductivity meter. Rainwater on the other hand is very pure water and its Spc does not exceed 235 $\mu S\ cm^{-1}$. The Spc of well water is relatively constant at around 1500 $\mu S\ cm^{-1}$ while the Spc values of the cave waters vary between 275 and 3800 $\mu S\ cm^{-1}$. The high values observed in Little Cayman Brac Cave are from sites close to the entrance which will reflect the influence of sea spray. In Great Cave the lowest Spc values are from the lake and the highest from a site 7 m from the entrance. The caves with a thin roof, such as Bats, Rebecca's and Hospital Cave, have lower Spc values than Great Cave and Little Cayman Brac Cave that have more than 20 m of bedrock on top of them. Peter's Cave seems to fall in between the two groups. The thickness of the roof influences the amount of bedrock the water comes into contact with and the time available for the chemical reactions to take place: the longer the journey the more ions there will be in the water and the higher the Spc.

3.2.1.4 pH versus specific conductivity.

Figure 3.1 shows that there is no relationship between the pH and the specific conductivity (Spc) of the rain, well and cave water samples. However, there appears to be an upper limit, increasing with both pH and Spc.

3.2.1.5 Temperature versus specific conductivity.

A relationship between temperature and Spc does not exist (Fig. 3.2). The temperature has no influence on the Spc of the well water nor the rain water. As for the cave waters, each cave behaves differently and no general pattern can be read from it (Fig. 3.2b).

3.2.2 Alkalinity and hardness.

The results of the chemical analysis of the different water samples are given in Table 3.2. The table reveals that all ion balance errors (IBE) are larger than the generally accepted limit of 5%. For the samples of sea and lake water this can be explained by the presence of other ions that have not been analysed. The IBE's of the cave and well waters are all well over the acceptable limit but they are close to each other which suggests the influence of (a) foreign ion(s). The most plausible explanation is the influence of chloride, sulfate and other ions in sea salt particles that are present in the air and that can be removed from it in three different ways: washout by precipitation, fallout by gravity and interception by obstacles (Junge and Gustafson, 1957).

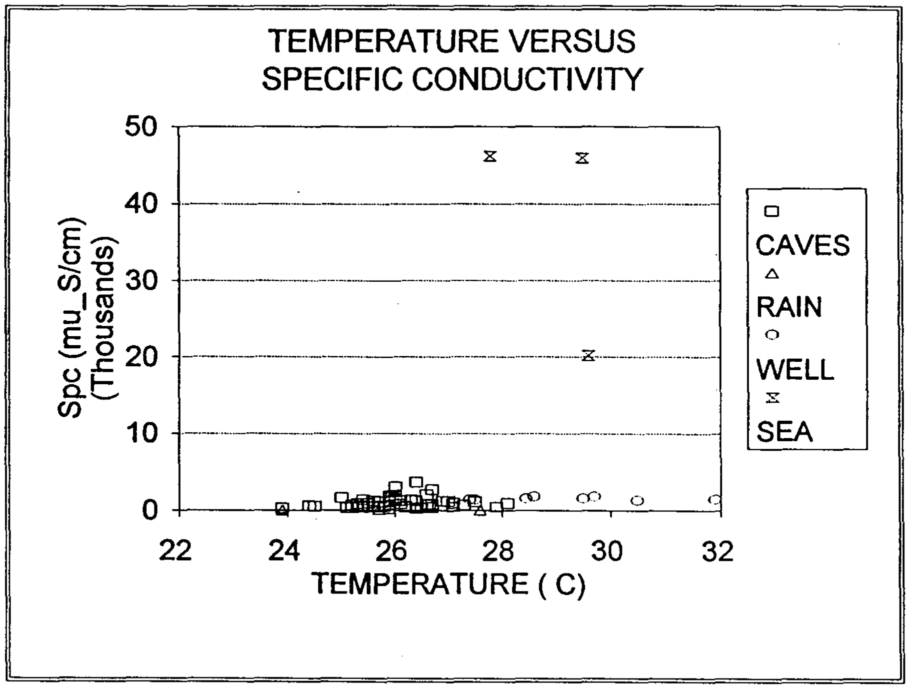

Fig. 3.2a. Temperature and specific conductivity on Cayman Brac.

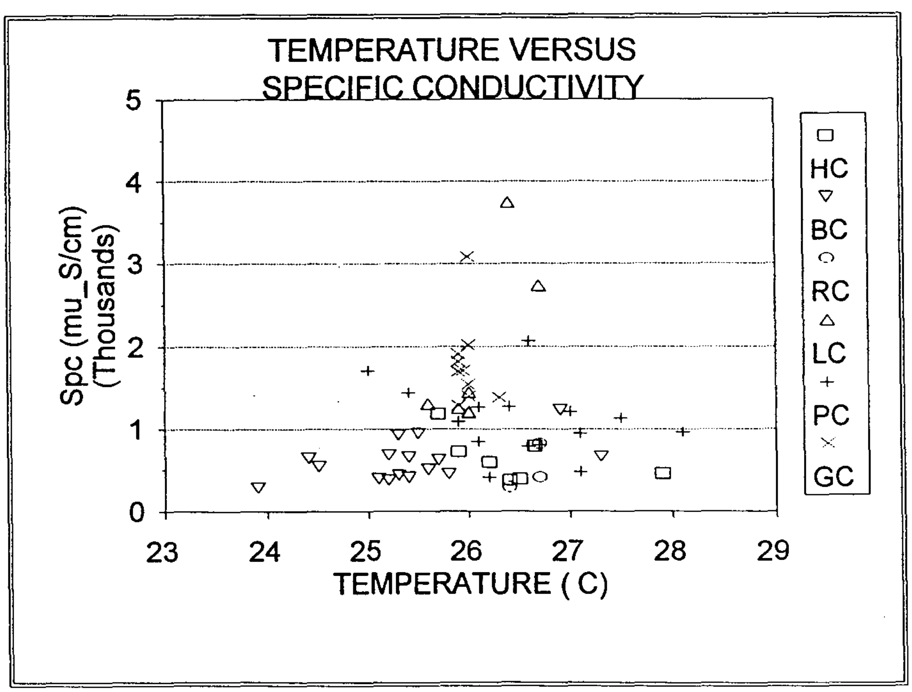

Fig. 3.2b. Temperature and specific conductivity of cave waters.

Table 3.2 Water Chemistry analysis.

Sample sit		Formation**	Spc (25 C) muS/cm	pH	Temp. (C)	Alkalinity (mg/l CaCO3)	Total Hardness (mg/l CaCO3)	Calcium Hardness (mg/l CaCO3)	Magnesium Hardness (mg/l CaCO3)	Non alkalin Hardness (mg/l CaCO3)	SI*** calcium (mm/L)	SI magnesium (mm/L)	SI gypsum (mm/L)	pPCO2 (atm)	IBE**** (%)
LC	23m IN*	BRAC (L)	1443	8.29	26.0	312	388	182	206	76	0.84	1.93	-1.77	3.05	28.19
LC	18m IN	BRAC (L)	1194	8.42	26.0	280	372	180	192	92	0.90	2.03	-1.69	3.24	26.48
PC	3m IN	CAY (D)	1706	8.36	25.0	410	574	258	316	164	1.09	2.46	-1.39	3.03	25.86
PC	8m IN	CAY (D)	1438	8.35	25.4	386	552	260	292	166	1.07	2.38	-1.37	3.04	25.18
GC	LAKE(40m IN)	BRAC (D)	1384	8.57	26.3	332	380	216	164	48	1.20	2.48	-1.88	3.33	31.47
GC	POOL(35m IN)	BRAC (D)	1393	8.99	26.0	282	406	222	184	124	1.42	2.95	-1.50	3.92	26.20
GC	7m IN	BRAC (D)	3086	8.72	26.0	450	636	230	406	186	1.36	3.15	-1.25	3.43	27.39
GC	5m IN	BRAC (D)	0	8.83	26.1	282	600	246	354	318	1.25	2.86	-1.16	3.75	17.67
RAIN			234	6.69	25.9	20	8	2	6	-12	-3.69	-6.69	-4.12	2.56	-47.26
WELL		IRON (L)	1781	7.27	28.6	284	414	296	118	130	0.04	-0.07	-1.35	2.01	23.24
WELL		IRON (L)	1840	7.43	29.7	298	450	266	184	152	0.18	0.45	-1.35	2.15	22.71
SEA			46197	8.08	27.8	141	8405	1475	6930	8264	0.46	1.81	0.17	3.33	-22.22
SEA			45918	8.50	29.5	128	8200	1375	6825	8072	0.73	2.39	0.08	3.96	0.87
LAKE			45964	8.83	33.6	147	10670	1685	8985	10523	0.97	2.97	0.18	4.44	0.83

* IN = from the entrance

**BRAC = Brac Fm
CAY = Cayman Fm
IRON = Ironshore Fm
L = limestone
D = dolostone

*** SI = Saturation Index
**** IBE = Ion Balance Error

3.2.2.1 Sea salt particles.

Due to the breaking of waves ("whitecaps") and some other less known processes, air bubbles are created in the water which then rise back up to the surface and break. The breaking of these bubbles forms jet and film drops and these drops may be transported away by wind owing to their small size. The exact size distribution of the air bubbles is not known but bubbles of < 20 to 30 μm and up to several millimetres in diameter have been observed (Blanchard and Woodcock, 1980). From each air bubble 1 to 10 jet drops are formed out of the unstable jet of water that rises rapidly from the bottom of the collapsing bubble cavity after this jet is formed due to the conversion of surface free energy of the bubble into kinetic energy. The maximum drop ejection height depends on the size of the bubble and peaks at nearly 20 cm for bubbles with a diameter of 2 mm. Film drops are formed from the bursting of the film of water which separates the air in the bubble from the atmosphere. The number of film drops from one air bubble can be many times more than the number of jet drops, e.g. a 6-mm bubble produces up to a 1000 drops but drops of < 0.3 mm do not give any film drops at all. While the size of a jet drop is about one tenth of the size of an air bubble, the size of film drops is more in the order of a few micrometers (*op. cit.*).

All these drops of sea water are more commonly called sea-salt particles because the water may or may not be evaporated, depending on the relative humidity (and other factors) of the atmosphere and on the drop size. Hence sea-salt exists as sea water drops, brine drops or sea-salt particles in the air. The composition of these sea-salt particles is close to the composition of sea water (*op. cit.*), i.e. over 55% is chloride, 30.6% sodium and 7.7% sulfate (Reilly and Goodman, 1985). The yearly production of sea-salt particles by the ocean is 10^9 to 10^{10} ton and was calculated based on the assumption that the rate of production equals the rate of reentering of the particles into the ocean (Blanchard, 1985).

Due to vertical mixing the size distribution of sea-salt particles is spatially uniform through out the troposphere although the concentration decreases with height. As mentioned above, the removal of these particles is by washout, fallout and interception by obstacles, like vegetation. Sea-salt particles are hygroscopic and thus constitute the condensation nuclei of raindrops. In their fall the raindrops coalesce with other sea-salt particles so that even more salt will reach the ground. Particles with a size of > 10-20 μm tend to fall back to the surface under their own weight which is large enough to overcome the upward force exercised by the wind. However, the removal by this process is only one quarter of that by washout. The impaction of the particles on obstacles such as trees and bushes seems to be quite an efficient way to remove the particles from the air (Junge and Gustafson, 1957). The efficiency of catch increases with increasing wind speed and decreasing radius of the obstacle. On account of the hygroscopic nature of these particles, it is almost impossible for the wind to remove them once they are caught. As the lower layers of the atmosphere get depleted of the particles others will be transported from higher levels by turbulence, especially under strong winds. An estimate of the amount of chloride intercepted by vegetation in northern

Sweden is in the order of several kg ha^{-1} yr^{-1} (Eriksson, 1955). Subsequently rainwater will wash the intercepted salt off the obstacles and transport it into the ground.

3.2.2.2 Hardness.

The total hardness, reflecting the cation (basically Ca^{2+} and Mg^{2+}) concentrations in the water, is in all but one case greater than the alkalinity which represents the bicarbonates. This is due to the salts that form between Ca^{2+}, Mg^{2+} and the anions from the sea salt particles. The alkalinity therefore best reflects the dissolution of the carbonate bedrock. Due to the lack of water it was not possible to repeat the analysis of one water sample in order to get a verification of the measurements. However, an average alkalinity of 342 mg l^{-1} as $CaCO_3$ was found for the cave water samples, 291 mg l^{-1} as $CaCO_3$ for the well water samples and 139 mg l^{-1} as CaCO3 for sea and lake water samples. Because the measurements of the alkalinity and the total hardness of the rain water sample do not agree with each other it is believed that the alkalinity of the rain water sample is overestimated and that the measurements should not be considered valid. The calculations of the saturation indices (SI) should also be interpreted with caution because

1. the concentrations of magnesium and sulfate have not been measured which decreases the accuracy of the $SI_{calcite}$,
2. they might be influenced by trace elements present in the sea salt particles and thus in the water and

3. the precision of the pH measurement might not be good enough to detect significant variations in saturation of the ion in question (Worthington, 1991).

The calculation of the theoretical partial pressure of CO_2 is very sensitive to pH (it changes one order of magnitude for each pH unit) and depends on the alkalinity. The $pPCO_2$ for the atmosphere is 3.30 and the values calculated for the cave water samples reveal that these waters have CO_2 partial pressure very close to the outside air.

CHAPTER FOUR

SPELEOTHEM ANALYSIS

4.1 Types of speleothem (Fig. 4.1).

Although the term "speleothem" embraces all secondary mineral deposits in caves, they consist largely of calcite which has been precipitated from supersaturated solutions as a consequence of the diffusion of CO_2 from the drip water into the cave atmosphere (Jennings, 1985). The different forms of speleothem can be grouped into dripstone, flowstone, rimstone and rimstone pool deposits, speleothems due to capillarity and cave pearls (Bögli, 1980). Speleothems may assume a wide range of colours depending on the type of impurity they contain. Pure calcite is transparent but red and black are very common colours.

In the caves on Cayman Brac, as in almost all caves, dripstone and flowstone predominate. However in one part of Peter's Cave "moonmilk" is the dominant form.

4.1.1 Dripstone

As the name indicates, dripstone is formed as a result of dripping water. It comprises stalactites, stalagmites, columns and draperies.

Stalactites hang from the ceiling or from any overhanging surface. A

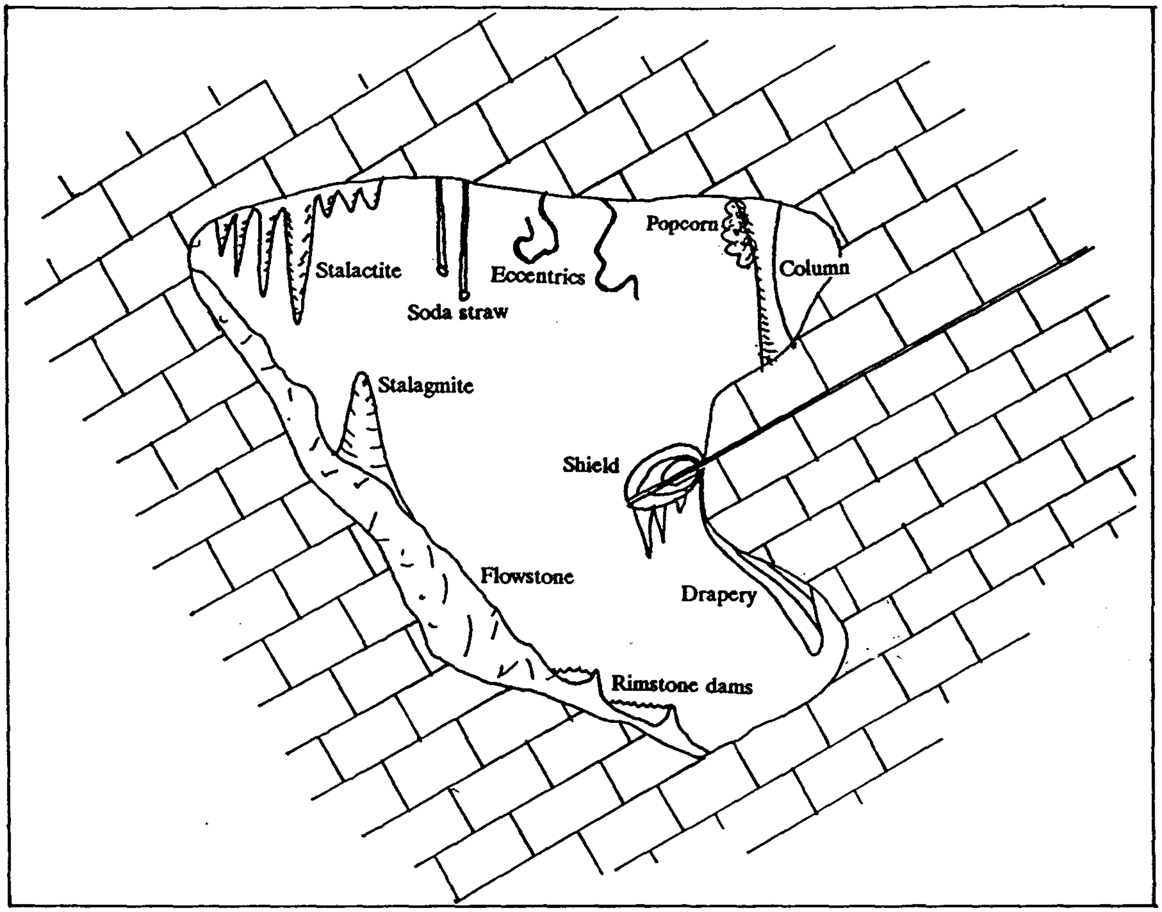

Fig. 4.1. Schematic sketch of speleothem types

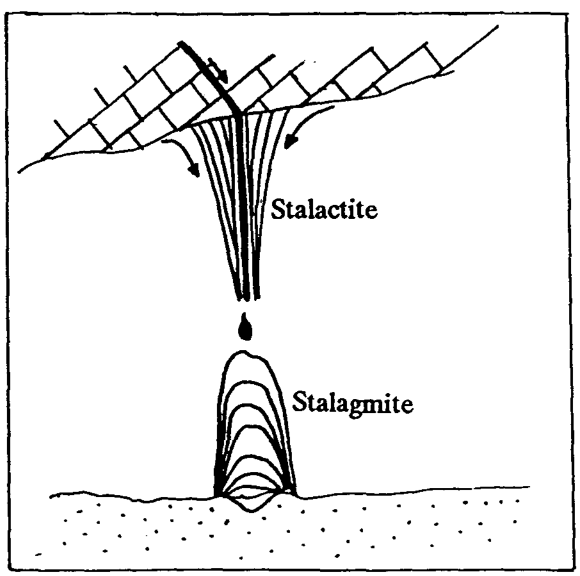

Fig. 4.2. Schematic cross section through a stalactite and stalagmite.

stalactite always starts as a "soda straw", a hollow sinter tube with the diameter of a water droplet (~5 mm). It grows only lengthwise at the end of the tube. When, for any reason, the tube is blocked, the water is diverted and flows along the outside of the tube, thus contributing to the growth in width and length of the stalactite. In cross section a stalactite always shows the inner initial tube with semi-circular growth layers around it.

Stalagmites grow upward from any available surface as a result of calcite deposition by water drops falling from a stalactite or directly from the ceiling. In contrast to stalactites, stalagmites grow by the deposition of cap-shaped layers that thin out along the sides (Fig. 4.2). The minimum diameter of a stalagmite is about 3 cm (Curl, 1973), one order of magnitude larger than for a stalactite.

Columns form when a stalactite meets a stalagmite or when either one reaches the opposite surface. It depends on the drip speed and/or on the speed of the reactions involved, which one of the two dripstone types will dominate.

A *drapery* is a form of hanging dripstone that results from water flowing down along an inclined ceiling or wall and which deposits calcite along the way.

4.1.2 Flowstone

Flowstone is caused by calcite deposition from a thin sheet of water flowing over bare rock or sediments. It might happen that the sediment on top of which the flowstone is formed is later washed away and the flowstone is left behind as a bridge, or "false" floor.

4.1.3 Rimstone and rimstone pool deposits

When a thin sheet of flowing water encounters a bump or rim, it thins when passing over it. This thinning causes an increased loss of CO_2 and thus preferential deposition of calcite. As a result the rim grows in height and may dam off the water to form a pool. After the formation of the pool, growth of the rim continues in the same way when the pool overflows. These pools vary in width and depth from a few millimetres (microgours) to several meters.

In pools, calcite may precipitate in the form of (among others) "cauliflowers", calcite ledges along the walls or floating calcite.

4.1.4 Speleothems due to capillarity

Eccentrics or helictites appear to defy the force of gravity and grow in every direction imaginable on bedrock as well as on speleothems. They are small, thin, twisted and often dendritic formations that posses a very fine channel into which water can be sucked through capillary action (Bögli, 1980).

Shields consist of two, spherical, parallel plates separated by a medial capillary crack. Growth is outward along the rim by water that is brought here through capillary action. Often the weight of the stalactites or draperies formed at the lower plate pulls the latter down and so widens the medial crack, inhibiting further growth. It might even happen that the lower plate breaks off all together (Hill and Forti, 1986).

4.1.5 Moonmilk

According to Hill and Forti (1986, p. 46) moonmilk is "a term used to describe aggregates of microcrystalline substances of varying composition....Moonmilk is soft, plastic, and pasty when wet, but crumbly and powdery when dry". The exact origin is not yet understood but the following hypotheses have been postulated (Hill and Forti, 1986):

1. Carbon dioxide is expelled from the limestone bedrock due to the freezing of the limestone by ice and a milky fluid is formed on the limestone wall.
2. Microorganisms are responsible for the formation of moonmilk.
3. Moonmilk is a form of disintegrated speleothem or bedrock.
4. As a result of particular physio-chemical conditions the crystals that precipitate from the water remain very small and do not grow larger. Moonmilk is thus a direct precipitate from water like any other speleothem.

4.2 Dissolution types of speleothems.

In all caves examined on Cayman Brac the majority of the speleothems were more or less attacked, dissolved. This is a state that has also been observed elsewhere in the Caribbean; e.g. on Grand Cayman Island (Smith, 1987), on Isla de Mona, Puerto

Rico (Field trip, May 1993) and on several islands of the Bahamas (Mylroie *et al.*, 1991; Mylroie, personal communications 1993).

The speleothems observed in the different caves on Cayman Brac can be divided into three dissolution types (Fig. 4.3):

1. Remnants of speleothems (mainly flowstone) in the walls or ceilings. Often associated with breccia. The transition between the wall, the speleothem and/or the breccia is so smooth that it is not perceivable when felt with closed eyes. The speleothem and/or breccia is seemingly attacked at the same time as the bedrock in which it is located. There is no active growth of new calcite.
2. Speleothems that still preserve their original form (stalactite, stalagmite, column, flowstone,..) but which, at closer look, appear to have been reduced considerably in size. Attack has often taken place preferentially on one side of the speleothem but in the individual caves these sides do not appear to indicate the same direction on all speleothems. Active growth has stopped.
3. Speleothems that are not or negligibly dissolved. The majority of these speleothems are still actively growing.

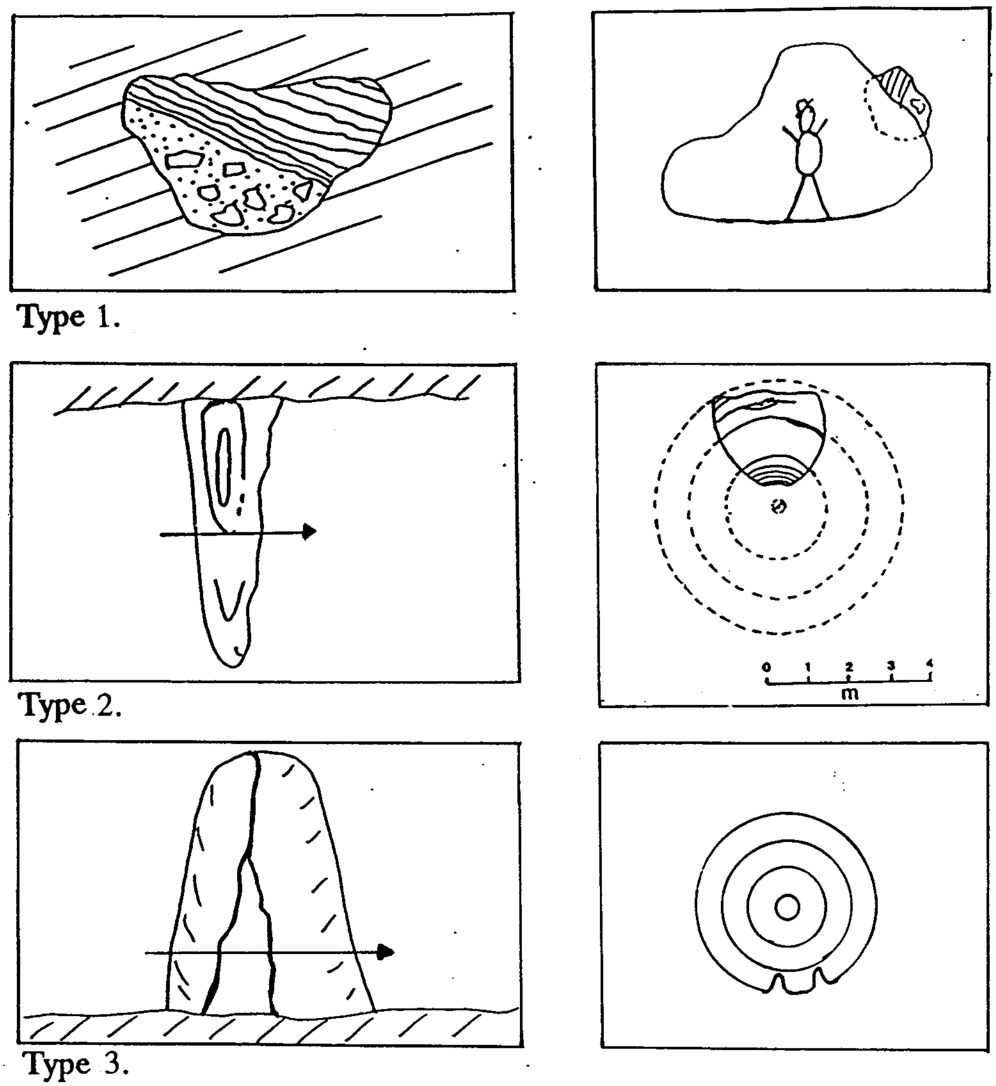

Fig. 4.3. Schematic sketch of the three dissolution types encountered on Cayman Brac.

4.3 Possible causes of dissolution.

The causes of the dissolution have not yet been established. Erosion by wave action does not seem to be very likely given the fact that dissolved speleothems have been found deep inside caves were waves could never have entered with full force, if at all.

Aggressive water is the most plausible agent of attack. It is however not clear where the water came from and how it happened to be aggressive. Several processes might be suggested:

1. The water forming the speleothem changes from (super)saturated to undersaturated with respect to calcite. The first signs of this type of dissolution are fluted and etched speleothems. This can evolve so far that the speleothem becomes perforated or completely disappears (Hill and Forti, 1986). This is "point source dissolution".
2. The cave passage is flooded by water from another source that is aggressive with respect to calcite ("body dissolution" - Gascoyne *et al.*, 1983).

   On Cayman Brac, during periods of high sea level the water may rise higher than the cave and the cave could be situated again in aggressive water, i.e. the fresh water lens or halocline.
3. Condensation corrosion, i.e. corrosion of bedrock or speleothem by

condensation water charged with a high level of carbon dioxide (Hill, 1986). This may be the result of changes in the physio-chemical environment of the cave due to climatic changes, the settling of a bat colony upwind or episodes of geothermal activity (Ford and Williams, 1989).

4.3.1 Dissolution due to change in the nature of the feedwater.

Changes in the nature of the feedwater of a speleothem can be caused by changes in the origin of the water, the vegetation and/or soil composition in the area where the water comes from or climatic changes inside and/or outside the cave. The percolation water reaching the cave is still undersaturated with respect to calcite and instead of depositing calcite to form speleothems, it can dissolve them. Thus, small dissolution features occur where this aggressive seepage water comes into contact with speleothem.

4.3.2 Dissolution due to flood water.

In the case of continental caves, passages might be flooded periodically by high river stands but on small oceanic islands, where rivers are absent, only relative rises in sea level can be responsible for the flooding of caves. As a result the caves are filled with water and the dissolution process that formed them in the first place may be renewed. The speleothems that have formed during dry periods may then be dissolved at the same time as the bedrock.

Theoretically, dissolution in the phreatic zone where water is stagnant or very slow flowing, is non-differential and results in relative equidimensional *solution pockets* (Hill, 1987; Bögli, 1980). These solution pockets vary in size from a few centimetres up to several meters in diameter. Caves in the phreatic zone often show a sort of "Swiss cheese" morphology (called *spongework* when the cavities are centimetric in diameter and depth or *boneyard* when larger) due to this non-differential dissolution (Hill, 1987). The cave maps of the notch caves show these rounded forms very clearly (Figs. 2.1 - 2.6).

4.3.3 Condensation corrosion

For condensation corrosion to take place three conditions need to be satisfied (Hill, 1986):

1. a high CO_2 (or any other acidic vapour) level in the cave atmosphere,
2. high relative humidity (close to 100%) and
3. a thermal gradient between the air in different parts of the cave.

Due to the thermal gradient, warm, moist air flows towards areas of lower temperature and humidity. In so doing the dew point of the air is reached and the surface on which the water condenses might be corroded by the latter (*op. cit.*). Therefore, dissolution is preferentially on the windward side of the speleothem or bedrock. As a consequence, deposition of calcite in the form of popcorn shaped speleothem might occur on the leeward side of speleothems or bedrock wall. It is also possible that the dissolved material is carried away in the water drops in the air. Due to evaporation of the water, the water drop becomes a dust particle, even easier to be transported by the wind.

The morphology resulting from condensation corrosion depends on where the water condenses and if it flows down along, drips down from or remains on the surface. Water condensing on the ceiling and falling back to the floor forms rillenkarren and spitzkarren in the floor, while water flowing down the wall forms corrosion channels. Concave pockets, caused by a corrosive air flow, resemble solution pockets that are formed in the phreatic zone but, according to Hill (1986, p. 31), the air scallops can be distinguished from the water-formed scallops by their much larger form and exhibition of blunt, rather than sharp, crests. It is possible that they are a mere modification by the air flow of a preexisting water-formed scallop, but it is also possible that the air was the sole agent responsible for the scallop. Corrosion of bedrock and speleothem appears to occur without any distinction and scallops are found crossing smoothly from one to the other (*op. cit.*).

4.4 Distribution of the speleothems.

Speleothems are present to some extent in all the caves studied on Cayman Brac. In general the notch caves have less speleothems than the caves located higher in the cliff. For each cave the speleothem content has been mapped by morphology and dissolution type.

4.4.1 The notch caves.

4.4.1.1 Rebecca's Cave (Fig. 4.4).

The northern wall of Rebecca's Cave is full of speleothem belonging to the first dissolution type. Figure 4.5 shows three different examples. The sites from which the examples are shown are indicated on Figure 4.4. At site 1 there is a layer of stalactites overtop of flowstone. This combination continues in a northern direction along the eastern wall of the most western part of the cave. The stalactites probably developed first in the cavity after which it was infilled with flowstone. Site 2 shows a complicated combination of probably three different stages of speleothem growth (Fig. 4.5b). The oldest consists of flowstone, the next stage of stalactite and flowstone, and the last one is again flowstone that does not appear to belong to the first dissolution type but more likely to the third. Figure 4.5c shows flowstone that probably infilled a crack and some small cavities.

Patches of old speleothem exist every where in the ceiling of the cave. The only speleothem belonging to the third type is situated in the western half of the cave around the skylights. The majority of these speleothems look like popcorn, indicating that their formation is probably due to the evaporation of the feed water. In the southern wall, east of the entrance, cauliflower-shaped speleothem that has not been dissolved is located close to the floor. It appears to have formed underneath the sediment cover as a result of a reaction between the sediment and the wall.

Legend to Figures 4.4 - 4.12.

(Turn over)

Legend to Figures 4.4-4.12:

- Stalactite
- Stalagmite
- Column
- Drapery
- Flowstone
- "Popcorn"
- Eccentrics
- Gours
- "Cauliflower"
- M Moonmilk
- Type 1 speleothem in the wall
- Type 1 speleothem in the ceiling
- Type 2 speleothem

- Type 3 speleothem
- Water
- Ceiling channel
- Breccia
- (Gypsum) crust on the ceiling
- (Gypsum) crust on the wall
- Mixture rock
- Coral-rich rock
- C Caymanite
- Breakdown blocks
- Roots
- Fracture
- Bellhole
- Skylight

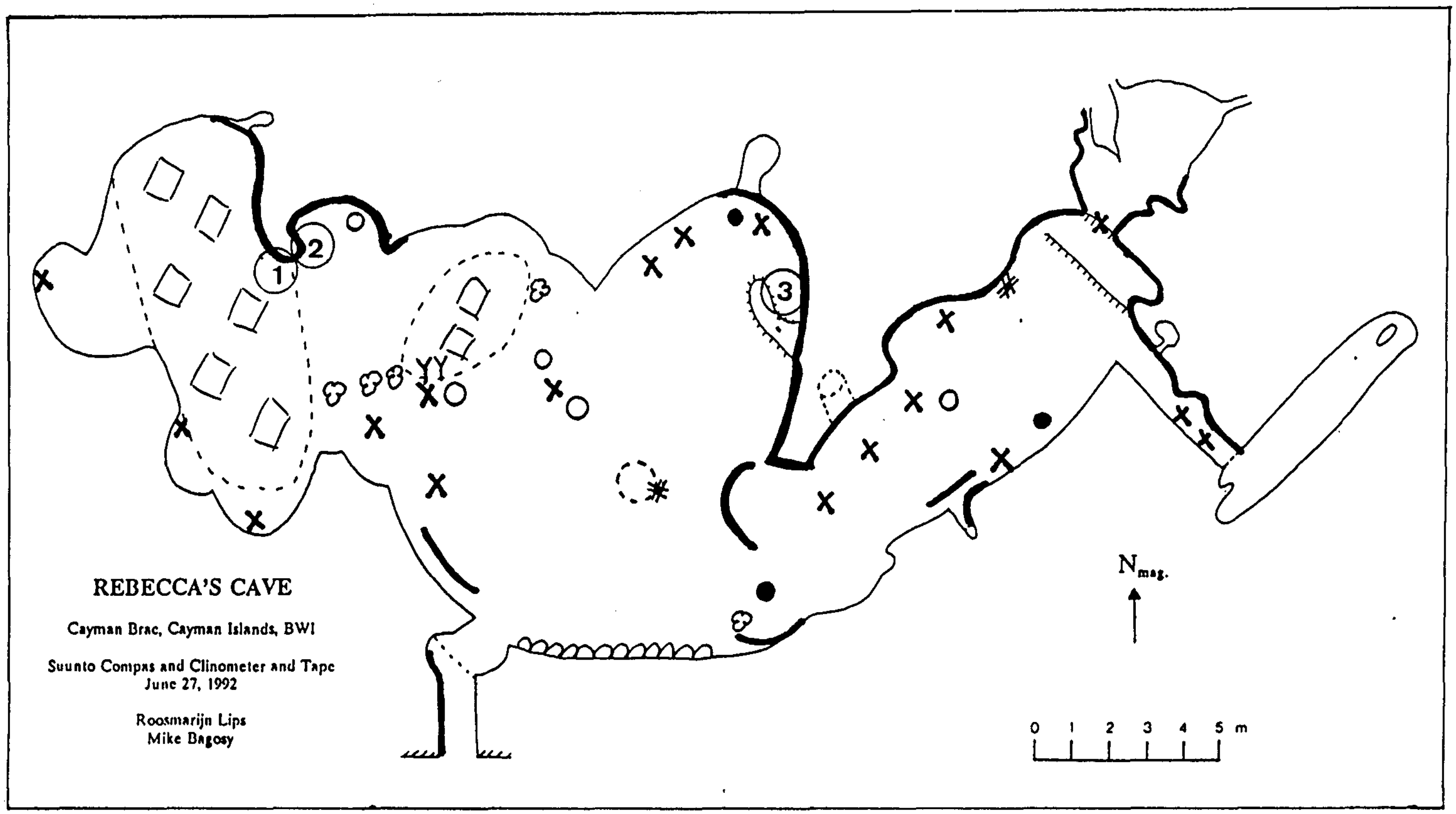

Fig. 4.4. Speleothem distribution in Rebecca's Cave.

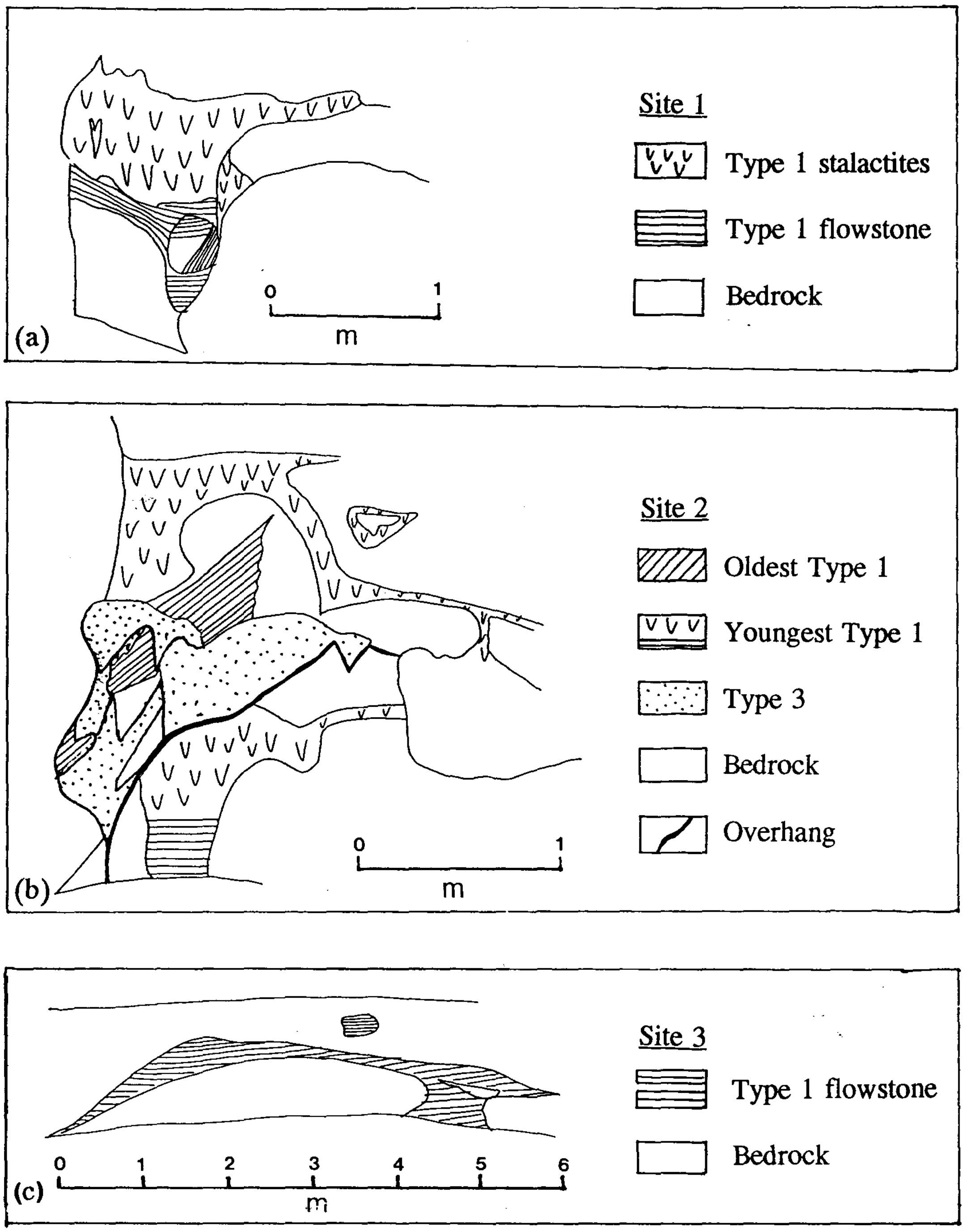

Fig. 4.5. Schematic sketches of the wall containing Type 1 speleothem in Rebecca's Cave.

4.4.1.2 Bats Cave (Fig. 4.6).

The majority of the speleothem in Bats Cave are situated close to the entrances and in the porch. However, walls of the passages where the roof has collapsed are covered by algae and small pockets which make it very difficult to examine them.

All three speleothem dissolution types and breccia are present. The first type is visible as lines of a few centimetres wide running along the wall for a few metres or as small patches in the ceiling or walls. The breccia is situated in the northern walls and in the ceiling. There is also a large patch of breccia in the ceiling close to the middle passage (Fig. 4.6) indicating that once there was a fairly large cavity or depression in which clastic debris collected.

Speleothems of the second type consist mainly of dripstone and some flowstone. All the dripstone is concentrated around the western entrances while the flowstone is mainly along the eastern wall. Almost all Type 3 speleothems are flowstone located in the western small cave. In the most eastern corner of the cave there is also flowstone of the third group with small dissolution gullies, formed by feed water that became acidic probably due to the presence of roots that are visible through the small opening from which the water must have come.

4.4.1.3 Great Cave (Fig. 4.7).

The speleothems in Great Cave are generally situated away from the entrance, in contrast to those in Bats Cave.

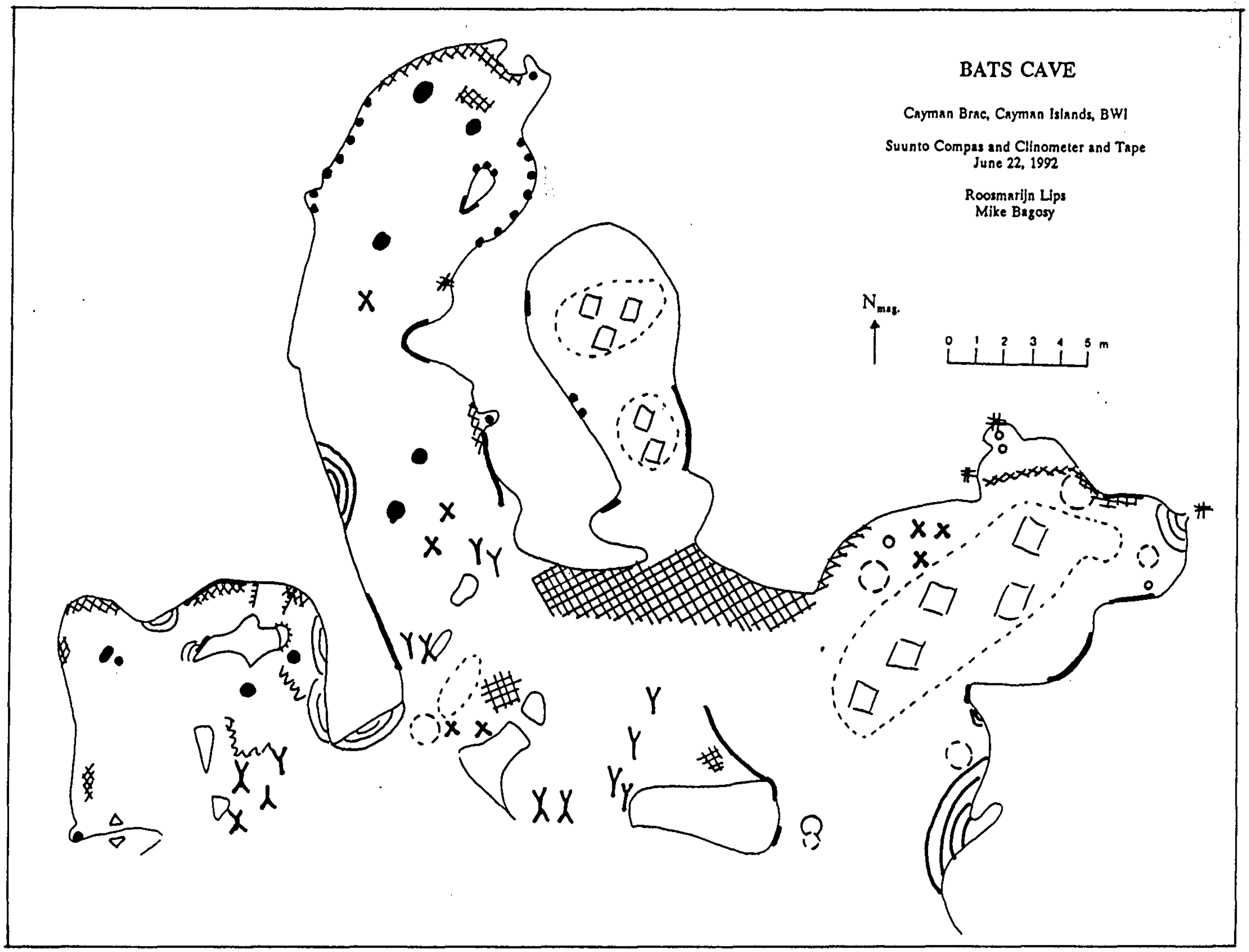

Fig. 4.6. Speleothem distribution in Bats Cave.

Apart from a little in the south western corner of the cave, there is no Type 1 speleothem. However, "mixture rock"[1] (Photo 4.1) is present at many places in the ceiling and walls of the cave. It is not clear if the mixture rock was formed before, after or at the same time as the speleothems of the first type.

Type 2 dripstone can be seen everywhere in the western passages, often covered by evaporites. On the floor of passage A there are also dry rimstone pools belonging to this type.

As in Bats Cave Type 3 is represented by flowstone. It is the only type of speleothem found close to the entrance, where it is often covered by popcorn. In the southern wall of the main room, the amount of flowstone and popcorn increases towards the entrance. Passage B does not contain any Type 3 speleothem while the floor of passage D appears to be covered completely by it.

4.4.1.4 Hospital Cave (Fig. 4.8).

Small patches of Type 1 speleothem can be seen everywhere inside the cave. They are often found in combination with breccia. Except for one stalagmite in the middle of the passage close to the main chamber, there are no Type 2 speleothems. This particular stalagmite is about one meter high and 0.5 m in diameter. It has been dissolved on all sides but preferentially along a gully going from top to bottom on the side facing

---

[1] Mixture rock is bedrock of which the fossil moulds and other vugs have been infilled with caymanite and/or calcite. It therefore composed of a "mixture" of bedrock, caymanite and calcite.

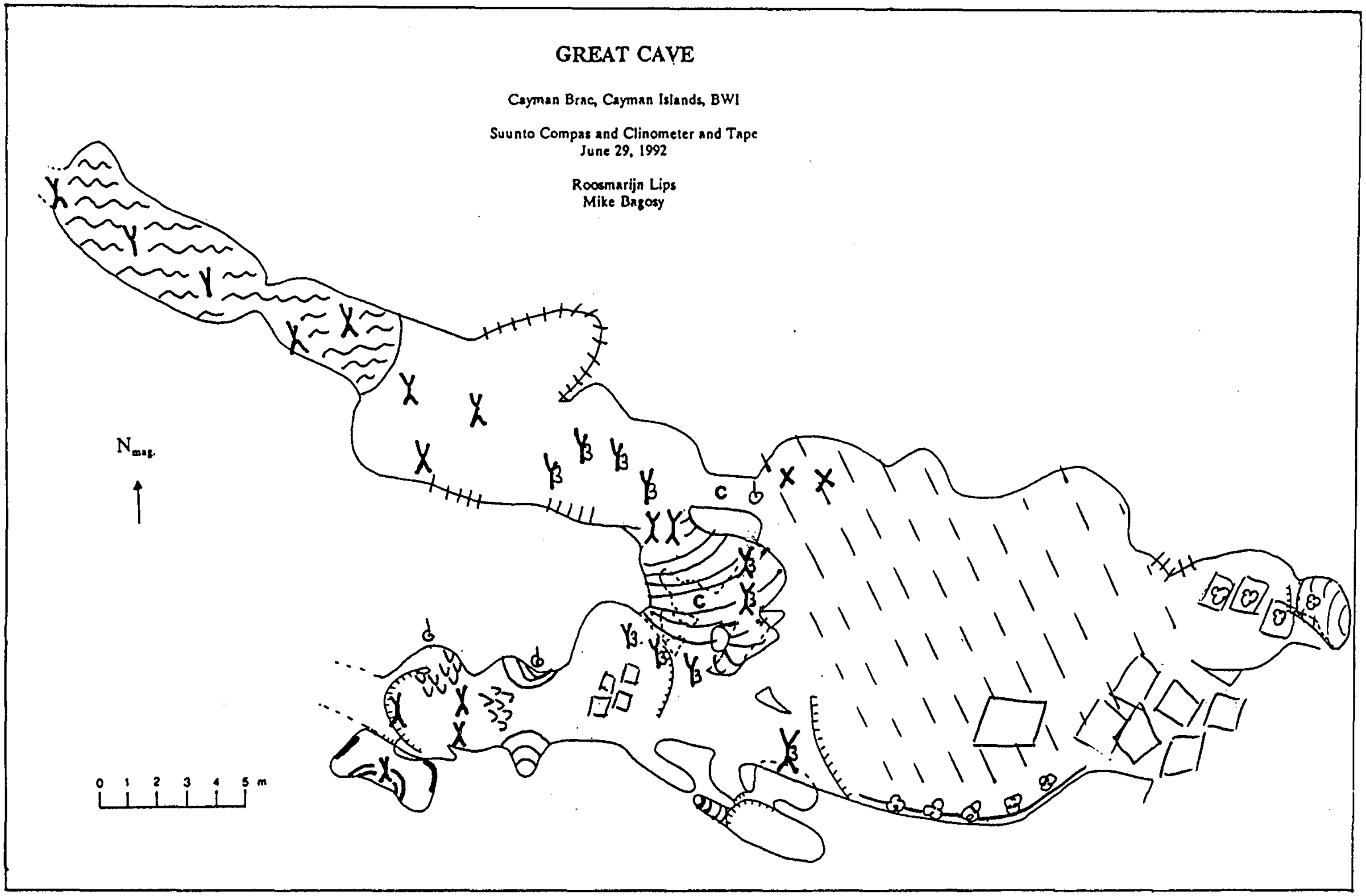

Fig. 4.7. Speleothem distribution in Great Cave.

Photo 4.1 Example of mixture rock from Great Cave

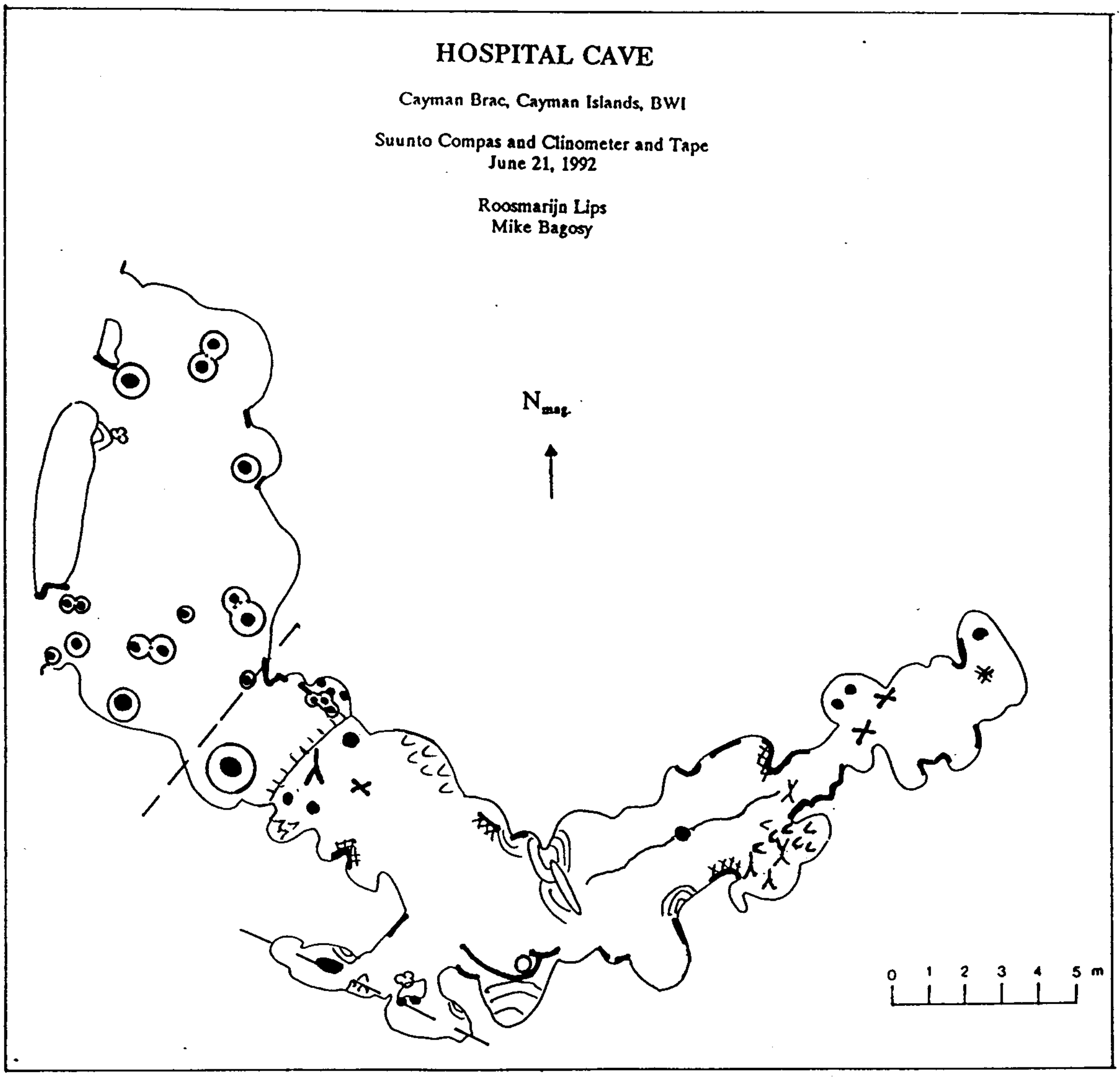

Fig. 4.8. Speleothem distribution in Hospital Cave.

the entrance (Photo 4.2). The last group of speleothems consist of dripstones which are still actively growing; the majority are concentrated in one alcove in the southern wall.

Crust remnants may be seen at many places in the walls and ceilings and in bellholes. Its origin is not known, but similar crusts have been observed in the Bahamas where they consist of gypsum and it is suggested that the gypsum is precipitated from water seeping uniformly from pores in the walls (Vogel *et al.*, 1990).

4.4.1.5 Cross Island Road Cave (Fig. 4.9).

This cave appears to be divided into a western and an eastern part by a large, inclined joint. The western part lies below the joint and consists of a series of rounded chambers connected to each other. It is almost completely devoid of speleothems. The eastern part is filled with Type 1 and three speleothems. It is possible that the western part does not get as much water as the eastern part because drainage is joint controlled, so that water can not penetrate further down. The few speleothems in the western part consist of some dripstone and popcorn of type three.

In the eastern part breccia is often found in association with Type 1 speleothem (Photo 4.3). Type 2 is not very common and consist of rimstone dams and dripstone. One Type 2 column is covered with popcorn and is broken and displaced horizontally approximately 5 cm. Type 3 flowstone forms a thin layer over the southern wall of the eastern part and over the western wall of the entrance chamber.

Photo 4.2 Type 2 stalagmite in Hospital Cave

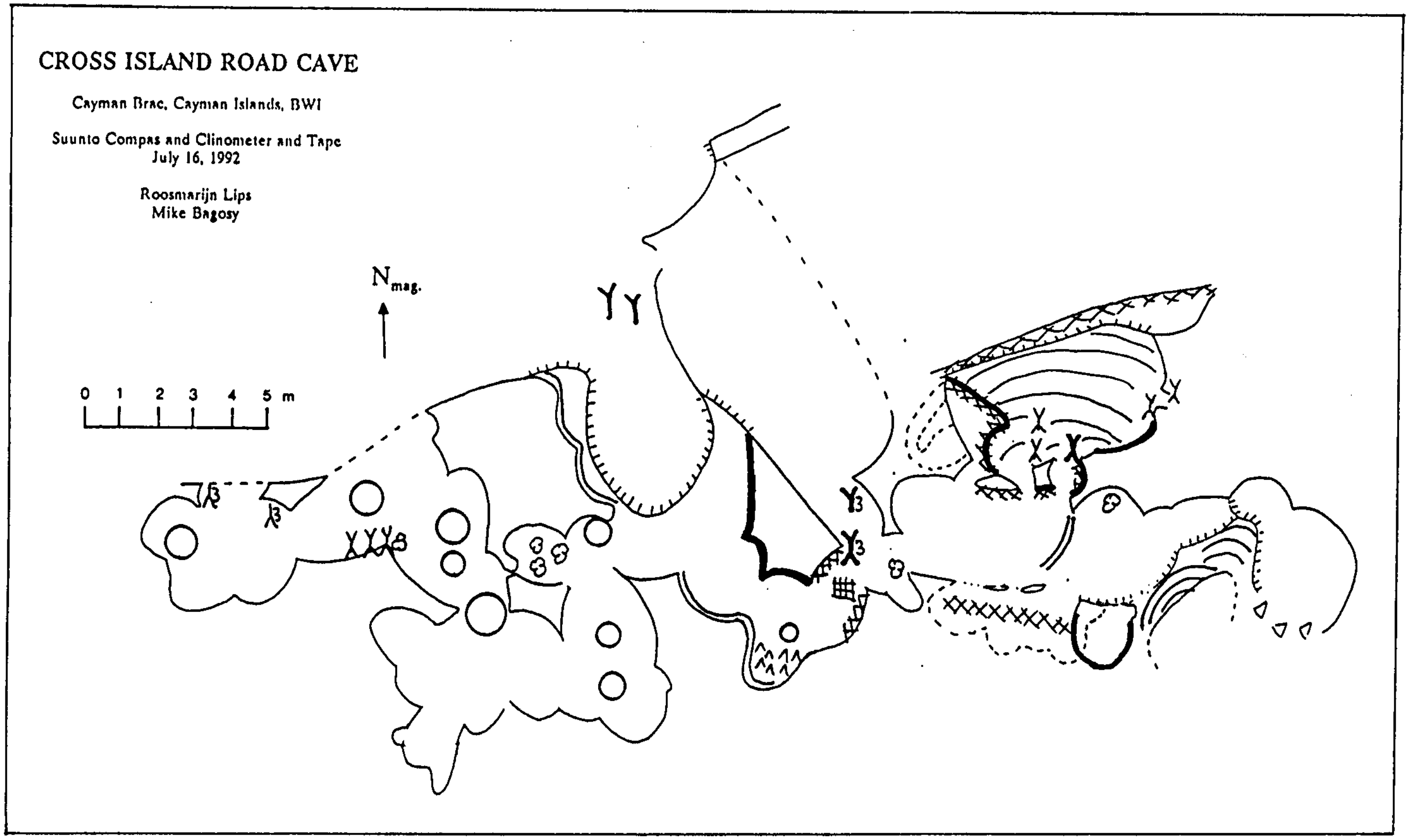

Fig. 4.9. Speleothem distribution in Cross Island Road Cave.

Photo 4.3 Type 1 flowstone and breccia in Cross Island Road Cave

4.4.2 The higher caves.

4.4.2.1 Tibbetts Turn Cave (Fig. 4.10).

The entrance of this cave is about 16 m above the notch, just underneath the plateau. Most of the walls, ceilings and floors are covered with Type 2 and three speleothem. No Type 1 speleothems have been observed. Type 2 speleothem consist of dripstones and some rimstone dams while Type 3 is represented by flowstone covering the wall and floor.

The dripstone is often in clusters, close to walls or along joints in the ceiling. The southern large chamber is divided into two sections by a row of columns. The southern section has stalactites on the ceiling but no speleothem on the floor. Instead it is covered with sandy sediments. In the northern section, there are more columns than stalactites and the floor is covered by a layer of flowstone.

In the northern large chamber, a big collapse block is covered with Type 3 speleothems, suggesting that the ceiling collapsed after the formation of Type 2 deposits. All the other collapse blocks in this room appear to have been cemented together or covered only by Type 3 speleothem.

In the western section of the cave some Type 2 columns have been broken at different heights above the floor (Fig. 4.10; Photo 4.4). This probably happened when the ceiling collapsed in the adjacent northern large chamber.

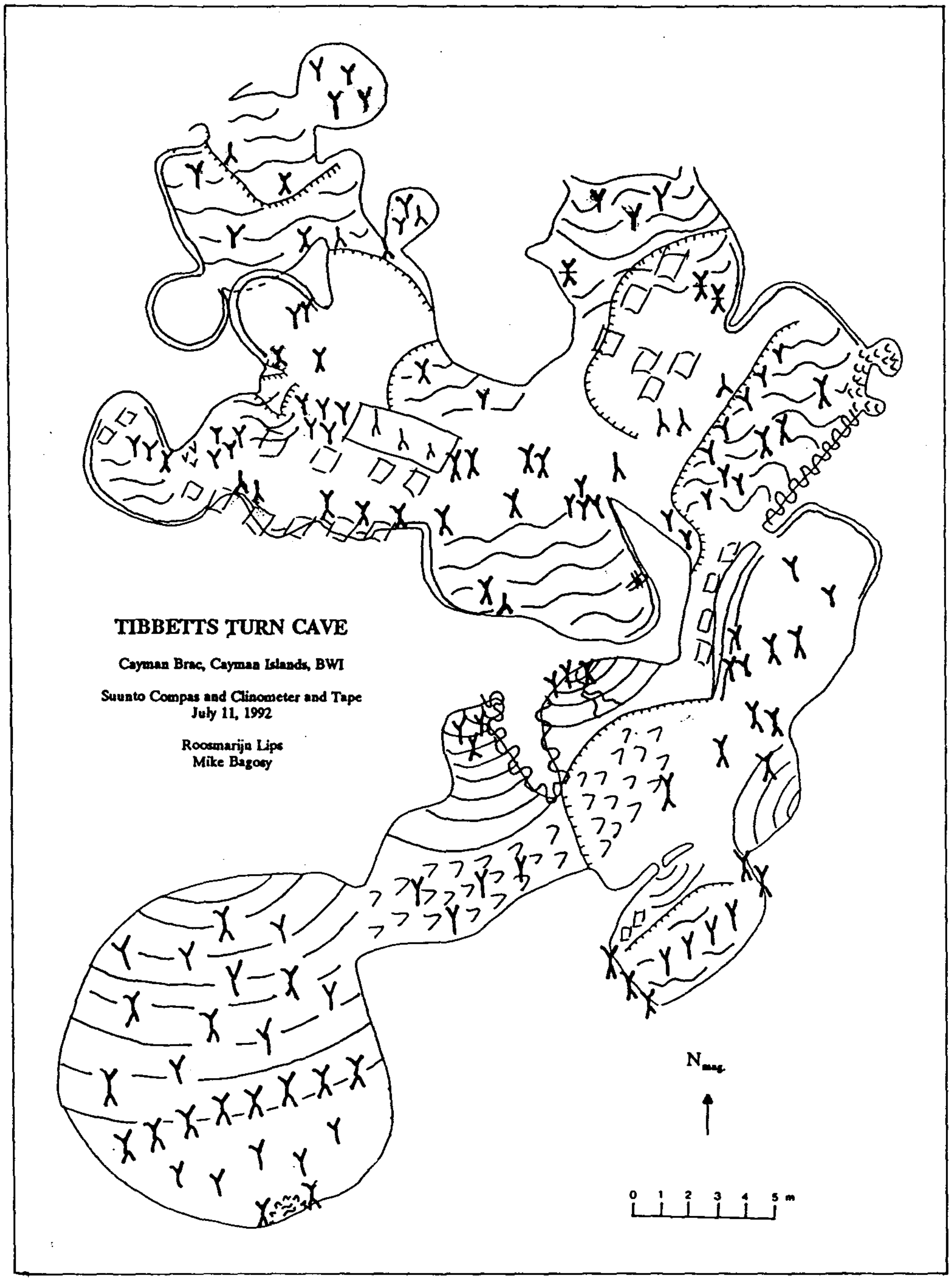

Fig. 4.10. Speleothem distribution in Tibbetts Turn Cave.

Photo 4.4 Broken Type 2 columns in Tibbetts Turn Cave

4.4.2.2 Peter's Cave (Fig. 4.11)

In Peter's Cave there is a strong contrast in morphology. The western half appears to have undergone extensive breakdown, sliding and shifting of large slabs of bedrock. The eastern half is much more stable and shows only some minor breakdown. A thin layer of Type 3 flowstone often covers and cements the large slabs of bedrock. In between them are many spaces through which the cave appears to continue.

The floor almost everywhere inside the cave consists of a (thin) layer of Type 3 flowstone. In the second main passage this has clearly followed the formation and dissolution of earlier dripstones. Further inside the cave speleothems consist increasingly of moonmilk.

Type 3 speleothems form a layer of flowstone on the floor and wall, thin layers of calcite on older speleothems and some small dripstones. However, the majority of the speleothems in the cave are Type 2 dripstones. They are present everywhere but the highest density is in the two main passages, especially in the eastern part of the second main passage. In this part there is also an old calcite shield; its lower plate has fallen to the floor, probably due to the weight of the draperies that formed on it. Close to it, there is another shield formed by capillary water from a fracture in the flowstone floor. The two plates protrude vertically from the floor with a thin crack between them.

There are a few sites where roots have penetrated into the cave. Where this occurred they have been covered by a layer of calcite that is broken at a few places, revealing the roots. Apparently these roots where not associated with enhanced

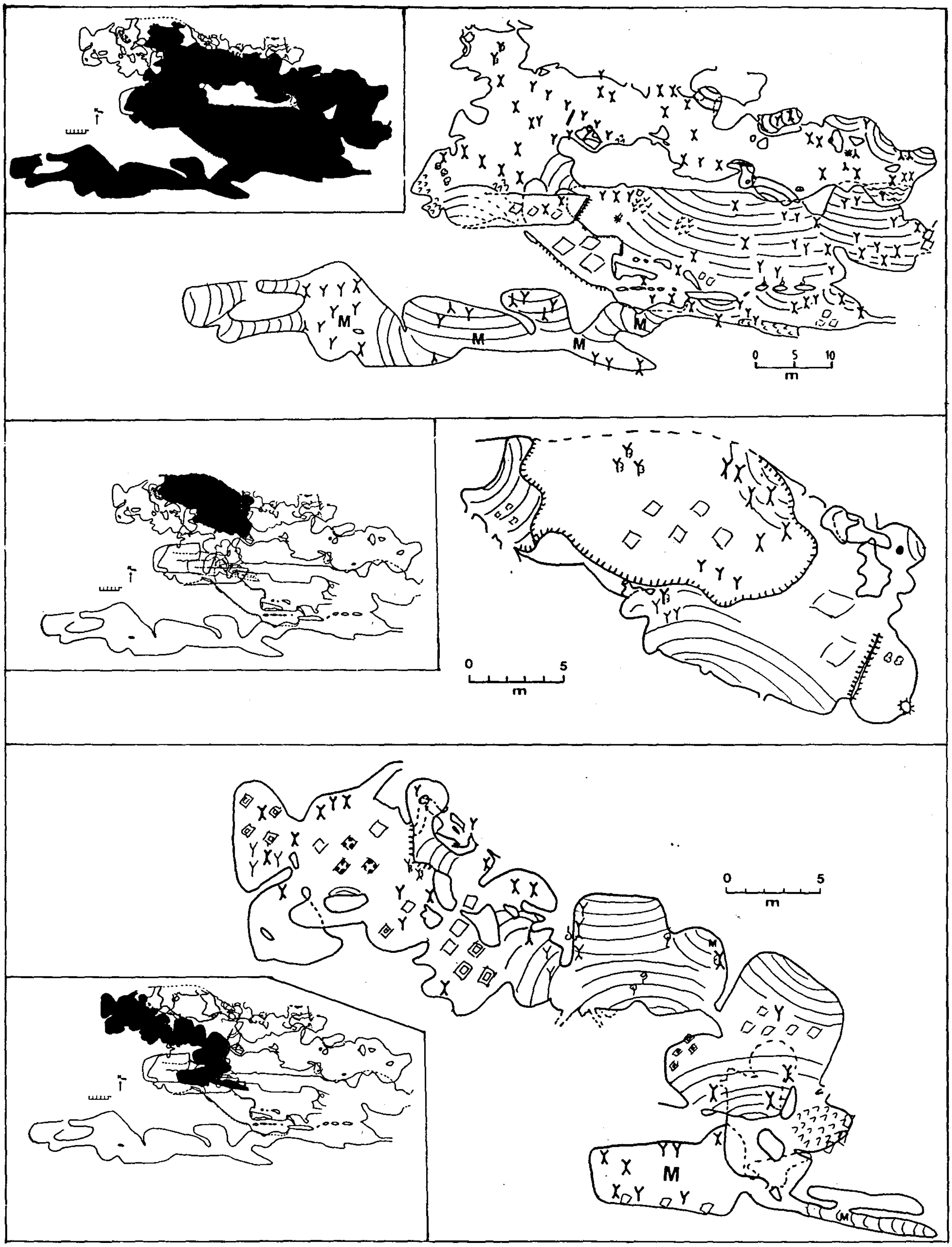

Fig. 4.11.a Speleothem distribution in Peter's Cave.

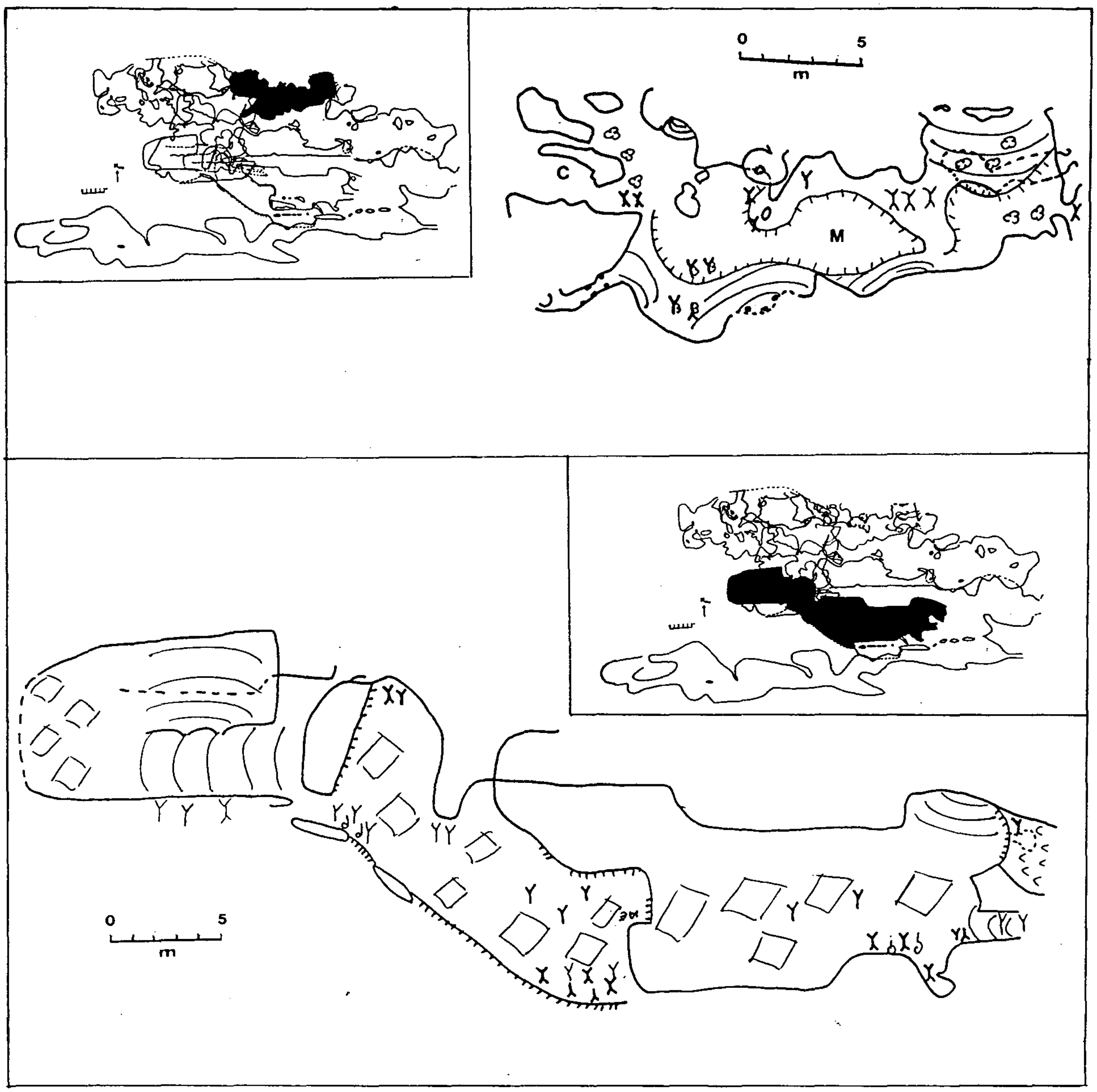

Fig. 4.11.b Speleothem distribution in Peter's Cave (cont.).

dissolution but rather with enhanced precipitation of calcite.

Small rimstone pools have been formed at different places in the cave, but only few of them still carry water. Popcorn only flourishes close to the second entrance, suggesting that it is indeed evaporation due to the passage of drier air that caused their formation.

4.4.2.3 Little Cayman Brac Cave (Fig. 4.12).

Little Cayman Brac Cave is a particulary interesting cave concerning its speleothems. There is a distinct increase in active speleothems together with a decrease of the dissolved types as one proceeds from the entrance deeper inside the cave.

Type 1 speleothem can be seen in cracks in the ceiling and in the walls of section A and the northern half of B. Type 2 speleothem consist mainly of dripstones and some flowstone. In sections D and E these speleothems appear to be increasingly covered by a layer of fresh calcite, which makes it difficult to tell if the entire speleothem is Type 3 or not.

This cave has a lot of eccentrics which also appear to be "fresher" (less dry) towards sections D and E. Deeper inside the cave some speleothems appear to be made of moonmilk but have the same forms as other speleothems close by that are made of calcite. It may be that they are weathered. Popcorn is only seen close to the entrance. This suggests an increase in humidity from the entrance inward, which is a normal phenomenon in caves; the entrance parts are under the influence of outside atmosphere

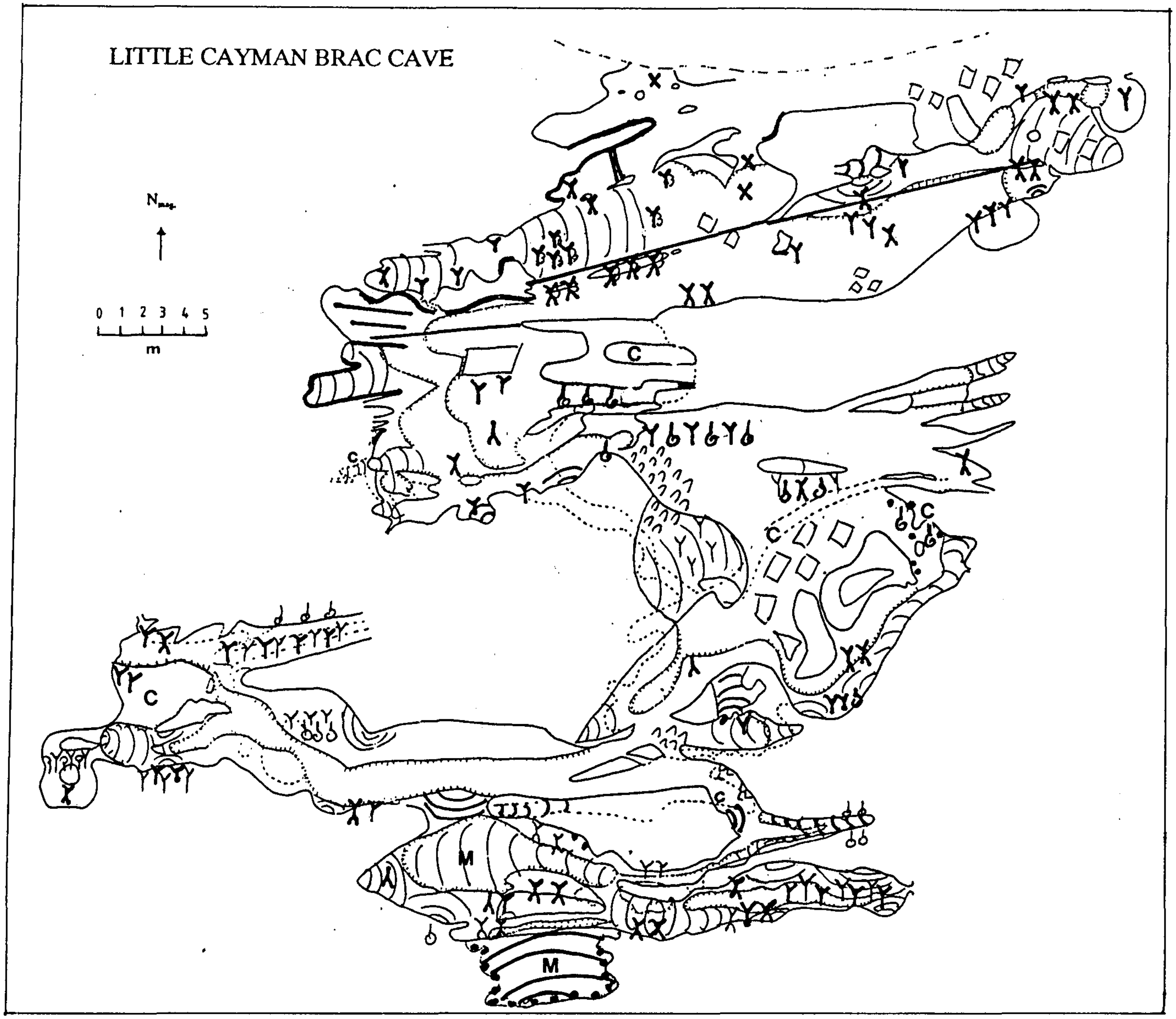

Fig. 4.12. Speleothem distribution in Little Cayman Brac Cave.

while deep inside the cave this diminishes and the cave atmosphere has close to 100% humidity with a stable temperature. The great amount of speleothems in the entrance part suggest that this part of the cave was once closed to the outside atmosphere as well and that they could have formed under conditions similar to those that prevail at present deeper inside the cave.

At many places inside the cave there are remnants of a brownish crust on the wall or ceiling. It is not clear of what this crust is made. In the southern most section the crust forms a line along the wall about 40 cm off the floor, suggesting that it has been deposited from standing water or as a reaction between the wall and a sediment cover. At present, the floor consists of flowstone that appears to be of moonmilk.

There is a lot of caymanite inside the cave. In the eastern wall of C it appears to have caused a boneyard like structure because it was more resistant than the bedrock, hence, less readily dissolved.

4.5 Discussion - speleothem deposition and dissolution.

Speleothems have been deposited inside the caves when the caves were air-filled. The higher caves are probably older than the notch caves and there has been more time for the formation of speleothems. The exact location of individual speleothems depends on where, how and how fast the water penetrates the bedrock. The different types of speleothem are caused by the way the water enters the cave and travels in it.

Dissolution of speleothems as a result of aggressive feedwater is present in the caves on Cayman Brac but it does not seem to be of more than local influence. Although this process can result in the total destruction of speleothem (Hill, 1986) it is believed to be in the initial stages and of local influence only in the caves on Cayman Brac, where it is solely observed on speleothems that are otherwise still intact.

Small dissolution features have been observed in flowstone in Bats and Tibbetts Turn Cave. In the case of Bats Cave the gullies appeared to be related to a root that came through the ceiling while in Tibbetts Turn Cave the water came out of two small holes in a flowstone wall and it left the imprint in the flowstone of a braided river going over into two main streams. The gullies are millimetric to centimetric in width and continue all the way to the floor in both caves.

Speleothems of the first and especially the second dissolution type have been observed in all the caves in great quantity and an island-wide change (or sequence of changes) in the physio-chemical environment of the caves is suspected. Sea level changes or changes in the relative humidity inside the caves have been the result of climatic changes and tectonism. Attention should therefore be concentrated on dissolution due to the flooding of the caves and/or possibly due to condensation corrosion.

4.5.1 Type 1 speleothems

Speleothems of the first dissolution type were observed mainly in the notch caves, whose entrances lie 1-2 m above the notch (Figs. 4.4 - 4.9), while speleothems of the second type dominate the higher located caves (Figs. 4.10 - 4.12). The latter contain much more speleothem which might conceal older Type 1 deposits in the walls.

As stated above, Type 1 speleothems are often associated with breccia (Fig 4.3). Therefore, the breccia and the speleothem must have coexisted. The speleothem consisted mainly of flowstone as can be seen from its cross sections. The cavities in the walls are completely filled with breccia and/or flowstone and are of small dimensions (less than 0.5 m in diameter). It is supposed that these cavities were formed prior to the caves. Subsequently the cavities filled with flowstone and/or fragments of rock that become lithified to form a collapse or fissure breccia. Cavities filled with flowstone and other material are common in the three Tertiary formations of the Cayman Islands (Jones *et al.*, in press a and b; Jones, 1992) which supports the idea that the cavities inside the Cayman Brac caves may have nothing to do with the caves themselves but are formed independently and prior to the caves during one or more paleokarst periods. As Figure 1.4 showed these karstification periods occurred each time the sea regressed. During a subsequent period of dissolution these cavity fills were dissolved in the same way as the surrounding bedrock. Dissolution in the phreatic zone and the chemical similarity between the bedrock and the cavity fills could make such a non-differential dissolution possible. Examination of pieces of bedrock collected inside the caves shows that the bedrock is very pure (containing less than 3% of impurities) and that chemical similarity might thus be possible. However, more detailed lithological study of the bedrock and the different types of cavity fill is necessary.

Dating of these speleothems would be very helpful too to derive a minimum age for the cavities. Unfortunately it was not possible to collect samples because core drilling is necessary and a drill was not available.

4.5.2 Type 2 speleothems

The majority of the speleothems found on Cayman Brac belong to the second group, i.e. they have been reduced (considerably) in size but they still show their original form. The higher caves have much more speleothem than the notch caves and the majority of it belongs to this group. Some of the speleothems present in the notch caves are also classified of this type.

Included in this group are all the different forms (stalactites, stalagmites, flowstone, etc) summarised above. They occur on ceilings, walls and floors. Figure 4.13a shows a cross-section through a stalactite from the second main passage in Peter's Cave. The dissolution asymmetry is very pronounced; assuming that the sample was perfectly round and did not undergo any dissolution on the outside of the lee side, about 36% of the sample is still present. This is however not very likely and more than 64% of the sample could have been dissolved. The same is very clear with a sample from the eastern part of Cross Island Road Cave (Fig. 4.13b) of which less than 20% of the initial speleothem is left. After dissolution the speleothem broke into pieces which then became coated with a younger layer of calcite.

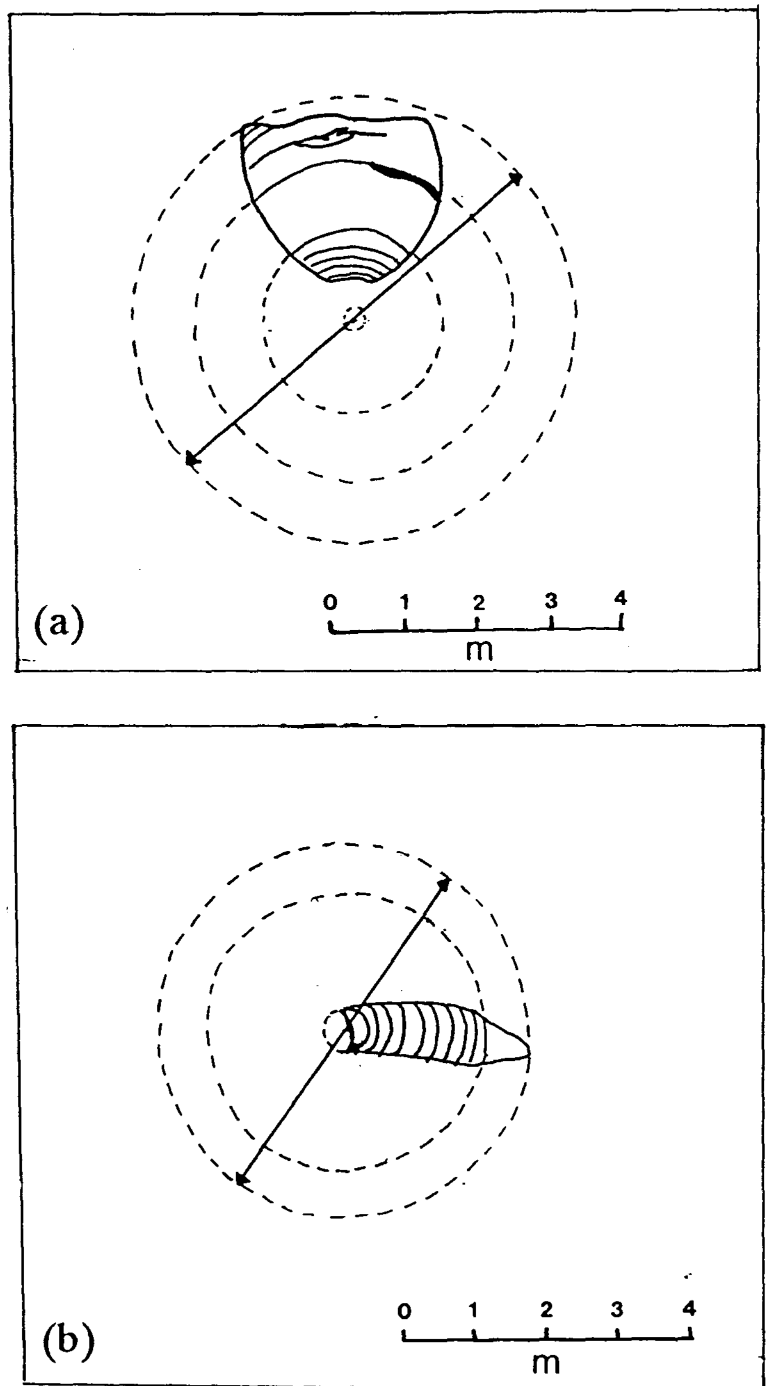

Fig. 4.13. Extent of dissolution of type two speleothems (a) HRC2, Peter's Cave, (b) CC2, Cross Island Road Cave.

At various places in Peter's Cave flowstone masses were scalloped (decimetric to metric). At one side in the first main passage, there is an opening of about 20 cm high and 40 cm wide at the foot of a flowstone "waterfall". It gives access to a small room that lies below the main passage the ceiling of which consist partly of dissolved flowstone. Another smaller opening is located in the floor not too far from the flowstone waterfall. Through these openings there is clear sound contact between the two main passages and air flows from the first towards the second main passage.

Each of the two proposed dissolution mechanisms has its problems. If the dissolution of speleothem took place during flooding of the caves, then why is there such widespread and distinct asymmetry? Dissolution in the phreatic zone of a small oceanic island is normally characterised by its non-differential, non-directional action. On the other hand if condensation corrosion was responsible, then what happened to the dissolved calcite in the condensation water? In Carlsbad Cavern there is deposition of some of the material on the lee side of the obstacle but in the caves on Cayman Brac such lee side deposition has not been observed. Neither is there any evidence that there was deposition of calcite at the foot of speleothems. In Tibbetts Turn Cave, for instance, the stalagmites in the big room seem to be "drowned" by a layer of flowstone. The angle between the stalagmites and the flowstone suggests that the flowstone came later and is not formed from calcite dissolved from the stalagmites themselves (Photo 4.4).

Little Cayman Brac Cave is a special case because it appears that speleothem dissolution changes gradually from the inside towards the entrance. Deep inside the cave, the speleothems are actively growing, Type 3 speleothems. Mid-way between the far end and the entrance the majority of the speleothems belong to Type 2 while those close to the entrance are Type 1. The change from a stable cave atmosphere deep inside to an atmosphere highly dependent on the outside fluctuations close to the entrance could have been the reason for the speleothems to stop growing, but was it also the cause of the dissolution of the speleothems? If the cave was air filled, condensation corrosion occurred close to the entrance and not deep inside the cave. Due to cliff retreat the condensation could penetrate further and further inside the cave, which explains the more pronounced dissolution close to the entrance where there was more time for dissolution. In the case of flooding of the cave as a result of sea level rise, there could be two possibilities, the cave was open or closed to the outside. If the cave was closed to the outside it could have happened that speleothems developed in the first part of the cave while the furthest part of the existing cave did not exist yet (Fig. 4.14). During the flooding the speleothems were dissolved in the part closest to the cliff while the cave itself developed deeper inland. In the same period the cave opened to the outside by cliff retreat and inhibited speleothem development close to the entrance after the water retreated. On the other hand, if the cave was already open to the outside at the time of the flooding, faster exchange of aggressive water (due to tidal fluctuations, the pumping effect of waves if the sea level was not much higher than the entrance of the cave,...) close to the entrance could have been responsible for more dissolution in the entrance

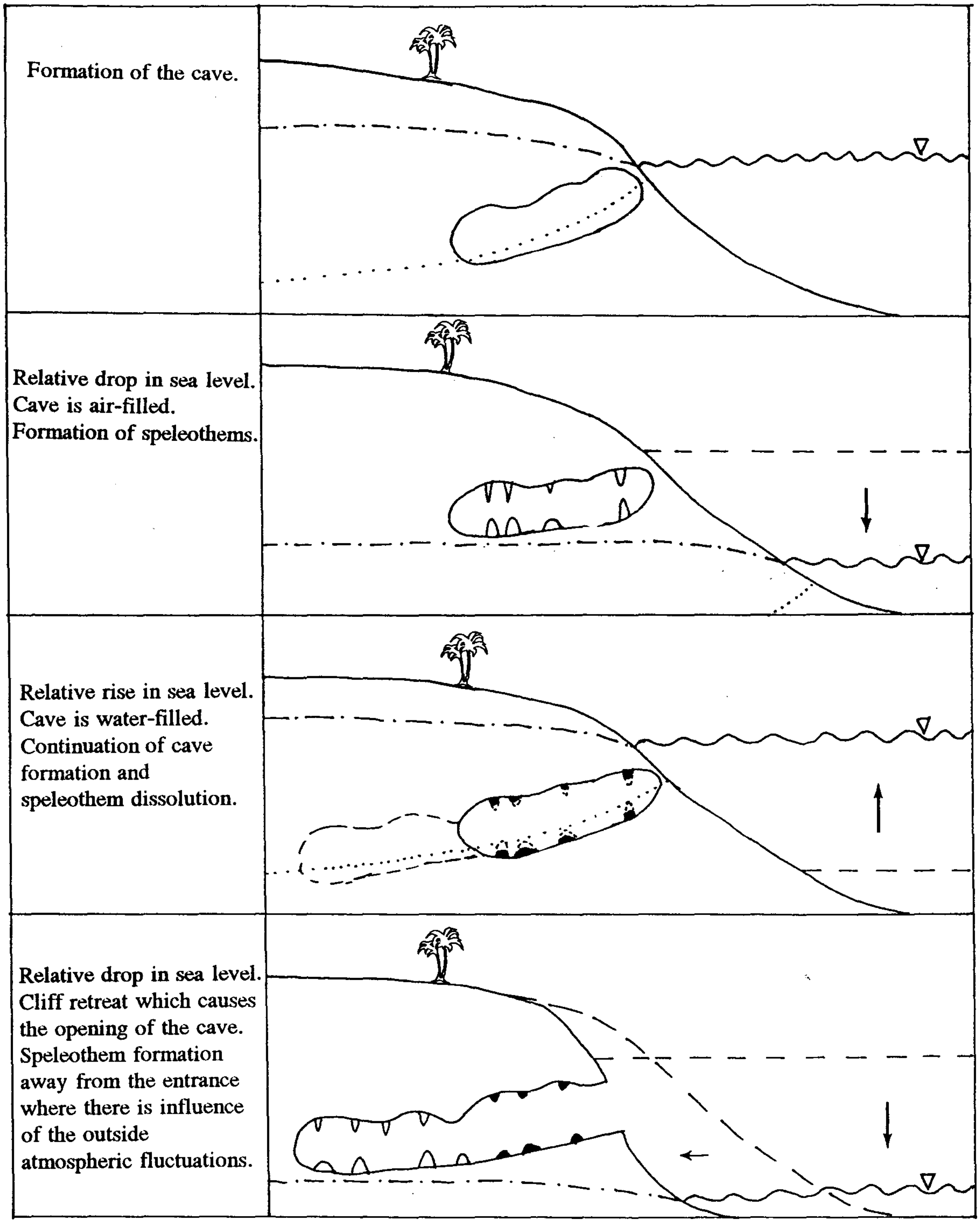

Fig. 4.14. Model explaining speleothem dissolution in Little Cayman Brac Cave in a closed system.

zone and less deeper inside the cave (Fig. 4.15). After the water retreated, only the cave atmosphere deep inside the cave allowed new speleothem development which now covers the evidence of dissolution. Of the three possibilities, it seems more likely that a change in the cave atmosphere caused the dissolution rather than aggressive water.

Considering the objections, it appears that, at present, condensation corrosion is the most likely dissolution mechanism for Type 2 speleothems. However, more study is certainly needed.

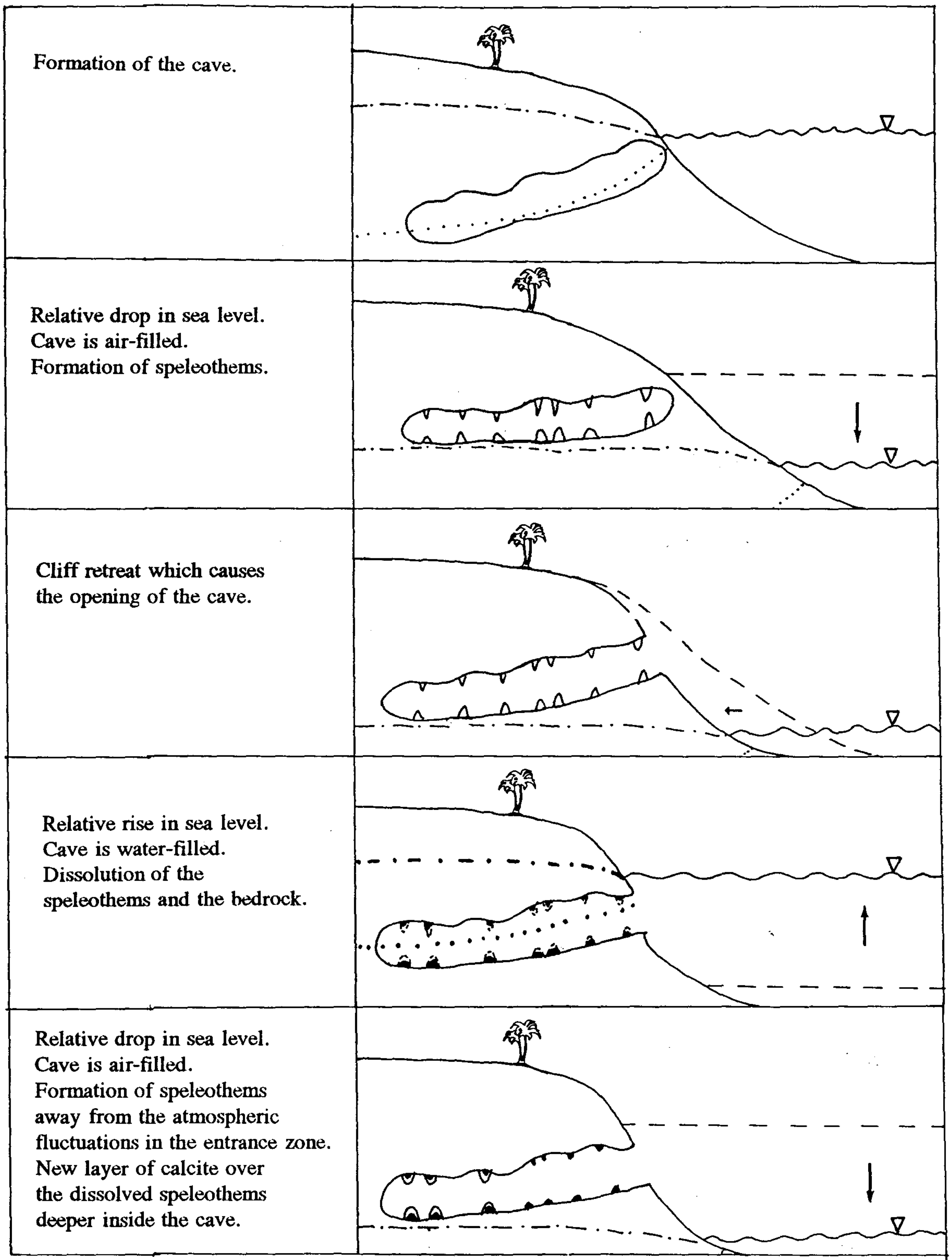

Fig. 4.15. Model explaining speleothem dissolution in Little Cayman Brac Cave in an open system.

CHAPTER FIVE

URANIUM-SERIES DISEQUILIBRIUM DATING OF SPELEOTHEMS BY ALPHA SPECTROMETRY.

5.1 Introduction.

Uranium series dating is, at present, the principal method of speleothem dating (Ford and Williams, 1989). It is based on the radioactive decay of ^{238}U and ^{235}U by the release of α and β particles, accompanied by the emission of γ radiation, to stable ^{206}Pb and ^{207}Pb (Fig. 5.1).

The most common method of dating relies on the build-up of ^{230}Th over time by radioactive decay of ^{234}U (itself decayed from ^{238}U) in a system where ^{230}Th is initially absent or at very low levels. In the case of speleothems, uranium present in the feed water is deposited in the crystal lattice of the calcite while the insoluble thorium is left behind in the soil, making it possible to determine the time of deposition.

The activity ratio of $^{230}Th/^{234}U$ is zero at the beginning and reaches equilibrium after about 600 ka (Lundberg, 1990). In the interim, the activity ratio can be calculated using the equation (Schwarcz and Gascoyne, 1984):

$$^{230}Th/^{234}U = (1 - e^{-\lambda 230\, t})\,(^{238}U/^{234}U) + [(1 - {}^{238}U/^{234}U) \times \lambda_{230}/(\lambda_{230} - \lambda_{234})]\,(1 - e^{-(\lambda 230 - \lambda 234)t}) \quad . \; . \; . \; . \quad (1)$$

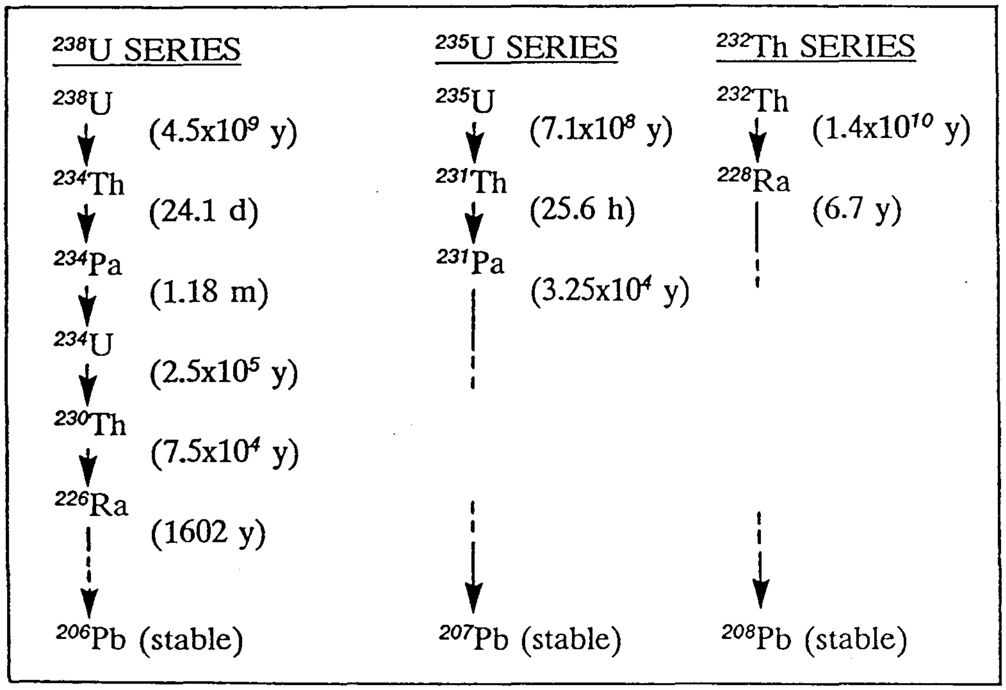

Fig. 5.1. Uranium and Thorium decay series. The half lives of the isotopes are included in brackets. The dashed line indicates that some steps are missing. The intermediate steps between ^{238}U and ^{234}U, and between ^{234}U and ^{230}Th are ignored for U-series dating because they are very rapid (Lundberg, 1990, Fig. 1.1).

where t is time, $^{230}Th/^{234}U$ and $^{238}U/^{234}U$ refer to the present activity ratios of the isotopes and λ_{230} and λ_{234} are the decay constants of ^{230}Th and ^{234}U respectively. To determine the time elapsed since the initiation of the system $^{230}Th/^{234}U$ and $^{238}U/^{234}U$ must be known. The activity ratios are measured in alpha spectrometry by estimating numbers of atoms from their emission of alpha particles at characteristic energy levels. Mass spectrometry counts isotopes directly by their mass.

The datable range for most speleothems is from about 1 ka to about 350 ka. The precision of a date is expressed as error margins of 1σ or 2σ on either side of the date, indicating that there is a 68% confidence level that the true date lies between $\pm$ 1 σ. Alpha spectrometry has a 1σ precision of the measurements of U ratios of 1% and for Th ratios of 3%. The cumulative error of a date from this techniques is about 10% in the estimated date. Mass spectrometry is more precise in the measurement of the ratios and errors range from 0.04 to 1.0% (2σ; i.e. a confidence level of 95% - Lundberg, 1990). The sample size needed for the two methods differs by more than one order of magnitude as well: 20 to 100 grams for α-spectrometry compared to 0.5 to 5 grams for mass spectrometry. Mass spectrometry is thus more precise and more accurate and allows for higher sampling densities. The main advantage of α-spectrometry is that it is much cheaper and has been in use much longer, hence it is better understood.

5.2 Results and discussion.

Thirty speleothem samples were collected from seven caves and the notch at Little Cayman Brac. It was tried to take at least one sample or better a series of samples from each cave. The samples were chosen so that they represent as much as possible the speleothems inside the cave in question, are not weathered and are taken from sites where their disappearance would not be noticed. In the case of Hospital Cave this was not possible and therefore there is no sample from this cave.

Fifteen uranium-thorium activity ratios and ages of eight speleothem samples from five caves and the notch are presented in Table 5.1. The ages range from about 10 ka to over 350 ka. Several growth periods alternating with periods of cessation of growth or even dissolution may be recognised. The periods of dissolution are distinguishable as hiatuses in three speleothems. The present time is for all the dated samples a period of dissolution.

5.2.1 Hiatuses.

The speleothem samples of which the ages were determined were selected because of the presence of hiatuses or of their position. The sub-samples were then chosen immediately above or below the hiatuses.

The hiatuses could be recognised by a layer of mud or dust, a difference in calcite structure or the evidence of truncated calcite followed by continuous calcite

Table 5.1Uranium-Thorium activity ratios and ages of speleothem samples.

CAVE	SAMPLE	U conc. (ppm)	230Th/234U	234U/238U	230Th/232Th	AGE (years)		+1sigma (years)	-1sigma (years)
						UNCORR	CORR		
GREAT CAVE	GC8 CORE	0.838+/-0.016	0.528+/-0.021	1.016+/-0.017	80.5 +/- 25.055	81400		5000	4800
	GC8 OUT	0.622+/-0.008	0.15 +/-0.007	1.066+/-0.017	101 +/-111.926	17600		900	900
BATS CAVE	BC5 CORE	0.159+/-0.005	0.84 +/-0.048	1.014+/-0.057	67.1 +/- 23.214	197200		37500	27900
	BC5 OUT	0.17 +/-0.012	0.697+/-0.061	1.153+/-0.095	161 +/-217.569	124700		21600	18100
NOTCH AT LC	LB3 OUT	0.623+/-0.017	0.107+/-0.024	1.037+/-0.026	8 +/- 6.541	10400		4400	4300
							12300	3000	2900
L. CAYMAN BRAC CAVE	LC1	0.089+/-0.003	1.094+/-0.111	0.939+/-0.093	55.333+/- 31.184	>350 000			
L. CAYMAN BRAC CAVE	LC2 MIDDLE	0.109+/-0.003	0.956+/-0.069	1.038+/-0.071	43 +/- 15.958	313600		39100	84900
L. CAYMAN BRAC CAVE	LC3 TOP	0.139+/-0.005	0.693+/-0.041	1.092+/-0.62	57.556+/- 18.698	125100		14600	12900
	LC3 BOTTOM	0.207+/-0.007	0.848+/-0.045	1.05 +/-0.04	35.571+/- 7.722	197900		33900	26000
PETER'S CAVE	HRC4 TOP	0.262+/-0.007	0.491+/-0.028	1.052+/-0.054	100.333+/- 99.062	72700		6000	5700
PETER'S CAVE	HRC2 OUT	0.17 +/-0.012	0.805+/-0.07	1.017+/-0.093	165 +/-195.035	176000		47200	32800
TIBBETTS TURN CAVE	TC12 A (core)	0.136+/-0.005	0.948+/-0.075	1 +/-0.079	252 +/-584.045	319700		165000	96500
	TC12 B	0.153+/-0.007	0.942+/-0.065	1.053+/-0.073	106.25 +/- 78.837	285100		124200	67400
	TC12 C	0.207+/-0.01	0.765+/-0.057	0.957+/-0.072	82.5 +/- 46.13	160200		31900	24500
	TC12 D	0.24 +/-0.017	0.581+/-0.057	1.121+/-0.12	93.667+/- 92.267	92600		15000	13200

deposition.

5.2.1.1 The appearance of the hiatuses.

5.2.1.1.1 Little Cayman Brac Cave

The three dated samples from Little Cayman Brac Cave, are all part of a speleothem section on the floor and ceiling close to the western entrance of the cave (Fig. 5.2). The phases indicated in Figure 5.2b are relative to each other (phase 1 being the oldest) and phase 1 on the floor and ceiling may not necessarily represent the same period. LC2 is a sample of ceiling phase 1, LC1 of floor phase 1 and LC3 of floor phase 2 (Fig. 5.2c).

LC2 is a piece of flowstone from the ceiling which presents very interesting features. It shows five hiatuses and one layer of evaporitic speleothem which is below hiatus 1, but separated from it by a layer of more compact calcite (Photo 5.1). Hiatus 1 can be recognised due to a thin white layer on top of a thin layer of reddish particles which appears to have been deposited together with calcite. The reddish and white particles are probably dust. The lower layers do not seem to be truncated during this period of growth cessation. The next two hiatuses are clearly visible due to the reddish (hiatus 2) and yellowish (hiatus 3) clay particles, which are most likely left behind by flood waters that stirred the clay up from the bottom after which it settled out among others on the ceiling when the water was calm again. Again the lower layer does not appear to be truncated by dissolution but it is not completely certain. LC2 is located

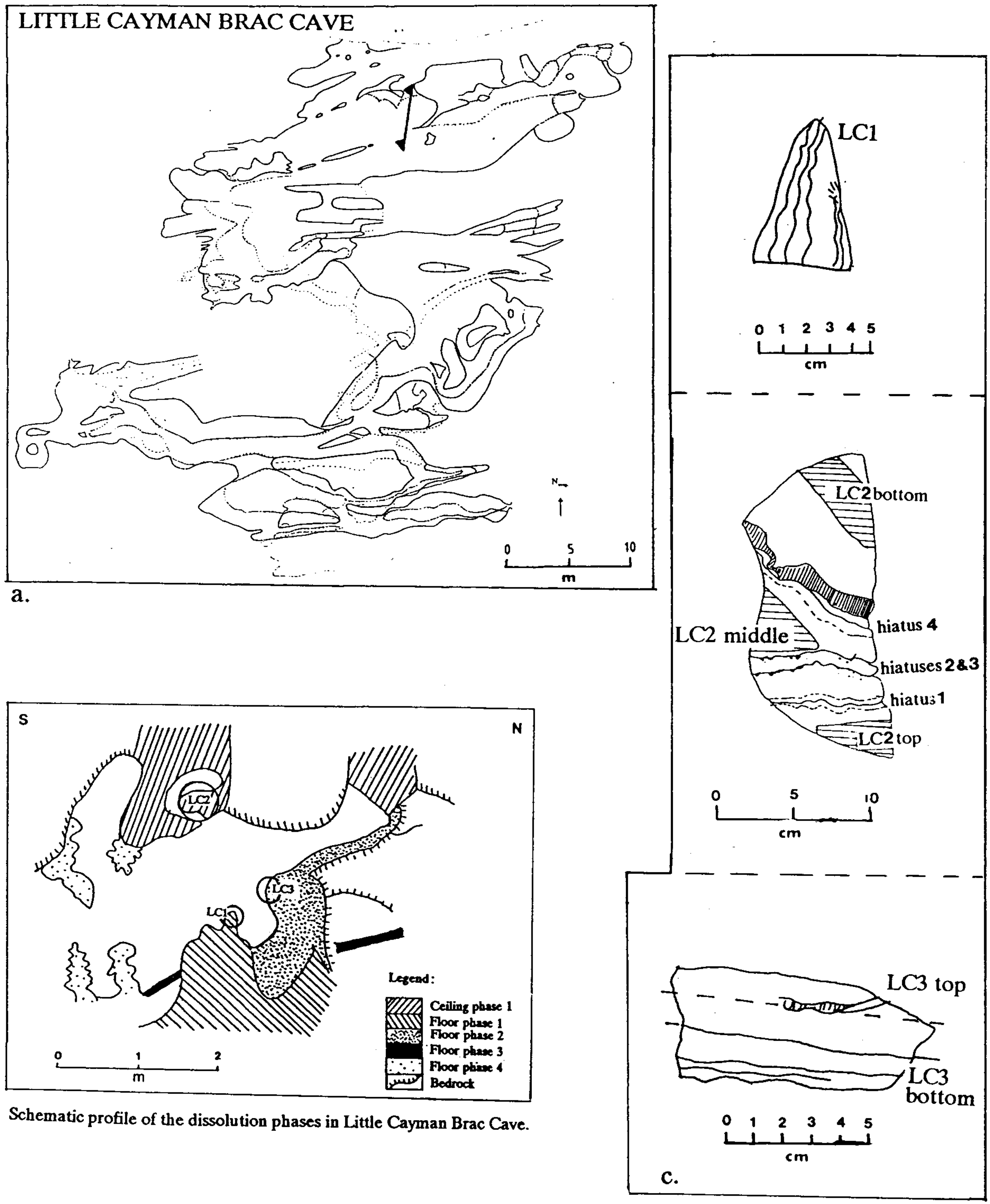

b. Schematic profile of the dissolution phases in Little Cayman Brac Cave.

Fig. 5.2a. Location of dated speleothems on Little Cayman Brac Cave
b. Schematic profile of dissolution phases
c. Cross section of dated speleothem samples

Photo 5.1 Cross section of LC2

about 15 m above modern sea level which suggests that the flooding must have been caused either simply because of tectonism or as the result of high sea level followed by tectonic uplift. The latter seems the more likely since the timing of these two hiatuses correspond very well with hiatuses 1 and 2 of DWBAH (see below; Fig. 5.7). More mud seems to have been deposited during hiatus 2 than during hiatus 3. Extensive dissolution does not appear to have taken place during either of the two periods. Hiatus 4 resembles hiatus 1 only this time the dust particles are more yellowish than reddish. The present period of dissolution shows a speleothem surface that is clearly sculptured and covered with a greyish dust.

As a result of too low thorium yields in the top and bottom sample of LC2 (Photo 5.1) no date could be obtained from them. This makes it impossible to date the three hiatuses after about 200 ka and the one before about 350 ka (Photo 5.1). However the oldest hiatus is believed to be around 350 ka because the dated sample from LC2 was taken close to this hiatus.

5.2.1.1.2 Tibbetts Turn Cave

Sample TC12 is a stalactite located about 31 m inside Tibbetts Turn Cave at the entrance of a relatively small rectangular room (Fig. 5.3). It consist of three parts: the centre is light in colour and is partially dissolved while the two sides are dark and still intact (Photo 5.2). The hiatus in TC12 is shown as a thin white layer, resembling a thin layer of speleothem weathering (Photo 5.2). The sample was clearly preferentially

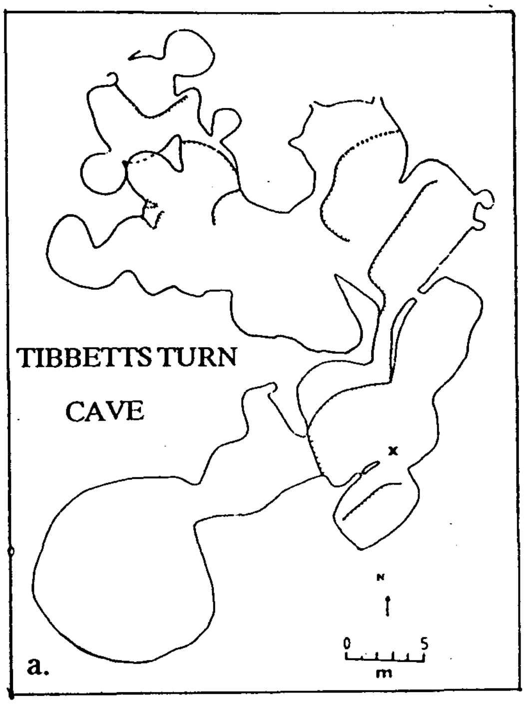

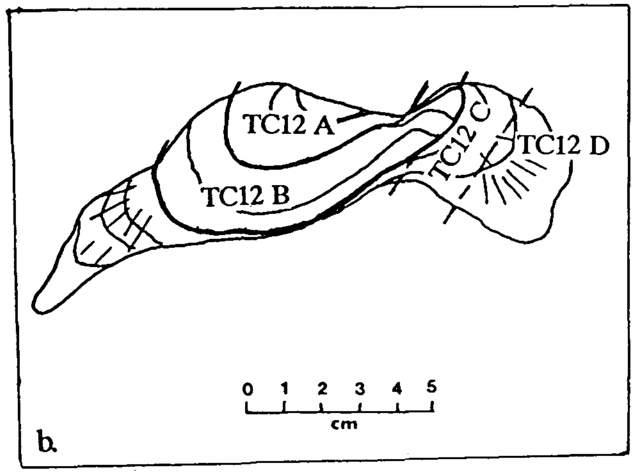

Fig. 5.3a. Location of TC12 in Tibbetts Turn Cave
b. Cross section of TC12

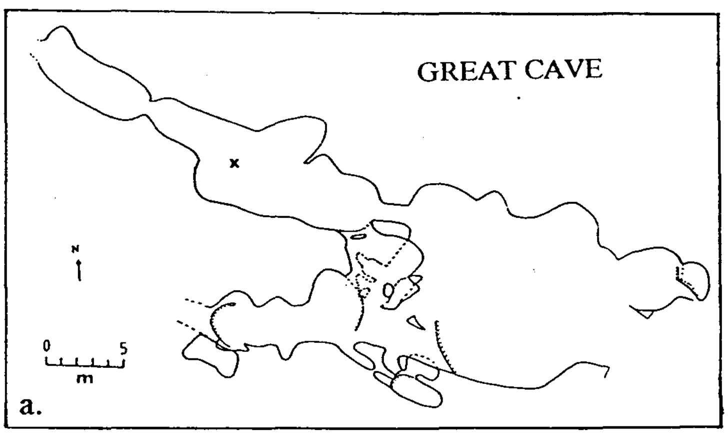

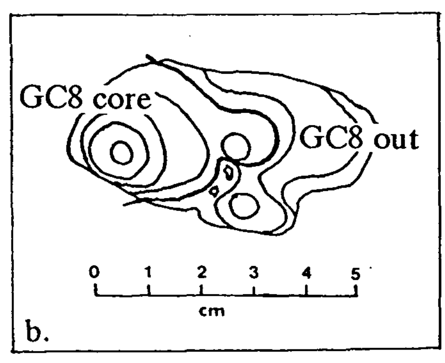

Fig. 5.4a. Location of GC8 in Great Cave
b. Cross section of GC8

Photo 5.2 Cross section of TC12

dissolved on one side, beyond the centre of the stalactite. There is a distinct colour difference between the calcite on either side of the hiatus, indicating a change in the characteristics of the feed water. The darker colour could indicate more mineral or organic material in the water. It is not clear if the two side parts have grown simultaneously or not. A thin white layer along one side of the non-dated part (Photo 5.2) suggests that the dated part grew later but only dating can confirm this.

The large errors in the age determination of the oldest part of TC12 are due to a low uranium content and relatively short counting time. In spite of these large errors all the dates are in stratigraphic order and a break clearly exist between the dates on either side of the hiatus which is probably around 200 ka.

5.2.1.1.3 Great Cave

The sample GC8 is taken from passage B, just before the passages lowers down to the pool in front of the lake (Fig. 5.4). GC8 is a stalactite composed of three stalactites grown together. The hiatus is mainly visible due to the different types of calcite structure on either side of the hiatus. Growth of the initial three stalactites started before the hiatus, two joined together before the hiatus. The other one was later connected to them by evaporitic calcite. This stalactite is composed of very clear calcite and contained the highest concentrations of uranium. The outside is milky white, resembling weathered calcite.

5.2.1.1.4 Bats Cave

BC5 is the top of a 1.4 m high and 0.45 m in diameter stalagmite at the entrance of the small westerly cave at Bats Cave (Fig. 5.5). The sample was taken from the cave side where the stalagmite was not yet as much eroded as on the outside. The base of the stalagmite is about 0.9 m above the centre of the notch.

5.2.1.1.5 Peter's Cave

HRC4 is a sample of the flowstone step at the main entrance (Fig. 5.6). It was taken about 0.75 m underneath the floor of the entrance. There is no hiatus visible, only a lightening of the calcite from dark brown at the bottom to white at the top, indicating a gradual change in the characteristics of the feedwater.

HRC2 is a Type 2 stalactite from the second main passage, east of the calcite shield in the ceiling. It shows a clear asymmetry in the direction of dissolution and no hiatuses.

5.2.1.1.6 Notch

The sample LB3 was collected from the notch about 50 m west of Little Cayman Brac Cave. At this site the Sangamon notch was filled with speleothems which subsequently have been eroded. This speleothem phase was succeeded by a phase of breccia formation which was then followed by another phase of speleothem formation. All the different materials that filled in the notch have undergone or undergo erosion by

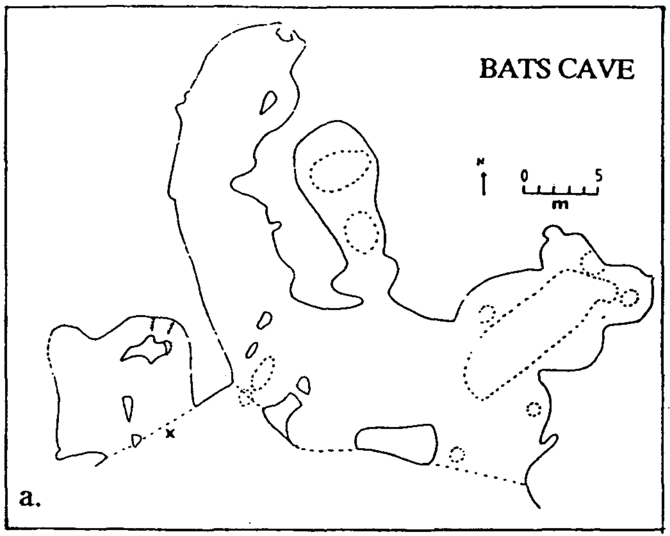

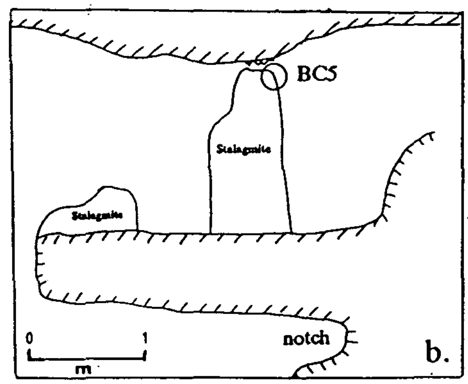

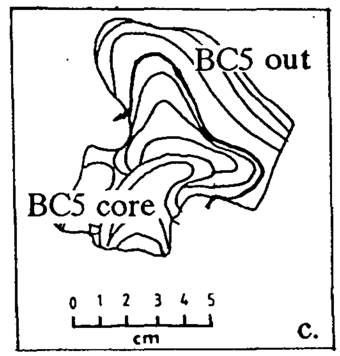

Fig. 5.5a. Location of BC5 in Bats Cave
b. Schematic sketch of the site
c. Cross section of BC5

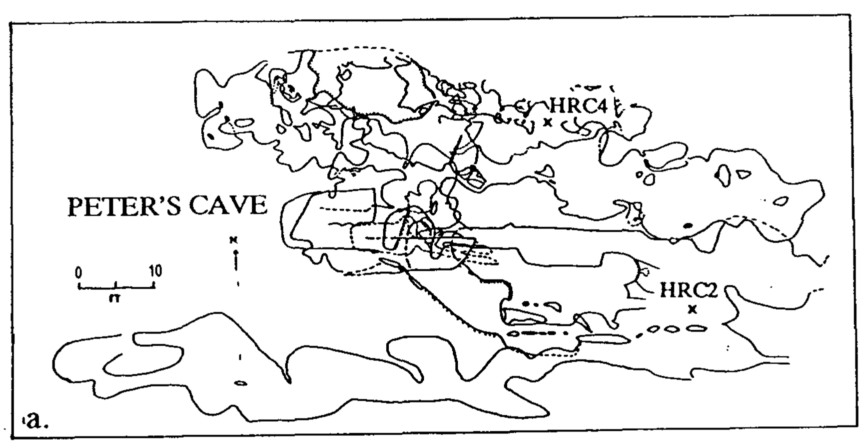

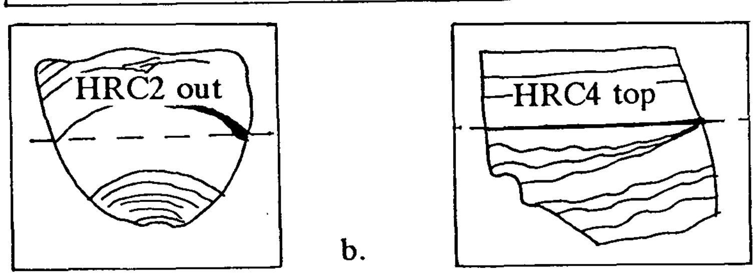

Fig. 5.6a. Location of HRC2 and HRC4 in Peter's Cave
b. Cross section of dated speleothem samples

the ocean and perhaps other agents. The dated piece of speleothem is from the latest phase of speleothem deposition. The sample has been contaminated with detrital thorium for which the date was corrected. The sample had grown continuously from an unknown date to at least 12 ka, but probably later if account is taken of the layers lost to erosion. The rise of sea level accompanying the melt of the continental ice sheets could have been responsible for the cessation of growth of this speleothem. It is possible that the close proximity of the sea changed the conditions favourable for speleothem growth; e.g. due to continuous wetting by sea spray, breaking of the waves against the speleothem in times of storm.

5.2.1.2 The ages of the hiatuses.

The exact date of the oldest hiatus (present in LC2) is unknown but is believed to have occurred before or around 350 ka (see above). The next hiatus is probably around 200 ka, broadly encompassing the oxygen isotope stage 7. It is present in TC12 and most likely in LC2 (again because the sample was taken close to the hiatus). The growth of speleothems LC3 and BC5 was probably initiated about this date. However, the date on the outside of stalactite HRC2 (176 ka) and the fact that there is no hiatus between the core and the outside suggest that this sample has grown during the oxygen isotope stage 7.

The last datable hiatus was somewhere between 75 ka and 20 ka, during stage 2 or 3. Apart from GC8 no other cave sample was dated beyond 65 ka which makes it impossible to give a more precise date to this period of dissolution.

Although, as mentioned previously, it is not possible to give a date of the hiatuses occurring in LC2, useful information may be inferred from their relative position. The hiatus immediately above the dated sample and the next hiatus are less than a centimetre apart. Using a growth rate of 1 mm in 1000 year (see below), there was approximately 10 ka years between these hiatuses (assuming there was no great loss of speleothem during the second hiatus). It is possible that these two hiatuses both correspond to the one hiatus in TC12 or that TC12 continued to grow while LC2 stopped for some time. If the two hiatuses were caused by flooding of the cave (see above), it is possible that Tibbetts Turn Cave stayed dry, because it lies approximately 6 m higher than Little Cayman Brac Cave. The youngest hiatus is about two cm further and might perhaps represent the same period as the one in GC8.

It is not certain either exactly when, and consequently why, the dissolution period that prevails today started. Further dating with mass spectrometry is certainly needed to answer these and other related questions.

5.2.1.3 Comparison with DWBAH.

DWBAH is a piece of flowstone collected at 15 m below modern sea level in Lucayan Caverns, Grand Bahama Island, which has been dated in detail by mass spectrometry by Lundberg (1990). It contains four hiatuses plus the present no growth (drowned) interval.

A comparison between DWBAH and the speleothems on Cayman Brac (at present all located above sea level on a tectonically unstable island) might be interesting to determine if the conditions accompanying the sea level high stands that caused the hiatuses in DWBAH were also responsible for the growth cessation of the speleothems on Cayman Brac.

The hiatuses found in this study show a general similarity with the ones obtained by Lundberg (1990) for DWBAH (Fig. 5.7). The oldest hiatus found in DWBAH and on Cayman Brac might correspond to each other. In the case of DWBAH the oldest dates by α spectrometry were > 350 ka while mass spectrometry gave a date of about 270 ka. It is possible that dating by mass spectrometry of LC2 will give better results as well, perhaps close to the one on DWBAH. Hiatus 1 and 2 in DWBAH and hiatus 2 on Cayman Brac, correspond very well, considering the differences in dating precision. Hiatuses 2 and 3 in LC2 are characterised by the presence of reddish and yellowish clay particles, resembling the description of the hiatal mud present in DWBAH (Lundberg, 1990) and which are deposited under submerged conditions. They are roughly 10 ka apart (see above) and occur around 235 ka. This suggests that these two hiatuses could correspond to hiatuses 1 and 2 in DWBAH and that these two hiatuses are represented as only one in TC12. Hiatuses 3 and 4 of DWBAH are not evident on Cayman Brac, certainly not in TC12, which covers their whole extent. These periods of growth cessation of DWBAH might account for why LC3 and BC5 stopped growing and

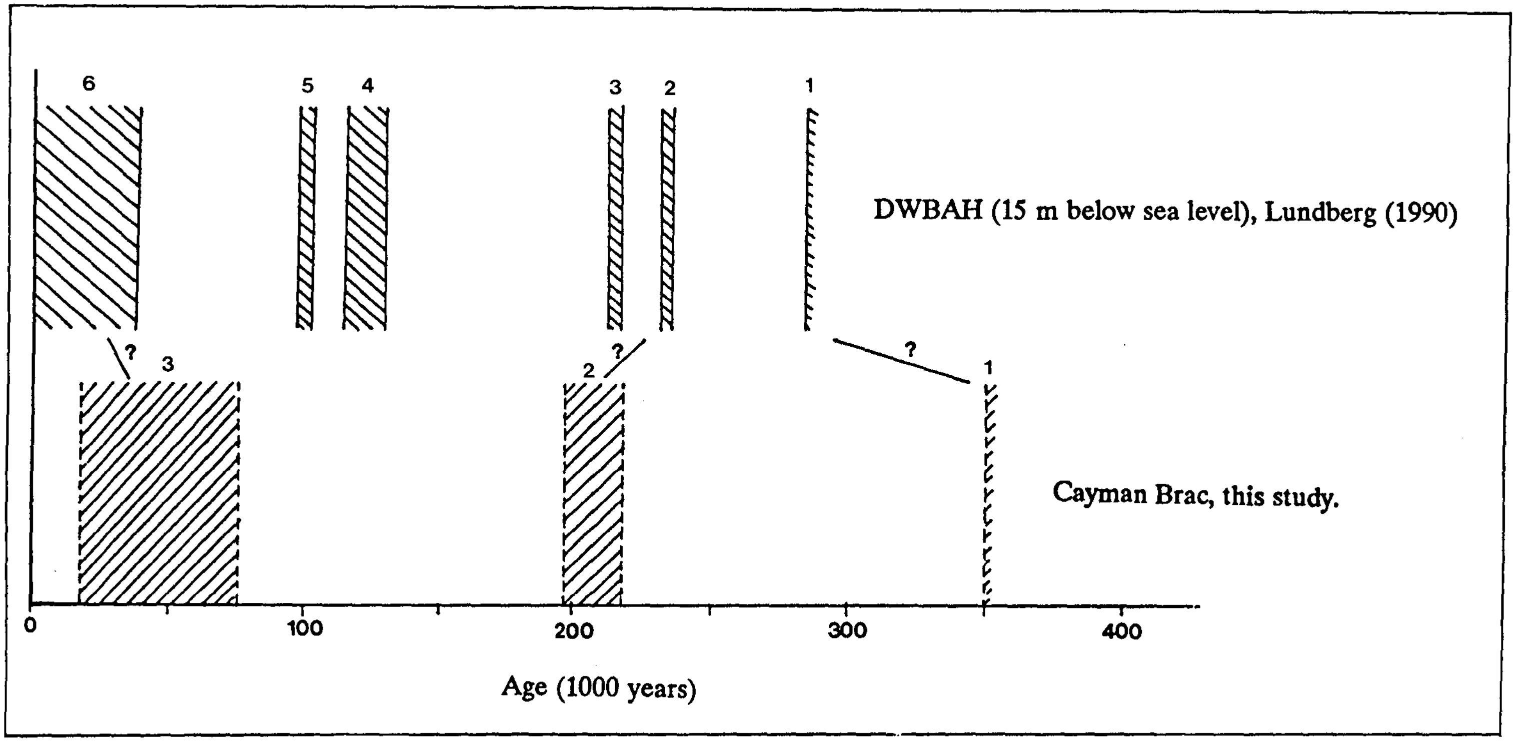

Fig. 5.7. Comparison of the speleothem growth hiatuses on Cayman Brac and in DWBAH.

GC8 started growing afterwards but there is no evidence of this. The last period of dissolution of DWBAH, might correspond to the last hiatus found on Cayman Brac, considering the fact that it is not possible to determine exactly when the latter occurred. It might also be that the dissolution period existing today for many speleothems is the one that corresponds to DWBAH.

The hiatuses before the last interglacial of both regions agree. During the last interglacial and afterwards there were more hiatuses in DWBAH than on Cayman Brac. It might just be coincidence that the two record agree before and disagree after the last interglacial but it might as well be an indication of some change occurring on the more unstable Cayman Brac. Although field evidence indicates that the island has been tectonically stable at least since the last interglacial (see 1.3 Geology).

More accurate dating with mass spectrometry is certainly needed to pinpoint the dissolution periods better and thus to be able to compare the two records better with each other.

5.2.2 Growth periods and growth rates.

5.2.2.1 Growth periods.

Growth appears to have taken place during four periods: > 350 ka, around 300 ka (transition from stage 9 to 8), between 200 ka and 70 ka (penultimate glaciation, stage 6, and last interglaciation, stage 5) and around 15 ka (last glaciation, stage 2).

Figure 5.8 shows that growth must have occurred during glacial and

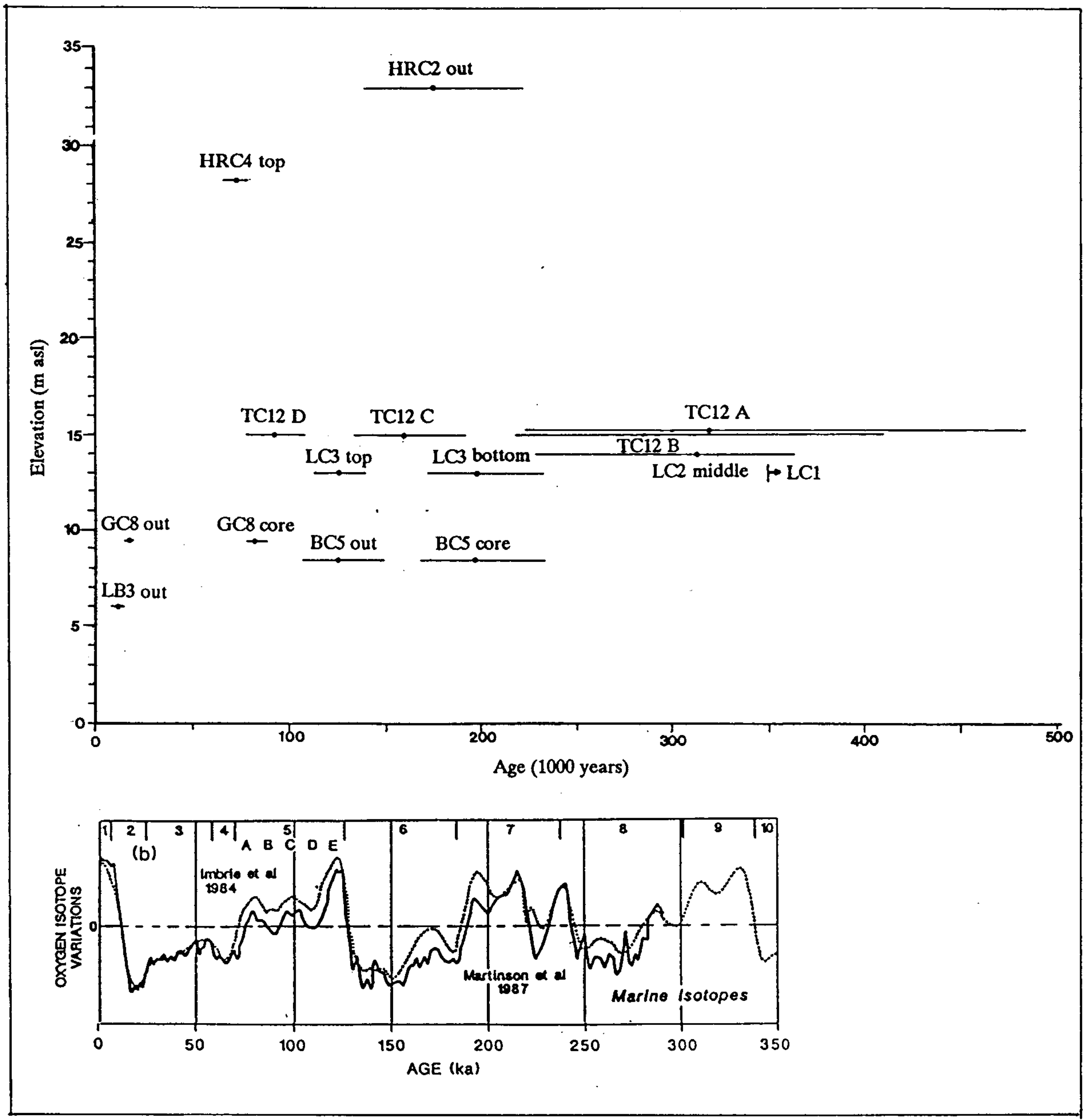

Fig. 5.8. Speleothem growth periods on Cayman Brac.

interglacial periods and that it does not appear to have been restricted to either period. As previously mentioned, the hiatuses occurred during stages 7, 3 and/or 4. Therefore, the succession of growth and dissolution periods does not appear to follow the glacial-interglacial sequences. A simple climatic correlation cannot be accepted at this stage in the investigation.

5.2.2.2 Growth rates.

Speleothem growth depends on many factors (e.g. feedwater channel length and diameter, soil and bedrock thickness overtop of the different sections of a cave, different climatic factors (rainfall, temperature)). Therefore, individual speleothems in a particular cave or in caves within one region can grow at different growth rates. Furthermore, different types of speleothem have different growth rates; e.g. flowstone will thicken more slowly than stalagmites extend upward. However, in spite of these individual differences, some broad uniformity of growth rates might be expected because the climatic factors play an important role. Especially the amount of rainfall and the rainfall regime are predominant because if there is no water there is no speleothem growth.

TC12 grew uninterrupted from about 320 ka to 285 ka and from 160 ka to 92.5 ka. Because alpha spectrometry uses large sample sizes the dates might represent averages of large growth periods and to calculate the growth rates it is necessary to take the middle of the area dated to compensate for this lack of precision. When this is done it is seen that TC12 grew approximately 3 cm during the first growth period, averaging about 0.85 mm ka^{-1}. The second period shows a rate of 0.3 mm ka^{-1}. The other two samples with continuous growth between two dates are BC5 and LC3, both covering the period 200 ka to 125 ka. Their growth rates are 0.55 and 0.4 mm ka^{-1} respectively.

Considering the last three growth rates, an average growth rate of about 0.4 mm ka^{-1} can be adapted for the period covering the penultimate glaciation and the last interglacial (200-90 ka). Growth during the transition from stage 9 to 8 might have been slightly faster, about 0.9 mm ka^{-1}, but this is only calculated from one sample. These growth rates are very similar to the ones obtained by Lundberg (1990) for DWBAH; growth rates of 0.3 mm ka^{-1} for isotope stage 8 (280-235 ka), 1.5 mm ka^{-1} during stage 7.4 (230-220 ka), 0.6 mm ka^{-1} for stage 7.2 to 6 (212-133 ka) and 0.45 mm ka^{-1} between 97 ka and 30 ka.

5.2.3 Discussion.

Speleothems grow where water enters a cave. Blockage of the feedwater channel or diversion of the feedwater can cause growth cessation of individual speleothems and the beginning of growth for another. Thus, there need be no phase correlation between the speleothems within a given cave or between different caves in a region (such as Cayman Brac). However, the abundance and widespread distribution of Type 1 and 2 speleothems and of the hiatuses observed in sectional samples from different caves suggests that there may be some kind of regional control. This discussion speculates upon it. It is clear that more samples and dates are needed from different islands to confirm this.

Considering the dates, the oldest part of sample LC2 and LC1 may have formed at the same time (Fig. 5.8), indicating that floor phase 1 and the beginning of ceiling phase 1 could represent the same growth period. Sample LC3 probably correspond to the top part of LC2, after hiatus 2 and even 3. The dated part of LC2 does not correspond to any of the other two samples. This might be because the flood waters that deposited the clay on the ceiling during hiatus 2 and 3 dissolved all the calcite deposited since 350 ka or because speleothem growth stopped on the floor, for instance because the floor was under water.

It was not possible to get a date from floor phase 3 and floor phase 4 was never dated. Phase 4, however, belongs to the third speleothem group and consist of popcorn shaped speleothem on stalactites and stalagmites. The popcorn speleothem is probably formed as a result of calcite deposition due to the evaporation of the feed water. The apparent orientation towards the entrance could be the result of higher evaporation rates on the sides facing the entrance where the wind comes from (Hill and Forti, 1986) or could have been deposited together with algal growth on the side facing the light.

The growth periods appear to cover glacial as well as interglacial periods (Fig. 5.8). The same is true for the dissolution periods; the present, for instance, is a period of growth cessation and even dissolution for the majority of the speleothems suggesting that interglacial periods are not necessarily growth periods. At present, the actively growing speleothems are few, localised and their size is small in comparison to the dissolved ones. In some cases they appear to form a new layer over older speleothems. There are no indications that the previous hiatuses resembled the present one but it might be that, similar to the present, not all the speleothems stopped growing at the same time. Therefore, it appears that the growth-dissolution periods of the individual speleothems do not necessarily follow the glacial-interglacial sequences.

Factors that might have played a role in the temporary cessation and dissolution of the speleothems could have been regional (the same speleothem dissolution has been encountered on other islands as well - Bahamas: Mylroie *et al.*, 1991; Mylroie, personal communications 1993; Mona, Puerto Rico: visited May 1993) or perhaps local, occurring at different islands at different times.

Climatic factors such as precipitation, temperature and wind have both direct and indirect influence on the amount of water and the saturation level of the water entering the caves. Indirectly they influence for instance the vegetation, the degree of soil formation and evapotranspiration rates. Global variations in CO_2 concentration of the atmosphere also interfere; the variations in the atmosphere outside are reflected in the cave atmosphere after some delay and dampening. For instance consider a decrease in the CO_2 concentration of the air but not of the feed water, an additional amount of calcite will have to be deposited from the feed water in order for the feed water to attain equilibrium with the CO_2 concentration of the air.

Climatic fluctuations are the result of the interaction of many different parameters such as temperature, precipitation, wind, barometric pressure, evaporation etc. In order to reconstruct the climatic fluctuations as a whole it is necessary to examine each of these factors individually, which is unfortunately rarely possible. That is why complicated atmospheric general circulation models have been developed to simulate the past climate (e.g. Gates, 1976, Manabe and Hahn, 1977; Kutzbach and Wright, 1985). These models are based on boundary conditions determined by CLIMAP (1976, 1981).

The climatic response of the tropical oceanic regions to the climatic and sea level fluctuations of the Quaternary is not yet completely understood. However, one thing is certain, these regions have never been glaciated and their position close to the equator was probably responsible for less drastic climatic fluctuations than those in the higher latitudes. Sea surface temperature reconstructions based on planktonic and benthic foraminefera indicate a decrease of about 2°C (CLIMAP, 1976, 1981; Broecker, 1986) during the last glacial period and a temperature range of approximately 5°C in the Caribbean Sea and 3-4°C for the Gulf of Mexico over the last 125 ka (Hecht, 1973). Towards the end of the last glaciation the influx of great quantities of cold melt water into the Gulf of Mexico might have caused a negative temperature anomaly. This resulted in the development of a high regional surface-pressure anomaly, which could have strengthened the western Atlantic trade winds and suppressed precipitation (Overpeck *et al.*, 1989). The absence of dates covering the end of the last glaciation inhibits any comparison between this climatic phenomena and growth or dissolution periods of the speleothems.

For a long time, it was widely believed that during glaciations in the higher latitudes pluvial periods existed in the tropics due to a southward shift of the climatic zonation. However, field evidence, for instance from lake level fluctuations and palynology (Hastenrath, 1985; Dawson, 1992), and numerical models (Gates, 1976; Manabe and Hahn, 1977; Kutzbach and Wright, 1985) show that the majority of the non glaciated areas were rather drier than wetter during the cooler periods of the Quaternary. One exception is western North American where numerous lakes developed during the last glaciation due to the southward steering of mid latitude cyclones around the southern margin of the Laurentide and Cordilleran ice sheets producing increased development of cyclones over the south western USA (Dawson, 1992). The eastern USA, however, appears to have experienced increased anticyclonic conditions due to a southward displacement of the westerly jet stream resulting in a reduction of precipitation and temperature (*op. cit.*).

The build-up and melt of the continental ice sheets resulted in sea level fluctuations. Curves of sea level fluctuations have been constructed over time based on drowned speleothems and raised coral reefs in tectonic stable areas such as the Bahamas or Bermuda (e.g. Land *et al.*, 1967; Harmon *et al.*, 1983; Lundberg, 1990; Richards *et al.*, in litt.). Comparison of the hiatuses of flowstone sample DWBAH of Lucayan Cavern, Grand Bahama Island (Lundberg, 1990), with the record obtained for Cayman

Brac, shows that the two records are similar except for the absence of the dissolution periods of 130-115 ka and 103-97 ka in the Cayman Brac record. DWBAH was collected from a depth of -15 m in a tectonic stable area and can thus be used for the reconstruction of sea level fluctuations. On the other hand, the samples dated on Cayman Brac were all collected from sites presently above sea level and in a region that has been tectonically unstable before the last interglacial. A direct connection between speleothem growth and sea level elevation is thus difficult to determine. The fact that speleothem appears to have grown during glacial periods and that there is presently a period of dissolution could indicate that the alternation of periods of growth and dissolution of speleothems on Cayman Brac did not necessarily follow the sequences of glacial and interglacial periods during the Quaternary.

CHAPTER SIX

DISCUSSION AND CONCLUSION

The distinction between the notch caves and the higher caves was originally based on the elevation above the notch. However, this study shows that there is more than just the elevation above the notch on which to base this separation.

In general the notch caves are characterised by

(i) a similar morphology,

(ii) well developed bellholes,

(iii) greatest volume close to the entrance and a rapid decrease after the first few meters,

(iv) development into the cliff in all directions, with a slight preference towards the N-NE.

(v) a low amount of speleothems, which belong largely to Type 1,

(vi) absence of breakdown inside the caves except there where partial collapse of the ceiling occurred and

(vii) smooth scallop-shaped rather than angular walls and ceilings.

The higher caves are not as similar to each other as the notch caves. Tibbetts Turn Cave resembles the notch caves morphologically but it contains much more speleothems and its greatest volume is not close to the entrance but rather furthest from the entrance. Little Cayman Brac Cave appears to follow a pre-existing vertical joint pattern sub-parallel to the cliff face and Peter's Cave has also large passages sub-parallel to the cliff face but they are not formed along vertical joints.

The morphology of the caves is determined by the process of cave formation and the events that follow. Therefore morphological similarities and differences can give some information about the relationship between caves.

6.1 Speleogenesis

6.1.1 Notch caves

The notch caves follow the description of flank margin caves, i.e. caves opening up in the cliff along the outer rim of the island and having a large, round or oval chamber sub-parallel to the cliff face and close to the entrance from which radiating passages lead inland where they pinch out or end abruptly. This suggest that these caves have been formed as a result of mixing corrosion along the halocline and/or water table. If the caves and the notch were formed at the same time then the point of discharge of the freshwater lens and the elevation of the notch would have to be at the same altitude, i.e. the sea level at the time of formation. However, the floor of the caves are situated at least one or more meters above the notch. Another point is that the caves form inside the rock and only open up as the result of surface erosion along the seaward side of the ridge or cliff. This would imply that the position of the notch should be located further seaward than the entrances of the caves, which is not the case. Therefore two possibilities exist:

1 the caves and the notch formed during the same sea level high stand but the caves formed first and the notch was formed when sea level lowered again and had a temporary halt long enough to cause cliff retreat and the formation of the notch at an elevation a few meters lower and

2 the caves and the notch formed at two different periods, the notch after the caves.

The age of the speleothems inside the caves could give the answer to this problem because speleothems only grow in air filled passages and thus should give a minimum age of the cave. The dated speleothem sample BC5 (Bats Cave) was taken on the outside, at the top of a 1.4 m high stalagmite located 0.9 m above the centre of the notch. Growth of this young part of the stalagmite started somewhere at the end of the penultimate interglaciation. Therefore, the entire stalagmite must be much older. Assuming that the notch was formed during the last sea level high stand 125 ka years ago, it is clear that Bats Cave is much older than the notch. Sample GC8 (Great Cave) started growth at the end of the last interglaciation which would not leave a long time to dissolve the cave. Furthermore, GC8 was only a small stalactite and dating of a bigger one might give older dates, leaving even less (or no) time for cave formation during the last interglacial sea level high stand. Further and more precise dating of speleothems inside these caves is necessary to get a better idea of the minimum age of these caves.

The relatively uniform elevation of these caves above the notch and their horizontality suggests that there has been no differential tectonic movement since their formation and between the formation of the caves and the notch.

6.1.2 Higher caves.

6.1.2.1 Tibbetts Turn Cave

As previously mentioned, this cave resembles the notch caves much more than the other two caves. The forms are rounded and cave development was in all directions. This is supported by the fact that there are no vertical or horizontal joints in the ceiling and walls. However, it contains much more speleothems and there does not appear to be a decrease in volume inland which would be expected if the cave formed from the shore inland. Furthermore, the floor is not horizontal as in the notch caves but it decreases stepwise inland.

It is possible that this cave also owes its formation to mixing corrosion but some kind of structural feature perhaps now disguised by speleothem growth, influenced the morphology.

6.1.2.2 Peter's Cave

The entrances to Peter's Cave lie along an arching joint in the cliff face (Photo 6.1). The passages of this cave are sub-parallel to the cliff face and decrease in height westward and landward. It is suggested that the main passages are formed along the sub-horizontal arching joint. The extensive breakdown in the western section of the

Photo 6.1 The entrances of Peter's Cave are situated along an arching joint in the cliff face

cave might be the result of instability at the western end of the joint where it appears to dip down. The eastern end of the joint is much more horizontal. The difference in orientation of the joint at the two end might have something to do with the difference in stability at the two ends. Perhaps the faster velocity and greater concentration of the water travelling along the vertical joint could have enhanced dissolution and breakdown. Another possibility is a localised vertical movement at the western end.

6.1.2.3 Little Cayman Brac Cave.

This is the only cave in which a vertical joint system (sub-parallel to the cliff face) exists and where the passages are clearly formed along these joints. The trend of the speleothems (i.e an increase of active speleothems and a decrease of the dissolved types from the entrance inward) in this cave might also give important information about its history.

There is no evidence of any stream inside the cave suggesting that it was formed in the phreatic zone. Water infiltrating along the joints could have mixed with the groundwater at the water table resulting in mixing corrosion. The pattern of groundwater flow may also have been dominated or controlled by the joints leading to preferential dissolution along the joints. The interplay of these processes together with mixing corrosion at the halocline may have contributed to the dissolution of the limestone and the formation of the cave.

6.2 Possible scenario for the karstification history of Cayman Brac.

A period of karstification followed the deposition of each formation in the Tertiary (Jones, 1992). Small cavities were dissolved in the bedrock during periods of submergence after lithification had taken place and subsequently were filled with caymanite, flowstone and clastic debris during periods of emergence.

The formation of the studied caves most likely occurred before the formation of the notch and the deposition of the Ironshore Formation during the last interglaciation. If the notch caves are indeed all formed in the same period and if speleothem Type 1 existed before the formation of the caves, then cave development must have taken place after the formation of the Pedro Castle Formation and at least one period of emergence during which speleothem Type 1 and breccia were formed. Speleothem sample BC5 suggest that Bats Cave was air-filled before the penultimate interglaciation, i.e. 200 ka ago. This then indicates the maximum lower time limit for cave formation. The higher caves appear to be older because of the older dates of the speleothems (>350 ka) and the greater abundance of speleothem suggesting that there has been more time available for speleothem development.

After the formation of the caves, speleothems were deposited during periods of emergence. Dating of some of the speleothems on Cayman Brac revealed that speleothem growth was not continuous over time but that the periods of growth cessation or dissolution were not necessarily linked to the glacial-interglacial sequence of the

Quaternary. Periods of growth cessation were dated at >350 ka, ~ 200 ka and between 75 and 20 ka. Some other hiatuses were visible but low thorium yield made it impossible to date them. During two of the undated hiatuses clay was deposited on the ceiling of the entrance section of Little Cayman Brac Cave. The most feasible explanation for this is flooding of the passage, which is situated about 10 m above mean sea level. These periods of dissolution might correspond to the high sea level stands recorded in a flowstone collected on Grand Bahama Island 15 m below mean sea level. It might also be the same period as the one dated in Tibbetts Turn Cave at 200 ka. Here there is no evidence of flooding, due, probably, to the higher location of this cave. Over the entire island the present interglacial appears to be a period of growth cessation.

Three different speleothem dissolution types were identified on Cayman Brac. Type 1 consist of speleothem that has lost its initial morphology and is visible in the wall, dissolved in the same manner as the walls; Type 2 speleothems have lost an extensive part of their volume but their original morphology is still recognisable and Type 3 speleothems only show point dissolution or none at all. As mentioned above the first type is believed to precede the cave formation but this can only be verified with more dating. Type 2 speleothems often show a distinct asymmetry in the direction of dissolution and it is believed that this is due to condensation corrosion caused by aggressive air flows. Type 3 speleothems might have some dissolution gullies caused by aggressive feedwater.

The particular trend of more actively growing speleothems inland and less dissolved types in Little Cayman Brac Cave provide useful information about the history of the cave since its emergence. Figures 4.15 and 4.16 showed two possible models by which this trend might have formed.

6.3 Further studies.

Further studies need to be done in many aspects. More widespread and more precise dating of all different speleothem types not only on Cayman Brac but also on other Caribbean islands is needed to establish authoritatively when the caves were formed, if the notch caves developed during the same period or not, when exactly dissolution took place and if the periods of growth and growth cessation were completely independent of the glacial-interglacial sequences of the Quaternary.

More water chemistry data might help understand why today is a period of growth cessation for the majority of the speleothems on Cayman Brac and elsewhere in the Caribbean.

Ways should be explored in the quantitative modelling of cave formation on small oceanic islands because the proposed karstification sequence and the flank margin model are only qualitative, revealing nothing about the rates of cave formation and cliff retreat or possible fresh water lens locations.

It appeared that a linear relationship exist between the logarithmic functions of cave plan area and volume. This means that decrease in volume inland, as is expected to occur if caves are formed from the shore inland, can be determined from existing cave plans without knowledge of the heights. However, this relationship warrants further studying.

REFERENCES

Back, W., Hanshaw, B.B., Herman, J.S. and Van Driel, J.N. (1986) Differential dissolution of a pleistocene reef in the ground-water mixing zone of coastal Yucatan, Mexico. *Geology*, 14, pp. 137-140.

Badon Ghyben, W. (1889) Nota in verband met de voorgenomen put boring nabij Amsterdam (Notes on the probable results of the proposed well drilling near Amsterdam). *K. Inst. Ing. Tijdschr., The Hague,* p.21.

Bearman, G. (ed.) (1989) *Seawater: its composition, properties and behaviour.* The Open University, 165 p.

Blanchard, D.C (1985) The oceanic production of atmospheric sea salt. *J. Geophys. Res.*, 90, pp. 961-963.

Bögli, A. (1980) *Karst Hydrology and Physical Speleology*. Berlin Heidelberg (Springer Verlag), 284 p.

Broecker, W.S. (1986) Oxygen isotope constraints on surface ocean temperatures. *Quat. Res.*, 26, pp. 121-134.

Brunt, M.A., Giglioli, M.E.C., Mather, J.D., Piper, D.J.W. and Richards, H.G. (1973) The Pleistocene rocks of the Cayman Islands. *Geol. Mag.*, 110, pp. 209-304.

Budd, D.A and Vacher, H.L. (1991) Predicting the thickness of fresh-water lenses in carbonate paleo-islands. *J. Sed. Petrol.,* 61, pp. 43-53.

Bugg, S.F. and Lloyd, J.W. (1976) A study of fresh water lens configuration in the Cayman Islands using resistivity methods. *Q. Jl Engng Geol.*, 9, pp. 291-302.

Bull, p.a. and Laverty, M. (1982) Observations on phytokarst. *Z. Geomorph. N.F.*, 26, pp. 437-457.

CLIMAP Project Members (1981) Seasonal reconstruction of the earth's surface at the last glacial maximum. *Geol. Soc. Am. Map and Chart Series,* MC-36.

CLIMAP Project Members (1976) The surface of the Ice-Age earth. *Science*, 191, pp. 1131-1137.

Cooper, H.H. (1959) A hypothesis concerning the dynamic balance of fresh water and salt water in a coastal aquifer. *J. Geophys. Res.*, 64, pp. 461-467.

Curl, R.L. (1973) Minimum diameter of stalagmites. *N.S.S. Bull.* 34, pp. 1-9.

Dawson, A.G. (1992) *Ice Age earth.* London (Routledge), 293 p.

Dreybrodt, W. (1988) *Processes in karst systems: Physics, Chemistry, and Geology.* Berlin (Springer), 288 p.

Eriksson, E. (1955) Air borne salts and the chemical composition of river waters. *Tellus*, 7, pp. 243-250.

Focke, J.W. (1978) Limestone cliff morphology on Curaçao (Netherlands Antilles), with special attention to the origin of notches and vermetid/coraline algal surf benches ("cornices", "trottoirs"). *Z. Geomorph.*, 22, pp. 329-349.

Folk, R.L., Roberts, H.H. and Moore, C.H. (1973) Black phytokarst from Hell, Cayman Islands, British West Indies. *Geol. Soc. Am. Bull.*, 84, pp. 2351-2360.

Folk, R.L. and Ward, W.C. (1957) Brazos River bar: a study in the significance of grain size parameters. *J. Sed. Petrol.,* 27, pp. 3-26.

Ford, D.C. and Williams, P.W. (1989) *Karst geomorphology and Hydrology.* London (Unwin Hyman), 601 p.

Foster, I.D.L., Grieve, I.C. and Christmas, A.D. (1982) The use of specific conductance in studies of natural waters and soil solutions. *Hydrol. Sci. Bull.*, 26, pp. 257-269.

Gascoyne, M., Latham, A.G., Harmon, R.S. and Ford, D.C. (1983) The antiquity of Castlegard Cave, Columbia Icefield, Alberta, Canada. *Arctic and Alpine Res.*, 15, pp. 463-470.

Gates, W.L. (1976) Modelling the Ice-Age climate. *Science*, 191, pp. 1138-1144.

Glover, R.E. (1959) The pattern of fresh-water flow in a coastal aquifer. *J. Geophys. Res.,* 64, pp. 457-459.

Hallam, A. (1984) Pre-Quaternary sea-level changes. *Ann. Rev. Earth Planet. Sci.*, 12, pp. 205-243.

Harmon, R.S., Mitterer, R.M., Kriausakul, N., Land, L.S., Schwarcz, H.P., Garrett, P., Larson, G.J., Vacher, H.L. and Rowe, M. (1983) U-series and amino-acid racemization geochronology of Bermuda: Implications for eustatic sea-level fluctuation over the past 250,000 years. *Palaeogeog.*

Palaeoclimatol. Palaeoecol., 44, pp. 41-70.

Hastenrath, S. (1985) *Climate and circulation of the tropics.* Dordrecht (D. Reidel Publishing Company), 455 p.

Hecht, A.D. (1973) Faunal and oxygen isotopic paleotemperatures and the amplitude of glacial/interglacial temperature changes in the equatorial Atlantic, Caribbean Sea and Gulf of Mexico. *Quat. Res.*, 3, pp. 671-690.

Henry, H.R. (1964) Effects of dispersion on salt encroachment in coastal aquifers. *in:* U.S. Geol. Surv., *Sea water in coastal aquifers*, Water-Supply Pap. 1613-C, pp. 70-84.

Herzberg, A. (1901) Die Wasserversorgung einiger Nordsee Bäder. *J. Gasbeleucht. Verw. Beleuchtungsarten Wasserversorg.*, 44, pp. 815-819, 842-844.

Hill, C.A. (1987) Geology of Carlsbad Cavern and other caves in the Guadalupe Mountains, New Mexico and Texas, *New Mexico Bureau of Mines and Mineral Resources*, Bulletin 117, 150 p.

Hill, C.A. and Forti, P. (1986) *Cave minerals of the world.* Huntsville, USA (Nat. Speleo. Soc.), 238 p.

Horsfield, W.T. (1975) Quaternary Vertical Movements in the Greater Antilles. *Geol. Soc. Am. Bull.*, 86, pp. 933-938.

Hubbert, M.K. (1940) The theory of ground-water motion. *J. Geol.*, 48, pp. 785-944.

Imbrie, J., Hays, J.D., Martinson, D.G., McIntyre, A., Mix, A.C., Morley, J.J., Pisias, N.G., Prell, W.L. and Shackleton, N.J. (1984) The orbital theory of Pleistocene climate: support from a revised chronology of the marine $\delta^{18}O$ record. *in:* A.L. Berger *et al.* (eds.) *Milankovitch and climate*. Dordrecht (Reidel), pp. 269-305.

Jennings, J.N. (1985) *Karst geomorphology*. Oxford (Basil Blackwell Ltd.), 293 p.

Jones, B. (1992) Caymanite, a cavity-filling deposit in the Oligocene-Miocene Bluff Formation of the Cayman Islands. *Can. J. Earth Sci.*, 29, pp. 720-736.

Jones, B., Hunter, I.G. and Kyser, K. (in press (b)) Revised stratigraphic nomenclature for Tertiary strata of the Cayman Islands, British West Indies. *Carib. J. Sci.*

Jones, B., Hunter, I.G. and Kyser, K. (in press (a)) Stratigraphy of the Bluff Formation (Miocene-Pliocene) and the newly defined Brac Formation (Oligocene), Cayman Brac, British West Indies. *Carib. J. Sci.*

Jones, B. and Hunter, I.G. (1989) The Oligocene-Miocene Bluff Formation on Grand Cayman. *Carib. J. Sci.*, 25, pp. 71-85.

Junge, C.E. and Gustafson, P.E. (1957) On the distribution of sea salt over the United States and its removal by precipitation. *Tellus*, 9, pp. 164-173.

King-Webster, W.A. and Kenny, J.S. (1958) Bat erosion as a factor in cave formation. *Nature,* 181, p. 1813.

Kohout, F.A. (1960) Cyclic flow of salt water in the Biscayne aquifer of southeastern Florida. *J. Geophys. Res.*, 65, pp 2133-2141.

Kutzbach, J.E. and Wright, H.E. (1985) Simulation of the climate of 18,000 years

BP: results for the North American/North Atlantic/European sector and comparison with the geologic record of North America. *Quat. Sci. Rev.*, 4, pp. 147-187.

Land, L.S., MacKenzie, F.T. and Gould, S.J. (1967) Pleistocene history of Bermuda. *Geol. Soc. Am. Bull.*, 78, pp. 993-1006.

Lundberg, J. (1990) *U-series dating of carbonates by mass spectrometry with examples of speleothem, coral and shell.* PhD Thesis, McMaster University, Hamilton, Ontario, Canada, 271 p.

Manabe, S. and Hahn, D.G. (1977) Simulation of the tropical climate of an Ice Age. *J. Geophys. Res.*, 82 (27), pp. 3889-3911.

Martinson, D.G., Pisias, N.G., Hays, J.D., Imbrie, J., Moore, T.C., Jr., and Shackleton, N.J. (1987) Age dating and the orbital theory of the Ice Ages: development of a high-resolution 0 to 300,000-year chronostratigraphy. *Quat. Res.*, 27, pp. 1-29.

Mather, J.D. (1975) Development of the groundwater resources of small limestone islands. *Q. Jl Engng Geol.*, 8, pp. 141-150.

Matley, C.A. (1926) The geology of the Cayman Islands (British West Indies), and their relation to the Bartlett Trough. *Quat. J. Geol. Soc. London*, 82, pp. 352-386.

McNeill, D.F., Ginsburg, R.N., Chang, S-B.R. and Kirschvink, J.L. (1988) Magnetostratigraphic dating of shallow-water carbonates from San Salvador, Bahamas. *Geology*, 16, pp. 8-12.

Miller, T. (1981) *Hydrochemistry, hydrology, and morphology of the Caves Branch Karst, Belize.* PhD Thesis, McMaster University, Hamilton, Ontario, Canada, 280 p.

Muskat, M. (1937) *The flow of homogeneous fluids through porous media.* McGraw-Hill, New York, N.Y., 763 p.

Mylroie, J.E. and Carew, J.L. (1990) The flank margin model for dissolution cave development in carbonate platforms. *Earth Surface Processes and Landforms*, 15, pp. 413-424.

Mylroie, J.E., Carew, J.L., Sealey, N.E. and Mylroie, J.R. (1991) Cave development on New Providence Island and Long Island, Bahamas. *Cave Science,* 18, pp. 139-151.

Ng, K-C., Jones, B. and Beswick, R. (1992) Hydrology of Grand Cayman, British West Indies: a karstic dolostone aquifer. *J. Hydrol.*, 134, pp. 273-295.

Niewolt, S. (1977) *Tropical Climatology.* Chichester (John Wigley & Sons), 207 p.

Ollier, C.D. (1975) Coral island geomorphology. *Z. Geomorph. N.F.*, 19, pp. 164-190.

Overpeck, J.T., Peterson, L.C., Kipp, N., Imbrie, J. and Rind, D. (1989) Climate change in the circum-North Atlantic region during the last deglaciation. *Nature*, 338, pp. 553-557.

Palmer, R.J., McHale, M. and Hartlebury, R. (1986) The caves and Blue Holes of Cat Island, Bahamas. *Cave Science*, 13, pp. 71-78.

Pissart, A. and Juvigné, E. (a.n.) *Methodes d'étude des formations détritiques* *continentales*. Université de Liège (unpublished).

Plummer, L.N. (1975) Mixing of sea water with calcium carbonate ground water. *Geol. Soc. Am. Mem.,* 142, pp. 219-236.

Reilly, T.E. and Goodman, A.S. (1985) Quantitative analysis of saltwater-freshwater relationships in groundwater systems - A historical perspective. *J. Hydrol.*, 80, pp. 125-160.

Richards, D.A., Smart, P.L. and Edwards, R.L. (in litt.) Sea levels for the last glacial period constrained using ^{230}Th ages of submerged speleothems. *Nature*.

Runnels, D.D. (1969) diagenesis, chemical sediments, and the mixing of natural waters. *J. Sed. Petrol.*, 39, pp. 1188-1201.

Schroeder, D. (1984) *Soils. Facts and concepts.* Bern (International Potash Institute), 140 p.

Schwarcz, H.P. and Gascoyne, M. (1984) Uranium series dating of Quaternary deposits. *in:* Mahaney, W.C. (ed.) *Quaternary dating methods* Amsterdam (Elsevier), pp. 33-51.

Smart, C.C. (1984) The hydrology of the inland Blue Holes, Andros Island. *Cave Science*, 11, pp. 23-29.

Smart, P.L., Dawans, J.M. and Whitaker, F. (1988) Carbonate dissolution in a modern mixing zone. *Nature*, 335, pp. 811-813.

Smith, D.S. (1987) *The speleothemic calcite deposits on Grand Cayman Island, British*

West Indies. M.Sc. Thesis, University of Alberta, Edmonton, Alberta, 171 p.

Spencer, T. (1985) Marine erosion rates and coral morphology of reef limestones on Grand Cayman Island, West Indies. *Coral Reefs*, 4, pp. 59-70.

Stenson, R.E. (1990) *The morphometry and spatial distribution of surface depressions in gypsum, with examples from Nova Scotia, Newfoundland and Manitoba.* MSc Thesis, McMaster University, Hamilton Ontario, Canada, 134 p.

Tarbox, D.L. (1986) Occurrence and development of water resources in the Bahama Islands. *in:* Curran, H.A. (ed.) *Proceedings of the 3rd Symposium on the Geology of the Bahamas, June 1983*, pp. 139-144.

Thornthwaite, C.W. (1948) An approach towards a rational classification of climate. *Geogr. Review*, 38, pp. 55-94.

Thrailkill, J. (1968) Chemical and Hydrologic factors in the excavation of limestone caves. *Geol. Soc. Am. Bull.*, 79, pp. 19-45.

Trudgill, S.T. (1985) *Limestone geomorphology*. (Geomorphology texts; 8). New York (Longman Group Limited), 196 p.

Trudgill, S.T. (1976) The marine erosion of limestone on Aldabra Atoll, Indian Ocean. *Z. Geomorph Suppl.*, 26, pp. 164-200.

Vacher, H.L. (1978) Hydrology of small oceanic islands-Influence of atmospheric pressure on the water table. *Ground Water*, 16, pp. 417-423.

Vogel, P.N., Mylroie, J.E. and Carew, J.L. (1990) Limestone petrology and cave morphology on san Salvador Island, Bahamas. *Cave Science*, 17, pp. 19-30.

Watson, R.A. and White, W.B. (1985) The history of American theories of cave origin. *Geol. Soc. Am., Centennial Special Vol.,* 1, pp. 109-123.

Wheatcraft, S.W. and Buddemeier, R.W. (1981) Atoll island hydrology. *Ground Water*, 19, pp. 311-320.

White, W.B. (1988) *Geomorphology and hydrology of karst terrains.* New York (Oxford University Press, Inc.), 464 p.

Whitten, D.G.A. and Brooks, J.R.V. (1972) *The Penguin dictionary of Geology.* London (Penguin Books), 516 p.

Wigley, T.M.L. and Plummer, L.N. (1976) Mixing of carbonate waters. *Geochim. Cosmochim. Acta,* 40, pp. 989-995.

Wilford, C.E. (1966) "Bell Holes" in Sarawak Caves. *N.S.S. Bull.*, 28, pp.179-182.

Woodroffe, C.D. (1988) Vertical movement of isolated oceanic islands at plate margins: evidence from emergent reefs in Tonga (Pacific Ocean), Cayman Islands (Caribbean Sea) and Christmas Island (Indian Ocean). *Z. Geomorph.*, 69, pp. 17-37.

Woodroffe, C.D., Stoddart, D.R., Harmon, R.S. and Spencer, T. (1983) Coastal morphology and late Quaternary history, Cayman Islands, West Indies. *Quaternary Research,* 19, pp. 64-84.

Worthington, S.R.H. (1991) *Karst hydrogeology of the Canadian Rocky Mountains.* PhD Thesis, McMaster University, Hamilton, Ontario, Canada, 370 p.